



UNIVERSIDADE FEDERAL DO ESPÍRITO SANTO
CENTRO DE CIÊNCIAS DA SAÚDE
PROGRAMA DE PÓS-GRADUAÇÃO EM BIOTECNOLOGIA

MARLONNI MAURASTONI ARAUJO

**Dynamics of the papaya meleira virus complex during the
development of papaya (*Carica papaya* L.)**

VITÓRIA, ES

2021

MARLONNI MAURASTONI ARAUJO

**Dynamics of the papaya meleira virus complex during the
development of papaya (*Carica papaya* L.)**

Tese apresentada ao Programa de Pós-Graduação em Biotecnologia do Centro de Ciências da Saúde da Universidade Federal do Espírito Santo, como requisito parcial para obtenção do título de Doutor em Biotecnologia.

Orientador: Prof. Dr. Patricia Machado Bueno Fernandes

VITÓRIA, ES

2021

Ficha catalográfica disponibilizada pelo Sistema Integrado de Bibliotecas - SIBI/UFES e elaborada pelo autor

A658d ARAUJO, MARLONNI MAURASTONI, 1996-
Dynamics of the papaya meleira virus complex during the development of papaya (*Carica papaya* L.) / MARLONNI MAURASTONI ARAUJO. - 2021.
173 f. : il.

Orientadora: PATRICIA MACHADO BUENO FERNANDES.

Tese (Doutorado em Biotecnologia) - Universidade Federal do Espírito Santo, Centro de Ciências da Saúde.

1. Totiviruses. 2. Proteína capsidial. 3. Interação proteína proteína. 4. Interação vírus-hospedeiro. 5. Meleira do mamoeiro. 6. Vetores de vírus. I. FERNANDES, PATRICIA MACHADO BUENO. II. Universidade Federal do Espírito Santo. Centro de Ciências da Saúde. III. Título.

CDU: 61

MARLONNI MAURASTONI ARAUJO

**Dynamics of the papaya meleira virus complex during the
development of papaya (*Carica papaya* L.)**

Tese apresentada ao Programa de Pós-Graduação em Biotecnologia do Centro de Ciências da Saúde da Universidade Federal do Espírito Santo, como requisito parcial para obtenção do título de Doutor em Biotecnologia.

Apresentada em 11 de novembro de 2021.

**Prof. Dr. Patricia Machado Bueno
Fernandes
Universidade Federal do Espírito Santo
Orientadora**

**Prof. Dr. Antônio Alberto Ribeiro
Fernandes
Universidade Federal do Espírito Santo**

**Prof. Dr. Anna Elizabeth Whitfield
North Carolina State University**

**Prof. Dr. Francisco Murilo Zerbini Junior
Universidade Federal de Viçosa**

Prof. Dr. Francisco José Lima Aragão
Empresa Brasileira de Pesquisa
Agropecuária – Recursos Genéticos e
Biotecnologia

Prof. Dr. Silas Pessini Rodrigues
Universidade Federal do Rio de Janeiro

VITÓRIA, ES

2021

DEDICATION

Dedicated to everyone fighting against the COVID-19 pandemic using Science as a weapon against the SARS-CoV.

ACKNOWLEDGEMENTS

I would like to thank the Federal University of Espírito Santo (UFES) and the UFES Biotechnology postgraduation program for the resources and infrastructure provided to develop my work.

I would also like to thank Coordenação de Aperfeiçoamento de Pessoal de Nível Superior (CAPES) for my scholarship and Fundação de Amparo à Pesquisa do Espírito Santo (FAPES) and Conselho Nacional de Desenvolvimento Científico e Tecnológico (CNPq) for funding.

I am grateful to all professors and professionals for their guidance and their institutions they belong.

In particular faculty, staff and students of UFES: P. M. B. Fernandes, A. A. R. Fernandes, J. A. Ventura, A. M. C. Santos, T. S. F. Antunes, O. F. Quadros, A. B. Vaz, A. C. Tosi, R. D. Moura, L. A. M. Castro, T. Carneiro, M. L. Silva, R. C. Pereira and F. Torres.

Federal University of Viçosa (UFV): F. M. Zerbini Jr. and A. F. Orílio;

Federal University of Rio de Janeiro (UFRJ): S. P. Rodrigues

EMBRAPA Genetic Resources and Biotechnology (CENARGEN): E. F. M. Abreu, F. J. L. Aragão, S. G. Ribeiro, D. M. A. Dusi, C. C. Lacorte, M. M. Sanches, A. Mehta, A. H. Vidal, H. M. Farias and Y. Santos.

University of Brasília: W. Fontes and N. M. F. S. Domingues

North Carolina State University: A. E. Whitfield, D. Rotenberg, C. A. D. Xavier, S. Kanakala, S. P. Rajarapu, J. Han, K. Lahre, Y. Chen, H. W. Teh, K. A. Shaw and E. Smith.

THESIS STRUCTURE

This thesis is presented in Scientific Article format. The lists of figures and tables contain the illustrations and tables presented in the papers in preparation for publication, as per ABNT. The item References contains the bibliographical references presented in the introduction of this thesis.

DINÂMICA DO COMPLEXO PAPAYA MELEIRA VIRUS DURANTE O DESENVOLVIMENTO DO MAMOEIRO (*Carica papaya* L.)

RESUMO

MAURASTONI, M. A. **Dinâmica do complexo papaya meleira virus durante o desenvolvimento do mamoeiro (*Carica papaya* L.)**. 2021. 173f. Tese de doutorado em Biotecnologia – Programa de Pós-graduação em Biotecnologia, UFES, Espírito Santo, Brasil.

A meleira do mamoeiro (PSD - do inglês, *papaya sticky disease*) está entre as doenças mais graves causadas por vírus e que afetam a produção de mamão. Essa doença foi relatada pela primeira vez no Brasil em 1993, associada a um vírus de RNA fita dupla, denominado papaya meleira virus (PMeV). Desde então, avançou-se no conhecimento da dispersão da doença no campo, na caracterização do agente etiológico e suas interações com o mamoeiro. Porém, em 2016, o papaya meleira virus 2 (PMeV2), com genoma de RNA fita simples de senso positivo, também foi identificado em plantas doentes, impondo um repensar no patossistema. Neste trabalho, avaliamos criticamente os achados dos últimos 30 anos para entender a dispersão da doença em campo. Mostramos que espécies de cigarrinhas e moscas-branca precisam ser melhor estudadas como potenciais vetores no Brasil uma vez que técnicas de diagnóstico molecular mais sensíveis estão disponíveis. Não obstante, desenvolvemos uma técnica de RT-PCR *multiplex* (mPCR) capaz de detectar ambos os vírus em uma única reação a partir de amostras de plantas em pré-florescimento, que é um método alternativo para o diagnóstico precoce de PSD. Mostramos também que os laticíferos da nervura central de folhas do mamoeiro doente são os locais preferenciais de infecção do PMeV e PMeV2. O capsídeo do PMeV é composto de dois polipeptídios principais com sequências sobrepostas, sendo que um fragmento central desses polipeptídios (aa 321-670) interage com a proteína ribossomal 50S L17 (RPL17), que especulamos como importante no acúmulo de ambos os vírus. Assim, esta tese discute a PSD em três esferas principais: biologia do agente etiológico e sua interação com o hospedeiro, a disseminação da doença no campo e o desenvolvimento de tecnologias para seu manejo.

Palavras-chave: Totiviruses. Proteína capsidial. Interação proteína-proteína. Interação vírus-hospedeiro. Meleira do mamoeiro. Vetores de vírus.

DYNAMICS OF THE PAPAYA MELEIRA VIRUS COMPLEX DURING THE DEVELOPMENT OF PAPAYA (*Carica papaya* L.)

ABSTRACT

MAURASTONI, M. A. **Dynamics of the papaya meleira virus complex during the development of papaya (*Carica papaya* L.)**. 2021. 173p. Thesis for the Degree of Ph.D. in Biotechnology – Postgraduation Biotechnology Programme, UFES, Espírito Santo. Brazil.

Among the most serious virus-incited diseases in papaya production is papaya sticky disease (PSD). This disease was first reported in Brazil in 1993, associated with a double-stranded RNA virus, called papaya meleira virus (PMeV). Since then, progress has been made in the knowledge of the disease dispersion in the field, the etiological agent characterization, and its interactions with papaya. However, in 2016, the papaya meleira virus 2 (PMeV2), with a positive single-stranded RNA genome, was also identified in diseased plants, imposing a rethinking of the pathosystem. Therefore, in this work, we critically evaluate the latest findings on PSD and the last 30 years of research done to understand its dispersion in the field. We show that leafhopper and whitefly species need to be better studied as potential vectors of the PSD-associated viruses in Brazil now that more sensitive molecular diagnostic techniques are available. Nevertheless, we developed a multiplex RT-PCR (mPCR) technique capable of detecting both viruses in a single reaction from pre-flowering plant samples, which is a useful tool for the early diagnosis of PSD. Here we show that laticifers of the main vein of papaya sticky diseased leaves are the preferential infection site of PMeV and PMeV2. We also show that the PMeV capsid is composed of two major polypeptides with overlapping sequences. A central fragment of these polypeptides (aa 321-670) interacts with the 50S ribosomal protein L17 (RPL17), which we speculate as an important player in virus accumulation. Overall, this thesis discusses PSD in three main spheres: the biology of the etiological agent and its interaction with the host, the spread of the disease in the field, and the development of technologies for its management.

Keywords: Totiviruses. Capsid protein. Protein-protein interaction. Virus-host interaction. Papaya sticky disease. Virus vectors.

LIST OF ABBREVIATIONS

3-AT	3-Amino-1,2,4-triazole
AAP	Acquisition access period
AD	Activation domain
BD	Binding domain
BiFC	Bimolecular fluorescence complementation
bp	Base pairs
CMV	Cucumber mosaic virus
CP	Capsid protein
DAPI	4,6-diamino-2-phenyl-indol
DDO	Double dropout
DDO/X/A	Double dropout plus X-alpha-gal and Aureobasidin A
DNA	Deoxyribonucleic acid
dsRNA	Double-stranded ribonucleic acid
EDTA	Ethylenediamine tetraacetic acid
ER	Endoplasmic reticulum
FAO	Food and agriculture organization of the United Nations
GFP	Green fluorescent protein
MATV	maize-associated totivirus
MP	Movement protein

nm	Nanometer
nt	Nucleotide
ORF	Open reading frame)
PCR	Polymerase chain reaction
PMeV	papaya meleira virus
PMeV2	papaya meleira virus 2
PMeV-ES	papaya meleira virus Espírito Santo isolate
PMeV-Mx	papaya meleira virus Mexico isolate
PMeV-RN	papaya meleira virus Rio Grande do Norte isolate
PnVA	panax notoginseng virus A
PPI	Protein-protein interaction
PpVQ	papaya virus Q
PVX	Potato virus X
QDO	Quadruple dropout
QDO/X	Quadruple dropout plus X-alpha-gal
QDO/X/A	Quadruple dropout plus X-alpha-gal and Aureobasidin A
RdRp	RNA-dependent RNA polimerase
RFP	Red fluorescent protein
RNA	Ribonucleic acid
RPL17	50S ribosomal protein L17
RT	Reverse transcriptase
RT-PCR	Reverse transcription-polymerase chain reaction

SD	Synthetic defined
SDO	Single dropout
SDS-PAGE	Sodium dodecyl sulphate–polyacrylamide gel electrophoresis
ssRNA	Single-stranded RNA
TMV	Tobacco mosaic virus
Y2H	Yeast two-hybrid
YFP	Yellow fluorescent protein

INDEX

GENERAL INTRODUCTION	16
REFERENCES.....	18
MANUSCRIPT #1. BATTLE OF THREE: THE CURIOUS CASE OF PAPAYA STICKY DISEASE	20
INTRODUCTION.....	22
PAPAYA STICKY DISEASE: TWO VIRUSES, ONE DISEASE.....	23
PAPAYA AND PMEV COMPLEX INTERACTION	26
EPIDEMIOLOGY	30
MANAGEMENT OF PAPAYA VIRUS DISEASES	32
CLOSING REMARKS AND FUTURE PROSPECTS	36
REFERENCES.....	39
THESIS OBJECTIVE	52
GENERAL OBJECTIVE.....	52
SPECIFIC OBJECTIVES.....	52
MANUSCRIPT #2. LATICIFERS OF PAPAYA STICKY DISEASED PLANTS ARE THE PREFERENTIAL INFECTION SITE OF A TOTIVIRUS-LIKE AND UMBRAVIRUS-LIKE ASSOCIATED RNA	53
ABSTRACT	54
INTRODUCTION.....	55
METHODS	57
RESULTS.....	60
DISCUSSION	62
REFERENCES.....	67
MANUSCRIPT #3. A CAPSID PROTEIN FRAGMENT OF A TOTI-LIKE VIRUS FOUND IN PAPAYA LATEX INTERACTS WITH THE 50S RIBOSOMAL PROTEIN L17	80
ABSTRACT	81
INTRODUCTION.....	82

METHODS	84
RESULTS.....	89
DISCUSSION	95
REFERENCES.....	100
MANUSCRIPT #4. A MULTIPLEX RT-PCR METHOD TO DETECT PAPAYA MELEIRA VIRUS COMPLEX IN ADULT PRE-FLOWERING PLANTS	120
MANUSCRIPT #5. EFFORTS TO UNDERSTAND TRANSMISSION OF THE PAPAYA MELEIRA VIRUS COMPLEX BY INSECTS	132
ABSTRACT	133
INTRODUCTION TO PAPAYA STICKY DISEASE	134
COULD PMEVC COMPLEX BE TRANSMITTED BY FUNGI?	136
HOW DOES AN INSECT ACQUIRE PMEVC COMPLEX VIRIONS FROM A DISEASED PLANT?	137
STUDIES OF PSD TRANSMISSION BY VECTORS	138
DO LEAFHOPPERS TRANSMIT PSD-ASSOCIATED VIRUSES?.....	139
DO WHITEFLIES TRANSMIT PSD-ASSOCIATED VIRUSES?.....	141
CONCLUSIONS.....	144
REFERENCES.....	145
THESIS CONCLUSIONS AND FUTURE PERSPECTIVES	160
ANNEX	162
ANNEX #1	162
ANNEX #2	163
ANNEX #3	175

1 GENERAL INTRODUCTION

2

3

4 Papaya (*Carica papaya* L.) has been widely cultivated in tropical and subtropical regions.
5 In 2019, the world production of papaya reached approximately 13.7 million tons. In 2018
6 the gross value of production reached \$4.9 billion, the highest yield since the 1990s (FAO,
7 2019). In 2019, Brazil was placed as the third-largest producer, after the Dominican
8 Republic and India. In the same year, more than 44 thousand tons of papaya fruit were
9 exported from Brazil, which placed the country as the third-largest exporter of fruit in the
10 world, only after Guatemala and Mexico (FAO, 2019).

11 The main importers of Brazilian papaya, the United States and European countries,
12 demand high-quality fruits, but the papaya crop is susceptible to pathogens which affect
13 exportation-quality fruit yields. From 2007 to 2015 more than 5.4 million diseased plants
14 were eliminated in Brazilian fields (IDAF, 2015). Part of the losses can be attributed to
15 viral diseases, including papaya sticky disease (PSD), known to affect the yield and
16 quality of fruit in Brazil (VENTURA *et al.*, 2004), Mexico (PEREZ-BRITO *et al.*, 2012), and
17 Australia (PATHANIA *et al.*, 2019). So far, the only method for disease control consists
18 of rouging symptomatic plants (VENTURA *et al.*, 2004).

19 To discuss and advance on what we know about the disease, this thesis produced three
20 research manuscripts and two review manuscripts, and a patent deposited at the *Instituto*
21 *Nacional da Propriedade Intelectual* (INPI). The first manuscript summarized recent
22 papers published regarding PSD, including its etiology, epidemiology, and its interaction
23 with the *C. papaya* host at the molecular level, and is attached to the introduction section.
24 The second manuscript localizes PMeV complex RNA in papaya leaf tissues and uses
25 somatic embryogenesis as a non-laticifer tissue system to show that the PMeV complex
26 preferentially accumulates in laticifer cells. The third manuscript characterizes the PMeV
27 ORF1 by adding a new non-structural function of totiviruses coat protein which we
28 speculate to be relevant during virus-host interaction. The fourth article was originated
29 from the need to develop a technique for early diagnosis of PSD that would include the

30 recently discovered class 1 umbravirus-like associated RNA (ulaRNA) virus associated
31 with diseased plants. The last manuscript is a synthesis of the work carried out over the
32 last 30 years in an attempt to identify the PSD vector in Brazil, and the main findings in
33 other countries.

34

REFERENCES

- 35
36
37
38 FAO. Food Outlook - Biannual Report on Global Food Markets. Rome, p. 164. 2019.
- 39 IDAF, I. D. D. A. E. F. D. E. S. Controle do mamão no Espírito Santo é apresentado em
40 workshop sobre defesa vegetal. DOI: [https://idaf.es.gov.br/controle-do-mamao-no-](https://idaf.es.gov.br/controle-do-mamao-no-espírito-santo-e-apresen)
41 [espírito-santo-e-apresen](https://idaf.es.gov.br/controle-do-mamao-no-espírito-santo-e-apresen).
- 42 PATHANIA, N.; VALERIANA JUSTO; PABLITO MAGDALITA; FE DE LA CUEVA;
43 LORNA HERRADURA; AIRA WAJE; ADELFA LOBRES; ARCANGEL CUETO; NATALIE
44 DILLON; LYNTON VAWDREY; LOUISE HUCKS; DONNA CHAMBERS; GRACE SUN;
45 CHEESMAN, J. Integrated disease management strategies for the productive, profitable
46 and sustainable production of high quality papaya fruit in the southern Philippines and
47 Australia (FR2019-89). ACIAR. Australia: Australian Centre for International Agricultural
48 Research (ACIAR) 2019: 64 p. 2019.
- 49 PEREZ-BRITO, D.; TAPIA-TUSSELL, R.; CORTES-VELAZQUEZ, A.; QUIJANO-
50 RAMAYO, A.; NEXTICAPAN-GARCEZ, A.; MARTÍN-MEX, R. First report of papaya
51 meleira virus (PMeV) in Mexico. African Journal of Biotechnology, 11, p. 13564-13570,
52 2012.
- 53 VENTURA, J. A.; COSTA, H.; TATAGIBA, J. D. S. Papaya Diseases and Integrated
54 Control. In: NAQVI, S. A. M. H. (Ed.). Diseases of Fruits and Vegetables: Volume II:
55 Diagnosis and Management. Dordrecht: Springer Netherlands, 2004. p. 201-268.

56

57

58

59 This work will be presented in the format of a Scientific Article in five chapters. Thus, the
60 items: Methods, Conclusions, and References will be presented in the chapters,
61 according to the methods and references used in each chapter.

62

63

64 **MANUSCRIPT #1. BATTLE OF THREE: THE CURIOUS CASE OF PAPAYA**
65 **STICKY DISEASE**

66

67

68 Paper published in the *Plant Disease journal* (ISSN 0191-2917; IF 4.438, 2021; Qualis A2
69 Biotecnologia, 2013-2016). <https://doi.org/10.1094/PDIS-12-19-2622-FE>

70

71 **Battle of three: The curious case of papaya sticky disease**

72

73 Tathiana F. Sá-Antunes¹, **Marlonni Maurastoni**¹, L. Johana Madroñero^{1,2}, Gabriela
74 Fuentes³, Jorge M. Santamaria³, José Aires Ventura⁴, Emanuel F. Abreu⁵, A. Alberto R.
75 Fernandes¹ and Patricia M. B. Fernandes^{1*}

76

77 ¹Núcleo de Biotecnologia Universidade Federal do Espírito Santo, Av. Marechal
78 Campos 1468, Vitória, Espírito Santo 29040-090, Brazil;

79 ²Universidad El Bosque, Vicerrectoría de Investigaciones, Bogotá, Colombia

80 ³Centro de Investigación Científica de Yucatán, Calle 43 No. 130, Col. Chuburná de
81 Hidalgo, 97200 Mérida, Yucatán, Mexico;

82 ⁴Instituto Capixaba de Pesquisa, Assistência Técnica e Extensão Rural, Vitória
83 29050790, Espírito Santo, Brazil

84 ⁵Embrapa Recursos Genéticos e Biotecnologia, PqEB W5 Norte, Brasília, DF, 70770-
85 900, Brazil.

86 *Corresponding author: P. M. B. Fernandes; E-mail: patricia.fernandes@ufes.br

87

ABSTRACT

88
89
90
91 Among the most serious virus-incited diseases in papaya production is papaya sticky
92 disease (PSD). PSD concerns producers worldwide because the disease is extremely
93 aggressive. As no resistant cultivar is available, several management strategies have
94 been used in affected countries, such as selecting healthy seeds for planting, excluding
95 the pathogen, and roguing. In the 1990s, a dsRNA virus, papaya meleira virus (PMeV),
96 was identified in Brazil as the causal agent of PSD. However, in 2016 a second virus,
97 papaya meleira virus 2 (PMeV2), with an ssRNA genome, was also identified in PSD
98 plants. PMeV has been detected in asymptomatic plants, whereas all symptomatic plants
99 contain both viruses. Viral RNAs are packaged separately in particles formed by the
100 PMeV capsid protein. PSD also affects papaya plants in Mexico, Ecuador, and Australia.
101 PMeV2-like viruses have been identified in the affected plants, but the partner virus(es)
102 in these countries are still unknown. In Brazil, PMeV and PMeV2 reside in laticifers,
103 stimulating latex exudation that results in the affected papaya fruit's sticky appearance.
104 Genes modulated in plants affected by PSD include those involved in reactive oxygen
105 species and salicylic acid signaling, proteasomal degradation, and photosynthesis, which
106 are key components of plant defenses against the PMeV complex. However, complete
107 activation of the defense response is impaired by the expression of negative effectors
108 modulated by the virus. This review presents a summary of the current knowledge of the
109 *Carica papaya*-PMeV complex interaction and disease management strategies.

110
111 Keywords: papaya meleira virus, papaya meleira virus 2, virus-host interactions, pre-
112 flowering tolerance.

113

INTRODUCTION

114

115

116

117 World papaya production is concentrated in five countries (India, Brazil, Mexico,
118 Indonesia, and the Dominican Republic), with global estimates of over 13 million tons in
119 2018 (FAOSTAT 2018). Production in India, the leading producer, is mainly destined for
120 internal consumption. Brazil is the second-largest papaya producer, accounting for 1
121 million tons of world production (FAOSTAT 2018). Mexico plays a pivotal role as a key
122 supplier to the USA, which is the largest import market. Approximately 80% of papayas
123 in the USA originate from Mexico (FAO 2019). Although most of the papaya produced
124 worldwide is consumed in the domestic markets, high levels of fruit export provide a
125 significant source of income and employment year-round (FAO 2017).

126 Papaya diseases have diverse biotic and abiotic etiologies that affect the plant and fruit
127 quality, causing severe economic losses. In the world's leading papaya production
128 regions, the major diseases are caused by viruses. Although more than ten different virus
129 species have been reported in papaya worldwide (Table 1), only three present a threat to
130 papaya cultivation in Americas: *Papaya ringspot virus* (PRSV-P), *Papaya mosaic virus*
131 (PapMV), and the papaya meleira virus complex, comprised of papaya meleira virus
132 (PMeV) and papaya meleira virus 2 (PMeV2).

133 PRSV-P causes severe damage in the main papaya production areas of Brazil and
134 Mexico with crop losses of up to 85%. PRSV-P is mainly transmitted by aphid species in
135 a non-persistent manner (Wu et al. 2018). PapMV was first reported in 1962 in Florida,
136 USA, and has spread to Bolivia, Peru, Venezuela, and Mexico (Varun et al. 2017). PRSV-
137 P and PapMV mixed infections present a synergistic interaction that leads to increased
138 virus accumulation and symptoms (Chávez-Calvillo et al. 2016; García-Viera et al. 2018).

139 Papaya sticky disease (PSD), first reported as early as 1980 in Brazil, reached Mexico in
140 2008 (Perez-Brito et al. 2012) and Australia in 2019 (Pathania et al. 2019). In recent
141 years, research on the etiology of the disease (Abreu et al. 2015b; Antunes et al. 2016),
142 transmission (García-Cámara et al. 2018; García-Cámara et al. 2019; Tapia-Tussell et

143 al. 2015), and the plant-virus interaction (Abreu et al. 2014; Madroñero et al. 2018;
144 Soares et al. 2016) has led to significant advances in the understanding of the PSD
145 pathosystem. Here, we review the key developments in the literature, propose an
146 interaction map for the *Carica papaya*-PMeV complex, and summarize the current
147 management strategies for PSD.

148

149

150

151 **PAPAYA STICKY DISEASE: TWO VIRUSES, ONE DISEASE**

152

153

154 In the northeast region of Brazil, in the late 1980s, papaya began to exhibit an exudation
155 of fluid and aqueous latex (Nakagawa et al. 1987). This was credited to boron and calcium
156 deficiencies as the symptoms were similar to those observed on plants with these abiotic
157 stresses (Nakagawa et al. 1987). In 1989, epidemiological studies identified a biotic
158 pattern, which was confirmed by the appearance of disease in healthy plants inoculated
159 with latex from diseased plants (Rodrigues et al. 1989). The sticky appearance of infected
160 papaya fruits after oxidation of the latex by exposure to the air led to the name papaya
161 sticky disease (“*meleira*” in Portuguese) (Figure 1). In Brazil, PSD is currently distributed
162 in the northeastern states of Ceará, Rio Grande do Norte, Pernambuco, Bahia, and
163 Espírito Santo (Meissner Filho et al. 2017).

164 Transmission electron microscopy images showed isometric particles of approximately
165 42 nm in the laticifers of diseased plants (Kitajima et al. 1993) (Supplementary Fig. S1).
166 The purification of those particles from papaya latex and subsequent inoculation on
167 healthy papaya seedlings that later developed typical symptoms of PSD confirmed the
168 causal agent as a virus (Maciel-Zambolim et al. 2003).

169 Initially, experiments to identify the causal agents involved nucleic acid extraction of the
170 latex tapped from papaya plants with typical symptoms of PSD (Maciel-Zambolim et al.
171 2003; Rodrigues et al. 2005). Total RNA was analyzed by gel electrophoresis leading to

172 the visualization of two bands: a double-stranded RNA (dsRNA) band estimated to be
173 either ~10 kb (Kitajima et al. 1993) or ~12 kb (Maciel-Zambolim et al. 2003), designated
174 PMeV, and another then-unnoticed band of approximately 4.5 kb (Antunes et al. 2016).

175 PMeV dsRNA sequences were obtained from isolates from Espírito Santo (Antunes et al.
176 2016) and Rio Grande do Norte (Abreu et al. 2015a). Sequence alignment showed a high
177 similarity between the PMeV isolates and totiviruses. This family includes viruses with a
178 single-component dsRNA genome that infects fungi and protozoa and forms virions
179 (Fauquet and Fargette 2005). PMeV dsRNA contains two open reading frames (ORFs)
180 coding for a capsid protein (CP) and an RNA-dependent RNA polymerase (RdRp) (Figure
181 2A) (Abreu et al. 2015a; Antunes et al. 2016).

182 Initially regarded as a PMeV subgenomic RNA, the 4.5 kb RNA band is now recognized
183 as a genomic RNA from a second virus, PMeV2, associated with PMeV in infected plants
184 from Brazil. Sequence alignment showed a high similarity between PMeV2 and
185 umbraviruses (Antunes et al. 2016). Umbraviruses are single-stranded RNA (ssRNA)
186 viruses that do not encode a CP gene and, consequently, do not form conventional virus
187 particles. Genome encapsidation and transmission requires an auxiliary virus, typically a
188 polerovirus or an enamovirus. The hybrid virus particles, formed of the umbraviral RNA
189 and the helper virus CP, are transmitted by the helper virus vector (Taliensky and
190 Robinson 2003).

191 Antunes et al. (2016) showed, using degenerate primers targeting conserved domains of
192 the CP gene from members of the *Luteoviridae* family, that there were no recognized
193 poleroviruses, enamoviruses or luteoviruses in symptomatic papaya plants. Peptides
194 obtained by mass spectrometry from viral particles containing PMeV2 RNA matched with
195 the predicted amino acid sequence of PMeV ORF1. This indicates that hybrid virus
196 particles are formed from PMeV CP and PMeV2 ssRNA, supporting the idea that PMeV
197 is an auxiliary virus for PMeV2 (Antunes et al. 2016).

198 To the best of our knowledge, this is the first known case of an umbra-like virus associated
199 with a totivirus and an early example in plants of a viral CP encapsidating viral ssRNA
200 and dsRNA genomes (Figure 2B). A similar relationship was shown by Zhang et al. (2016)

201 in which the capsidless ssRNA mycovirus, yado-kari virus 1 (YkV1), using the CP of the
202 dsRNA mycovirus yado-nushi virus 1, forms hybrid particles encasing the YkV1 RdRp,
203 allowing replication as a dsRNA virus.

204 PMeV, but not PMeV2, can be detected in asymptomatic papaya plants, suggesting that
205 this virus alone cannot induce PSD symptoms (Antunes et al. 2016). This is similar to
206 persistent viruses, which induce little or no overt effects on their hosts and do not encode
207 a movement protein (Roossinck 2013). Although PMeV systemically infects papaya
208 plants, no PMeV movement protein was reported (Abreu et al. 2015a). PMeV localization
209 in laticifers and the increased latex exudation and fluidity during PSD (Kitajima et al. 1993)
210 could be used by the virus to move systemically throughout the plant. Another possibility
211 is that PMeV replicates in meristematic cells, allowing it to infect all plant tissues.

212 PMeV2 does not infect papaya on its own and all papaya plants displaying typical PSD
213 symptoms have a double infection by PMeV and PMeV2. The apparent requirement of
214 both PMeV and PMeV2 for PSD symptoms led to a reconsideration of the disease etiology
215 in Brazil (Antunes et al. 2016).

216 In Mexico, similar symptoms to those of PSD were observed in papaya cv. Maradol. Gel
217 electrophoresis of total RNA extracted from fruit latex also displayed two bands at
218 approximately 10 and 4.5 kb. The disease could also be transmitted through the latex of
219 infected papaya to healthy papaya plants (Perez-Brito et al. 2012). Together, these
220 findings indicated the same viral etiology for the Brazilian and Mexican diseases.

221 A cDNA library obtained from symptomatic plants identified an 1154 bp sequence,
222 partially covering the genome of the Mexican isolate (PMeV-Mx), showed high similarity
223 to an umbravirus found in Ecuador (papaya virus Q - PpVQ) (Quito-Avila et al. 2015) and
224 PMeV2, but no similarity to PMeV. Only one ORF with the characteristic domains of an
225 RdRp has been predicted for PpVQ, while both PMeV2 and PMeV-Mx have a putative
226 uncharacterized ORF upstream to their RdRp (Figure 2B). In addition, primers based on
227 the Mexican isolate sequence amplified fragments from both Brazilian and Mexican
228 symptomatic plants, and the amplicons had 100% nucleotide identity (Zamudio-Moreno
229 et al. 2015).

230 In 2019, PSD was officially reported for the first time in Queensland, Australia (Pathania
231 et al. 2019). Although virus particles were observed in Australian plants with PSD
232 symptoms, next-generation sequencing revealed only an umbra-like virus (PMeV2-Au)
233 (Campbell 2018). Currently, the auxiliary virus for the Mexican and Australian isolates is
234 unknown.

235

236

237

238 **PAPAYA AND PMeV COMPLEX INTERACTION**

239

240

241 During the interaction between viruses and plants, the virus hijacks host factors to
242 complete its infection cycle and the plant responds with a complex multilayered immune
243 defense. In PSD, the outcome of this interaction depends on the papaya's development
244 stage. Papaya is susceptible to the PMeV complex, but infected plants remain
245 asymptomatic for 6–8 months (Ventura et al. 2004). This phenomenon supports the idea
246 that a tolerance mechanism in pre-flowering plants allows the co-existence of plant and
247 virus without causing significant loss of vigor or fitness to their hosts (Madroñero et al.
248 2018). For this reason, several physiological, biochemical, structural, and molecular
249 aspects have been investigated to elucidate the interaction between the PMeV complex
250 and pre- and post-flowering papaya. We present a schematic view of this interaction in
251 Figure 3.

252

253

254

255 **PMeV complex effect on the laticifers**

256

257

258 Alteration in the physical and chemical properties, and spontaneous exudation of papaya
259 latex during PSD, suggested that the PMeV complex viruses could be directly involved in

260 PSD symptoms (Rodrigues et al. 2009). Papaya proteases are usually activated during
261 latex exudation and contribute to latex viscosity, the clotting process, and antiviral
262 defense (Rodrigues et al. 2009). In PSD-affected plants, the reduction of protease levels
263 and activity seems to have an inhibitory effect on latex coagulation, thus increasing its
264 fluidity which could facilitate its flow through laticifers and allow virus spread within the
265 plant (Rodrigues et al. 2012). Additionally, the accumulation of H₂O₂, a systemic response
266 elicitor (Rodrigues et al. 2009), could play a negative regulatory role in cysteine-protease
267 activity, possibly by oxidizing and inactivating the active site of the enzyme. The negative
268 modulation of papaya latex cysteine proteases could also be a viral strategy to delay the
269 progression of programmed cell death (PCD) in laticifers (Solomon et al. 1999) and
270 minimize virus particle degradation.

271

272

273

274 **PMeV complex effect on the proteasome**

275

276

277 The PMeV complex also has a role in other papaya tissues, including necrotic lesions on
278 the leaf tip (Ventura et al. 2004). The global protein expression profile of PSD leaf tissues
279 showed an accumulation of calreticulin, proteasome-related proteins such as 20S
280 proteasome b subunit, and stress-response proteins such as pathogenesis-related (PR)
281 proteins, endochitinase and PR-4, while proteins related to metabolism are down-
282 regulated (Rodrigues et al. 2012), demonstrating a major investment in plant defense (El
283 Moussaoui et al. 2001).

284 The involvement of the ubiquitin/26S proteasome system (UPS) in the signaling and
285 regulation of plant–pathogen interactions has been described in several studies (Sorel et
286 al. 2018). The UPS machinery contributes to antiviral immunity by degrading viral
287 effectors but viruses can usurp the UPS machinery to target proteins that inhibit viral
288 infection to the degradation pathway (Verchot 2016). The accumulation of proteasome-
289 related proteins in PSD symptomatic papaya plants supports the idea that defense host

290 proteins, which are essential for the plant response against viral infection, are targeted
291 for degradation (Rodrigues et al. 2011).

292 During PMeV complex infection, the levels of several microRNAs (miRNAs) involved in
293 the modulation of genes related to the UPS system are reduced. This indicates that PMeV
294 coopts the UPS system for its benefit, promoting virus replication, movement, and a rapid
295 turnover of viral proteins. For example, structural proteins, generally produced in large
296 amount in a short time, are not able to fold correctly leading to the formation of misfolded
297 proteins which are targeted for degradation (Alcaide-Loridan and Jupin 2012). Thus, we
298 suggest that the rapid turnover of viral proteins can favor viral infection since it maintains
299 an ideal cellular environment for plant and virus coexistence (Abreu et al. 2014; Verchot
300 2016).

301 In another study, the global protein profile of field-grown PMeV-infected pre-flowering *C.*
302 *papaya* plants exhibited low levels of 26S proteasome-related proteins (Soares et al.
303 2016), an opposite pattern to that previously observed for symptomatic plants (Rodrigues
304 et al. 2011). Lower activity of the 20S and 19S proteasome increases the levels of
305 polyubiquitinated proteins that result in increased PCD, which could successfully contain
306 a virus infection (Rodrigues et al. 2011). However, the full spectrum of anti-viral defenses
307 involves the activity of caspase-like serine proteases (Citovsky et al. 2009; Rodrigues et
308 al. 2011), such as subtilase 1.3, whose levels are reduced in PMeV-infected pre-flowering
309 *C. papaya* tissues.

310

311

312

313 **PMeV complex effect on redox balance and defense gene expression**

314

315

316 Photosynthesis light-dependent reactions are important in plant responses against
317 viruses and disturbances in this process favor viral accumulation (Soares et al. 2016). A
318 higher electron flow ratio induced by the accumulation of photosynthesis-related proteins

319 in pre-flowering infected papaya (Soares et al. 2016) promotes a cascade of events in
320 chloroplasts leading to reactive oxygen species (ROS) production. Low ROS levels
321 induce antioxidant enzymes; however, when the ROS levels reach a certain threshold, a
322 signal transduction pathway is activated that eventually leads to PCD (Solomon et al.
323 1999). ROS-related metabolic changes occur in *C. papaya*-PMeV complex interactions,
324 including an increase in H₂O₂ production in the laticifers (Rodrigues et al. 2009).
325 Moreover, pre-flowering *C. papaya* leaves treated with nitric oxide (NO) show an
326 accumulation of compounds used for defense and an increased activity of detoxification
327 enzymes (Buss et al. 2011). Supporting these data, several genes coding for ROS-
328 detoxifying enzymes in PMeV complex-infected plants are up-regulated at pre-flowering
329 (Madroño et al. 2018). Although defense mechanisms such as ROS-signaling features
330 are present at an early stage of infection, this is not enough to mediate resistance.

331 ROS have signaling effects in the chloroplast itself and other parts of the cell, often
332 involving hormonal cross-talk that regulates the activation of defenses in plants,
333 especially salicylic acid (SA) (Xia et al. 2015). At pre-flowering, *PR1*, *PR2*, *PR5*, and other
334 genes involved in SA signaling are up-regulated. Moreover, the exogenous application of
335 SA on pre-flowering plants before virus inoculation results in a trend of diminished viral
336 load (Madroño et al. 2018). These insights indicate the existence of defense
337 mechanisms at pre-flowering, which could hamper the development of PSD symptoms.
338 However, other genes known for their antagonistic roles in SA signaling, such as genes
339 involved in ethylene metabolism and the NPR1-inhibitor, are also up-regulated, which
340 could prevent full-scale and durable resistance. At post-flowering, the *PR1* gene is down-
341 regulated and negative modulators of SA signaling are up-regulated (Madroño et al.
342 2018). Together, the development of symptoms during post-flowering implies an
343 incomplete activation of defense response mechanisms upon PMeV complex infection.

344

345

346

347 **PMeV complex effect on cell wall structure**

348

349
350 Spread of the PMeV complex could also be facilitated by changes in structure and
351 composition of the papaya cell wall during the switch to the flowering stage. At pre-
352 flowering, infected plants show modulation of transcripts coding for cell wall remodeling
353 and structural proteins that may be part of the papaya response to hamper PMeV complex
354 traffic (Madroñero et al. 2018; Soares et al. 2016). At post-flowering, in contrast, cell wall
355 genes are induced in infected plants, which indicates that the PMeV complex could be
356 inducing cell wall turnover at the plasmodesmata site to promote systemic viral infection.
357 Analysis of the topography and mechanical properties of papaya leaves infected by PSD
358 show that their midribs are fragile and susceptible to breakage (Magaña-Álvarez et al.
359 2016), which suggests a weakening in the cell walls of leaf tissues that could extend to
360 laticifers. Cell rupture and latex exudation, the main symptoms in PSD plants, could be
361 explained by cell wall turnover associated with increased water content and internal
362 pressure.

363
364
365

366 **EPIDEMIOLOGY**

367
368
369 The epidemiological behavior of PSD has been extensively studied (Abreu et al. 2015a;
370 Rodrigues et al. 1989; Tapia-Tussell et al. 2015; Ventura et al. 2003). Environmental
371 factors and agricultural practices have been the main factors responsible for the disease
372 progression and appearance of symptoms in the field, which may vary according to the
373 source of virus inoculum—seed, alternative hosts, or vectors—and papaya variety.

374 Until 2012 most studies on PSD were based on virus detection through the visualization
375 of the viral dsRNA band in agarose gel electrophoresis. The sequencing of both PMeV
376 and PMeV2 (Antunes et al. 2016) allowed the development of more sensitive techniques
377 such as RT-PCR (Abreu et al. 2012; Antunes et al. 2016; Maurastoni et al. 2020) and

378 qRT-PCR (Abreu et al. 2012), which have been applied to understand key aspects of
379 PSD epidemiology.

380 Observations of PSD dispersal patterns in orchards pointed to insects as PMeV complex
381 vectors. In a study conducted in Brazil, after exposure to whiteflies (*Bemisia tabaci* type
382 B) that fed on infected plants, asymptomatic papaya plants developed PSD symptoms
383 and PMeV dsRNA was detected. However, the virus was not detected in these whiteflies,
384 which are not a papaya pest (Vidal et al. 2003). Several whiteflies can transmit viruses in
385 a non-propagative manner in which viruses are not internalized inside the insect cells.
386 Viral retention time in the insect's body depends on the virus half-life and viral load is
387 often low (Whitfield et al. 2015). Therefore, the absence of PMeV dsRNA in *B. tabaci* type
388 B does not exclude an ability to transmit the PMeV complex.

389 A whitefly commonly found in papaya orchards and considered a pest to Brazilian papaya
390 is *Trialeurodes variabilis*. This whitefly appears unable to transmit viral dsRNA from
391 inoculated plants to healthy plants (Rodrigues et al. 2009). The dsRNA was detected in
392 adults and nymphs but not in latex collected from plants 20 days after being exposed to
393 the viruliferous whiteflies. However, the ability of *T. variabilis* to vector the PMeV complex
394 cannot be ruled out, as the time required for dsRNA visualization may be longer than that
395 analyzed.

396 Recently, leafhoppers (Hemiptera,: Cicadellidae) were proposed as a potential PMeV
397 complex insect vector in Brazil as their distribution in the crop is correlated with the
398 distribution of the disease (Gouvea et al. 2018). In Mexico, *Empoasca papayae* Oman
399 (Hemiptera: Cicadellidae) adults, but not nymphs, have been shown to transmit PMeV-
400 Mx to *C. papaya* cv. Maradol. These leafhoppers can acquire the virus after 6 hours
401 exposure to infected plants and viral titer increases with longer exposure time (up to 5
402 days). Little is known about the biology of *E. papayae* and research is now focused on
403 understanding the behavior of this insect in the field (García-Cámara et al. 2019). In
404 Brazil, transmission experiments to study leafhoppers' ability to vector PMeV complex are
405 necessary to implement adequate management strategies.

406 Identification of alternative hosts for the PMeV complex is also essential for the
407 development of control strategies. In Brazil, several plants were tested for their
408 susceptibility to PMeV infection, but the dsRNA was detected only in *Brachiaria*
409 *decumbens* (*Poaceae*) (Maciel-Zambolim et al. 2003), which is commonly found close to
410 papaya plantations. In Mexico, intercropping between watermelon (*Citrullus lanatus*
411 Thunb.) and papaya led to the hypothesis that watermelon could be an alternative host
412 for PMeV-Mx. Indeed, PMeV-Mx can replicate in watermelon seedlings and, more
413 surprisingly, induce necrotic lesions on the leaf tip, a typical PSD symptom (García-
414 Cámara et al. 2018). The alternative hosts proposed by Maciel-Zambolim et al. (2003)
415 need to be revisited using more sensitive techniques, with additional detection for PMeV2.
416 *B. decumbens* and *C. lanatus* Thunb. also need to be assessed as viral reservoirs.

417 Understanding PSD etiology, dynamics of viral populations, and transmission are
418 imperative for integrated management of papaya production. Since PSD symptoms
419 appear only after flowering, an infected asymptomatic plant may remain an undetected
420 virus source for months before being eradicated. Thus, developing an efficient strategy
421 for virus control remains a challenge.

422

423

424

425 **MANAGEMENT OF PAPAYA VIRUS DISEASES**

426

427

428 The papaya crop has experienced significant improvements through the use of innovative
429 technologies (Costa et al. 2019). However, there are significant challenges, necessitating
430 quality- and genetically-certified seeds and cultivars, and most of all, resistance to major
431 crop diseases (Ventura et al. 2019). Several strategies have been recommended for
432 papaya virus control. The major control strategies applicable to all papaya viruses are the
433 following:

434

435

436 **1. Use of healthy seeds and exclusion of the pathogens by seedling/crop**
437 **certification.**

438

439

440 PSD has been reported as a seed-borne disease in Mexico and Australia, and the use of
441 healthy seeds in new plantations has been recommended (Tapia-Tussell et al. 2015). The
442 Australian government initiated a program to produce clean seeds (Campbell 2019b)
443 using embryo rescue and tissue culture, which was able to produce 98% PMeV2-free
444 plants (Campbell 2019a).

445 A seed transmission route has not yet been confirmed for the PMeV complex in Brazil.
446 However, measures have been adopted by Brazilian farmers to mitigate the possible
447 dispersion of PSD and other viral diseases: (i) the use of certified seedlings in the
448 establishment of new orchards; (ii) the use of seeds from plants that have been grown
449 under conditions that will prevent infection; (iii) the establishment of nurseries and
450 orchards as far as possible from other orchards especially if viral diseases had been
451 reported in the region; and (iv) exclusion of the pathogens by crop quarantine.

452

453

454

455 **2. Control of pathogen by eradication (roguing) of infected plants.**

456

457

458 Viruses can spread both within and between orchards. Growers and field workers must
459 learn to identify the early symptoms of viral diseases. The best way to manage the virus
460 is the prompt identification and immediate destruction of diseased trees, as delays enable

461 the virus to spread to additional trees (Ventura et al. 2003). Additionally, the possibility of
462 virus spread from asymptomatic papaya implies a need for additional disease
463 management strategies such as early detection of the PMeV complex (Maurastoni et al.
464 2020).

465 In Brazil, roguing of papaya is governed by Normative Instruction number 17, May 27th,
466 2010. Weekly inspections are performed throughout the crop, and plants with PSD
467 symptoms are removed (Figure 4A) (Ventura et al. 2004). From 2011 to 2014 more than
468 4.9 million plants were eradicated in the largest papaya exporting state in Brazil,
469 preventing the spread of various diseases to healthy orchards (Figure 4) (Fernandes et
470 al. 2018).

471

472

473 **3. Control of pathogen vectors.**

474

475

476

477 Several viral pathogens of papaya have insect vectors and their control plays an important
478 role in the management of papaya diseases. Efficacy of insecticide application is
479 determined by the manner of transmission, vector population dynamics, and vector host
480 range (Perring et al. 1999). In non-circulative transmitted viruses such as PRSV-P, the
481 use of insecticides results only in reduction of the populations of potential vectors, without
482 preventing the transmission. While the insect which vectors PSD-associated viruses is
483 still unknown in Brazil, Mexico, and Australia, measures used to control the PRSV-P
484 vectors have also been adopted for PSD control. An insecticide control strategy can be
485 enhanced by using additional control measures, such as the elimination of weeds before
486 the major peak of aphid flights, which could prevent the vector from acquiring virus from
487 reservoir plants, disrupting the virus cycling.

488

489

490

491 4. Selection of tolerant and/or resistant cultivars.

492

493

494 The development of resistant papaya cultivars has been recognized as the most effective
495 strategy for virus control. Since *C. papaya* cultivars are susceptible to several viruses,
496 breeders have been seeking sources of resistance in other species within the family
497 *Caricaceae*. Resistance to PRSV-P has been found in the genus *Vasconcellea* but its use
498 in conventional breeding has been hampered by sexual incompatibility between species
499 (Haireen and Drew 2014; Lin et al. 2019). No resistance to the PMeV complex has yet
500 been found in thirty *C. papaya* genotypes or in non-cultivated plants (Meissner Filho et al.
501 2017).

502 Expression of pathogen-derived genes can interfere with the virus cycle in the host plants,
503 inhibiting viral infection. So far, PRSV-resistant transgenic papaya have been developed
504 based on a sequence homology-dependent strategy (Azad et al. 2014; Jia et al. 2017)
505 which requires knowledge of virus diversity for its success. Transgenic resistance to
506 PRSV-P has already been broken due to the emergence of divergent virus strains (Jia et
507 al. 2017). To date, two PMeV isolates have been identified in Brazil (Abreu et al. 2015a;
508 Antunes et al. 2016). Although their CPs share 75% similarity, studies with more isolates
509 are required to understand PMeV diversity so that unlike PRSV, the PMeV complex will
510 not overcome transgenic resistance.

511

512

513

514 5. Control of alternative hosts.

515

516

517 The possibility of papaya virus spread from alternative hosts necessitates management
518 strategies for weed control (Alcalá-Briseño et al. 2020). Pathogen emergence results from
519 interactions between susceptible hosts and pathogenic viruses in conducive

520 environments, causing disease outbreaks in new geographic regions or hosts (Alcalá-
521 Briseño et al. 2020). In addition to the removal of weeds that grow close to papaya plants,
522 special attention should be given to plants that are confirmed as a reservoir for the PMeV
523 complex in Brazil and Mexico.

524
525
526

527 **6. Cleaning harvesting tools.**

528
529

530 Spatial distribution of the PMeV complex was studied in experimental plots over a year,
531 and a high percentage of infected plants (~78%) per row during and after the harvest
532 pointed to mechanical transmission (Abreu et al. 2015b; Ventura et al. 2003). This implies
533 that agricultural practices, including fruit thinning, may also be responsible for the spread
534 of PSD within orchards.

535 In orchards where appropriate agricultural practices were not carried out, the disease
536 spread to the whole crop and led to total yield loss. In contrast, in orchards that strictly
537 followed these principles including a weekly plant eradication based on the presence of
538 initial PSD symptoms, the incidence of eradicated plants was less than 5% during the
539 crop cycle (Ventura et al. 2004; Ventura et al. 2019).

540
541
542

543 **CLOSING REMARKS AND FUTURE PROSPECTS**

544
545

546 Over the last decade, much has been learned about PSD including details of the etiology,
547 epidemiology, defense mechanisms of papaya against the PMeV complex, and disease

548 management strategies. In the 1990s, the causal agent of PSD was identified as a dsRNA
549 virus, PMeV, but in 2016 a second virus, PMeV2, with an ssRNA genome, was also
550 discovered in PSD plants. All PSD symptomatic papaya plants are infected by both
551 viruses; however, asymptomatic plants analyzed in Brazil were positive only for PMeV.
552 Thus, evidence suggests that contrary to what was originally believed, PMeV is not the
553 etiological agent of PSD. Interestingly, in countries other than Brazil where PSD has been
554 reported, only the umbra-like virus has been identified. Thus, it is possible that a different
555 helper virus may be identified in these countries.

556 An intriguing question has been why infected plants remain asymptomatic until flowering.
557 Proteomic and transcriptomic data have increased our understanding of the interaction
558 between papaya and the PMeV complex. The infected papaya plant mounts an anti-viral
559 defense mechanism during pre-flowering, when several genes related to the SA pathway
560 and other defense pathways are highly expressed. After flowering, however, increased
561 expression of genes that negatively regulate SA production leads to depression in
562 defense responses.

563 The susceptibility of papaya plants to viruses results in economic and environmental
564 impact as it increases the use of agrochemical products and water resources, without
565 achieving the predicted crop yield. PSD may affect 20% of the plants during the economic
566 cycle of the crop in orchards where roguing is performed, but it affects up to 100% of the
567 plants where phytosanitary protocols are not implemented, causing a total yield loss
568 (Abreu et al. 2015a).

569 The development of papaya plants resistant to viruses is urgently needed. Plants
570 challenged by viral RNA initiate defense responses based upon RNA silencing, and this
571 strategy was used to develop virus-resistant crops (Lindbo and Falk 2017). Resistance to
572 infection against a range of individual viruses has been engineered into several plant
573 species. Because of the durability and success of transgenic papaya cultivars in Hawaii
574 (USA), similar transgenic papaya plants have been engineered in other countries.
575 Resistance, however, was inconsistent for many reasons, such as the emergence of

576 recombinant strains, increased strength of viral silencing suppressors, and unfavorable
577 environmental conditions.

578 Brazilian researchers have been working on the development of resistant papaya to
579 combat PSD. Until 2016, PSD was associated only with PMeV, and all efforts to obtain a
580 resistant plant considered only this virus. Now, groups working towards this goal must
581 consider both viruses, as well as the defense mechanisms activated in papaya-
582 PMeV/PMeV2 interactions reviewed in the present paper, if a breeding program to
583 develop a PSD resistant papaya plant is to succeed.

584

585

586

587 **ACKNOWLEDGEMENTS**

588

589

590 **Author Contributions:** All the authors have equal contribution. All authors read and
591 approved the manuscript.

592 **Acknowledgments:** Tathiana F. Sá Antunes and L. Johana Madronero would like to
593 thank the Coordenação de Aperfeiçoamento de Pessoal de Nível Superior, CAPES
594 (Ministry of Education of Brazil), and Marlonni Maurastoni thanks the Fundação de
595 Amparo à Pesquisa do Espírito Santo, FAPES for their fellowship. P.M.B. Fernandes and
596 J.A. Ventura acknowledge the Conselho Nacional de Desenvolvimento Científico e
597 Tecnológico, CNPq for their research productivity award (grants # 303432/2018-7 and #
598 308631/2016-1). This work was supported by the Fundação de Amparo à Pesquisa do
599 Estado do Espírito Santo (FAPES) grants # 76437906/16 and # 80598609/17. Thanks
600 are due to Dr. Raul Tapia for providing the papaya Maradol picture presented in Fig.1.

601 **Conflicts of Interest:** The authors declare that they have no conflict of interest.

602

603 **REFERENCES**

- 604
- 605
- 606 Abreu, E. F. M., Daltro, C. B., Nogueira, E. O., Andrade, E. C., and Aragão, F. J. 2015a.
607 Sequence and genome organization of papaya meleira virus infecting papaya in Brazil.
608 Arch. Virol. 160:3143-3147.
- 609 Abreu, P., Antunes, T., Magaña-Álvarez, A., Pérez-Brito, D., Tapia-Tussell, R., Ventura,
610 J., Fernandes, A., and Fernandes, P. 2015b. A current overview of the Papaya meleira
611 virus, an unusual plant virus. Viruses 7:1853-1870.
- 612 Abreu, P. M. V., Piccin, J. G., Rodrigues, S. P., Buss, D. S., Ventura, J. A., and
613 Fernandes, P. M. B. 2012. Molecular diagnosis of Papaya meleira virus (PMeV) from leaf
614 samples of *Carica papaya* L. using conventional and real-time RT-PCR. J. Virol. Methods
615 180:11-17.
- 616 Abreu, P. M. V., Gaspar, C. G., Buss, D. S., Ventura, J. A., Ferreira, P. C. G., and
617 Fernandes, P. M. B. 2014. *Carica papaya* microRNAs are responsive to Papaya meleira
618 virus infection. PLoS One 9.
- 619 Alcaide-Loridan, C., and Jupin, I. 2012. Ubiquitin and Plant Viruses, Let's Play Together!
620 Plant Physiol. 160:72-82.
- 621 Alcalá-Briseño, R. I., Casarrubias-Castillo, K., López-Ley, D., Garrett, K. A., and Silva-
622 Rosales, L. 2020. Network Analysis of the Papaya Orchard Virome from Two
623 Agroecological Regions of Chiapas, Mexico. mSystems 5:e00423-00419.
- 624 Antunes, T. F. S., Amaral, R. J. V., Ventura, J. A., Godinho, M. T., Amaral, J. G., Souza,
625 F. O., Zerbini, P. A., Zerbini, F. M., and Fernandes, P. M. B. 2016. The dsRNA Virus
626 Papaya Meleira Virus and an ssRNA Virus are Associated with Papaya Sticky Disease.
627 PloS One 11:e0155240.
- 628 Azad, M. A. K., Amin, L., and Sidik, N. M. 2014. Gene Technology for Papaya Ringspot
629 Virus Disease Management. Sci. World. J. 2014:768038.
- 630 Bau, H.-J., Kung, Y.-J., Raja, J., Chan, S.-J., Chen, K.-C., Chen, Y.-K., Wu, H.-W., and
631 Yeh, S.-D. 2008. Potential threat of a new pathotype of *Papaya leaf distortion mosaic*
632 *virus* infecting transgenic papaya resistant to *Papaya ringspot virus*. Phytopathology
633 98:848-856.
- 634 Buss, D. S., Dias, G. B., Santos, M. P., Ventura, J. A., and Fernandes, P. M. B. 2011.
635 Oxidative Stress Defence Response of *Carica papaya* Challenged by Nitric Oxide,
636 Papaya meleira virus and *Saccharomyces cerevisiae*. Open Nitric Oxide J. 3:55-64.
- 637 Campbell, P. 2018. Papaya Press. Page 1 in: New test to offer early detection of Papaya
638 Sticky Disease G. Kath, ed., Australia.

- 639 Campbell, P. 2019a. Papaya Press. Page 1 in: Papaya clean seed update G. Kath, ed.,
640 Australia.
- 641 Campbell, P. 2019b. Papaya Press. Page 1 in: Papaya Clean Seed Program Underway,
642 G. Kath, ed., Australia.
- 643 Chávez-Calvillo, G., Contreras-Paredes, C. A., Mora-Macias, J., Noa-Carrazana, J. C.,
644 Serrano-Rubio, A. A., Dinkova, T. D., Carrillo-Tripp, M., and Silva-Rosales, L. 2016.
645 Antagonism or synergism between papaya ringspot virus and papaya mosaic virus in
646 *Carica papaya* is determined by their order of infection. *Virology* 489:179-191.
- 647 Citovsky, V., Zaltsman, A., Kozlovsky, S. V., Gafni, Y., and Krichevsky, A. 2009.
648 Proteasomal degradation in plant-pathogen interactions. *Semin. Cell Dev. Biol.* 20:1048-
649 1054.
- 650 Costa, A. d. F. S. d., Abreu, E. F. M., Schimdt, E. R., Costa, A. N. d., and Schimdt, O.
651 2019. Advances observed in papaya tree propagation. *Rev. Bras. Frutic.* 41.
- 652 El Moussaoui, A., Nijs, M., Paul, C., Wintjens, R., Vincentelli, J., Azarkan, M., and Looze,
653 Y. 2001. Revisiting the enzymes stored in the laticifers of *Carica papaya* in the context of
654 their possible participation in the plant defence mechanism. *Cell. Mol. Life Sci.* 58:556-
655 570.
- 656 FAO. 2017. Food Outlook - Biannual Report on Global Food Markets. Rome.
- 657 FAO. 2019. Food Outlook - Biannual Report on Global Food Markets. Page 164, Rome.
- 658 FAOSTAT. 2014. Food and Agriculture Organization of the United Nations. FAO, Rome,
659 Italy.
- 660 Fauquet, C., and Fargette, D. 2005. International Committee on Taxonomy of Viruses
661 and the 3,142 unassigned species. *Viol. J.* 2:64.
- 662 Fernandes, P. M. B., Fernandes, A. A. R., Ventura, J. A., Antunes, T. F. S., Quadros, O.
663 F., Madroñero, J., Carminati, L. S., and Maurastoni, M. 2018. Um novo complexo viral: o
664 caso da meleira do mamoeiro. in: VII Simpósio do Papaya Brasileiro. Produção e
665 Sustentabilidade, Vitória-Espírito Santo, Brazil.
- 666 García-Cámara, I., Pérez-Brito, D., Moreno-Valenzuela, O., Magaña-Álvarez, A.,
667 Fernandes, P. M. B., and Tapia-Tussell, R. 2018. Molecular and experimental evidence
668 of Watermelon (*Citrullus lanatus*) as host of the Mexican variant of Papaya meleira virus.
669 *Eur. J. Plant Pathol.* 151:117-123.
- 670 García-Cámara, I., Tapia-Tussell, R., Magaña-Álvarez, A., Cortés Velázquez, A., Martín-
671 Mex, R., Moreno-Valenzuela, O., and Pérez-Brito, D. 2019. *Empoasca papayae*
672 (Hemiptera: Cicadellidae)-Mediated Transmission of Papaya Meleira Virus-Mexican
673 Variant in Mexico. *Plant Dis.* 103:2015-2023.

- 674 García-Viera, M., Sánchez-Segura, L., Chavez-Calvillo, G., Jarquín-Rosales, D., and
675 Silva-Rosales, L. 2018. Changes in leaf tissue of *Carica papaya* during single and mixed
676 infections with *Papaya ringspot virus* and *Papaya mosaic virus*. *Biol. Plant.* 62:173-180.
- 677 Gouvea, R., da Vitória, R., Rosa, R., Alves, W. d. S., Giuriatto, N., Calatroni, D., Fanton,
678 C., Martins, D. d. S., and Queiroz, R. 2018. Flutuação populacional de cigarrinhas
679 (Hemiptera: cicadellidae) e ocorrência do vírus da meleira do mamoeiro. in: VII Simpósio
680 do Papaya Brasileiro. Produção e Sustentabilidade, Vitória-Espírito Santo, Brazil.
- 681 Haireen, M. R. R., and Drew, R. A. 2014. Isolation and Characterisation of PRSV-P
682 Resistance Genes in *Carica* and *Vasconcellea*. *Int. J. Genomics* 2014:145403-145403.
- 683 Jia, R., Zhao, H., Huang, J., Kong, H., Zhang, Y., Guo, J., Huang, Q., Guo, Y., Wei, Q.,
684 Zuo, J., Zhu, Y. J., Peng, M., and Guo, A. 2017. Use of RNAi technology to develop a
685 PRSV-resistant transgenic papaya. *Sci. Rep.* 7:12636.
- 686 Kitajima, E. W., Rodrigues, C. H., Silveira, J. S., and Alves, F. 1993. Association of
687 isometric viruslike particles, restricted to lacticifers, with "meleira" (sticky disease) of
688 papaya (*Carica papaya*). *Fitopatol. Bras.* 18:118.
- 689 Lin, Q., Singh, R., and Yu, Q. 2019. Isolation and characterization of translation initiation
690 factor 4E in *Carica papaya* and *Vasconcellea* species. Pages 39-44 International Society
691 for Horticultural Science (ISHS), Leuven, Belgium.
- 692 Lindbo, J. A., and Falk, B. W. 2017. The Impact of "Coat Protein-Mediated Virus
693 Resistance" in Applied Plant Pathology and Basic Research. *Phytopathology* 107:624-
694 634.
- 695 Maciel-Zambolim, E., Kunieda-Alonso, S., Matsuoka, K., De Carvalho, M., and Zerbini, F.
696 2003. Purification and some properties of Papaya meleira virus, a novel virus infecting
697 papayas in Brazil. *Plant Pathol.* 52:389-394.
- 698 Madroñero, J., Rodrigues, S. P., Antunes, T. F. S., Abreu, P. M. V., Ventura, J. A.,
699 Fernandes, A. A. R., and Fernandes, P. M. B. 2018. Transcriptome analysis provides
700 insights into the delayed sticky disease symptoms in *Carica papaya*. *Plant Cell Rep.*
701 37:967-980.
- 702 Magaña-Álvarez, A., Vencioneck Dutra, J. C., Carneiro, T., Pérez-Brito, D., Tapia-Tussell,
703 R., Ventura, J. A., Higuera-Ciapara, I., Fernandes, P. M. B., and Fernandes, A. A. R.
704 2016. Physical Characteristics of the Leaves and Latex of Papaya Plants Infected with
705 the Papaya meleira virus. *Int. J. Mol. Sci.* 17:574.
- 706 Maurastoni, M., Sá-Antunes, T. F., Oliveira, S. A., Santos, A. M. C., Ventura, J. A., and
707 Fernandes, P. M. B. 2020. A multiplex RT-PCR method to detect papaya meleira virus
708 complex in adult pre-flowering plants. *Arch. Virol.* 165:1211-1214.
- 709 Meissner Filho, P., Lima Neto, F., de Oliveira, C., Santana, S., and Dantas, J. 2017.
710 Avaliação da resistência de genótipos de mamoeiro ao vírus da meleira no Semiárido.
711 Report No. 1809-5003. Page 21. Embrapa Mandioca e Fruticultura, Cruz das Almas, BA.

- 712 Nakagawa, J., Takayama, Y., and Suzukama, Y. 1987. Exudação de látex pelo
713 mamoeiro. Estudo de ocorrência em Teixeira de Freitas, BA. Pages 555-559 in:
714 Congresso Brasileiro de Fruticultura.
- 715 Pathania, N., Valeriana Justo, Pablito Magdalita, Fe de la Cueva, Lorna Herradura, Aira
716 Waje, Adelfa Lobres, Arcangel Cueto, Natalie Dillon, Lynton Vawdrey, Louise Hucks,
717 Donna Chambers, Grace Sun, and Cheesman, J. 2019. Integrated disease management
718 strategies for the productive, profitable and sustainable production of high quality papaya
719 fruit in the southern Philippines and Australia (FR2019-89). Page 64, ACIAR, ed.
720 Australian Centre for International Agricultural Research (ACIAR) 2019, Australia.
- 721 Perez-Brito, D., Tapia-Tussell, R., Cortes-Velazquez, A., Quijano-Ramayo, A.,
722 Nexticapan-Garcez, A., and Martín-Mex, R. 2012. First report of papaya meleira virus
723 (PMeV) in Mexico. *Afr. J. Biotechnol.* 11:13564-13570.
- 724 Perring, T. M., Gruenhagen, N. M., and Farrar, C. A. 1999. Management of plant viral
725 diseases through chemical control of insect vectors. *Annu. Rev. Entomol.* 44:457-481.
- 726 Quito-Avila, D. F., Alvarez, R. A., Ibarra, M. A., and Martin, R. R. 2015. Detection and
727 partial genome sequence of a new umbra-like virus of papaya discovered in Ecuador.
728 *Eur. J. Plant Pathol.* 143:199-204.
- 729 Rodrigues, C., Ventura, J., and Maffia, L. 1989. Distribuição e transmissão da meleira em
730 pomares de mamão no Espírito Santo. *Fitopatol. Bras.* 14:118.
- 731 Rodrigues, S., Andrade, J., Ventura, J., Lindsey, G., and Fernandes, P. 2009. Papaya
732 meleira virus is neither transmitted by infection at wound sites nor by the whitefly
733 *Trialeurodes variabilis*. *J. Plant Pathol.* 91:87-91.
- 734 Rodrigues, S. P., Galvao, O. P., Andrade, J. S., Ventura, J. A., and Fernandes, P. M. B.
735 2005. Simplified molecular method for the diagnosis of Papaya meleira virus in papaya
736 latex and tissues. *Summa Phytopathol* 31:281-283.
- 737 Rodrigues, S. P., Ventura, J. A., Aguilar, C., Nakayasu, E. S., Almeida, I. C., Fernandes,
738 P., and Zingali, R. B. 2011. Proteomic analysis of papaya (*Carica papaya* L.) displaying
739 typical sticky disease symptoms. *Proteomics* 11:2592-2602.
- 740 Rodrigues, S. P., Ventura, J. A., Aguilar, C., Nakayasu, E. S., Choi, H., Sobreira, T. J. P.,
741 Nohara, L. L., Wermelinger, L. S., Almeida, I. C., Zingali, R. B., and Fernandes, P. M. B.
742 2012. Label-free quantitative proteomics reveals differentially regulated proteins in the
743 latex of sticky diseased *Carica papaya* L. plants. *J. Proteomics* 75:3191-3198.
- 744 Roossinck, M. J. 2013. Plant virus ecology. *PLoS Pathog* 9:e1003304.
- 745 Soares, E., Werth, E. G., Madroñero, L. J., Ventura, J. A., Rodrigues, S. P., Hicks, L. M.,
746 and Fernandes, P. M. B. 2016. Label-free quantitative proteomic analysis of pre-flowering
747 PMeV-infected *Carica papaya* L. *J. Proteomics* 151:275-283.

- 748 Solomon, M., Belenghi, B., Delledonne, M., Menachem, E., and Levine, A. 1999. The
749 involvement of cysteine proteases and protease inhibitor genes in the regulation of
750 programmed cell death in plants. *Plant Cell* 11:431-444.
- 751 Sorel, M., Mooney, B., de Marchi, R., and Graciet, E. 2018. Ubiquitin/Proteasome System
752 in Plant Pathogen Responses. *Annu. Plant Rev.* online 2:65-116.
- 753 Taliansky, M. E., and Robinson, D. J. 2003. Molecular biology of umbraviruses: phantom
754 warriors. *J. Gen. Virol.* 84:1951-1960.
- 755 Tapia-Tussell, R., Magaña-Alvarez, A., Cortes-Velazquez, A., Itza-Kuk, G., Nexticapan-
756 Garcez, A., Quijano-Ramayo, A., Martin-Mex, R., and Perez-Brito, D. 2015. Seed
757 transmission of Papaya meleira virus in papaya (*Carica papaya*) cv. Maradol. *Plant*
758 *Pathol.* 64:272-275.
- 759 Tuo, D., Shen, W., Yan, P., Li, C., Gao, L., Li, X., Li, H., and Zhou, P. 2013. Complete
760 genome sequence of an isolate of papaya leaf distortion mosaic virus from
761 commercialized PRSV-resistant transgenic papaya in China. *Acta Virol.* 57:452-455.
- 762 Varun, P., Ranade, S. A., and Saxena, S. 2017. A molecular insight into papaya leaf
763 curl—a severe viral disease. *Protoplasma* 254:2055-2070.
- 764 Ventura, J. A., Costa, H., and da Silva Tatagiba, J. 2004. Papaya diseases and integrated
765 control. Pages 201-268 in: *Diseases of Fruits and Vegetables: Volume II.* Springer.
- 766 Ventura, J. A., Costa, H., Tatagiba, J. d. S., Andrade, J. d. S., and Martins, D. d. S. 2003.
767 Meleira do mamoeiro: Etiologia, sintomas e epidemiologia. Pages 267-276 in: *Papaya*
768 *Brasil: Qualidade do mamão para o mercado interno, Vitória-Espírito Santo, Brazil.*
- 769 Ventura, J. A., Lima, I. d. M., Martins, M. V. V., Culik, M. P., and Costa, H. 2019. Impact
770 and management of diseases in the propagation of fruit plants. *Rev. Bras. Frutic.* 41:e-
771 647.
- 772 Verchot, J. 2016. Plant Virus Infection and the Ubiquitin Proteasome Machinery: Arms
773 Race along the Endoplasmic Reticulum. *Viruses* 8:314.
- 774 Vidal, C., Nascimento, A., and Habibe, T. 2003. Transmissão do vírus da meleira do
775 mamoeiro por insetos. Pages 612-615 in: *Papaya Brasil: Qualidade do Mamão Para o*
776 *Mercado Interno, Vitória, Espírito Santo, Brazil.*
- 777 Whitfield, A. E., Falk, B. W., and Rotenberg, D. 2015. Insect vector-mediated transmission
778 of plant viruses. *Virology* 479-480:278-289.
- 779 Wu, Z., Mo, C., Zhang, S., and Li, H. 2018. Characterization of Papaya ringspot virus
780 isolates infecting transgenic papaya 'Huanong No. 1' in South China. *Sci. Rep.* 8:8206.
- 781 Xia, X.-J., Zhou, Y.-H., Shi, K., Zhou, J., Foyer, C. H., and Yu, J.-Q. 2015. Interplay
782 between reactive oxygen species and hormones in the control of plant development and
783 stress tolerance. *J. Exp. Bot.* 66:2839-2856.

- 784 Zamudio-Moreno, E., Ramirez-Prado, J., Moreno-Valenzuela, O., and Lopez-Ochoa, L.
785 2015. Early diagnosis of a Mexican variant of Papaya meleira virus (PMeV-Mx) by RT-
786 PCR. *Gen. Mol. Res.* 14:1145-1154.
- 787 Zhang, R., Hisano, S., Tani, A., Kondo, H., Kanematsu, S., and Suzuki, N. 2016. A
788 capsidless ssRNA virus hosted by an unrelated dsRNA virus. *Nat. Microbiol.* 1:15001.
- 789

790 TABLES

791

792

793 Table 1 –Viruses of papaya, by family and genus, in main growing regions
794 worldwide.

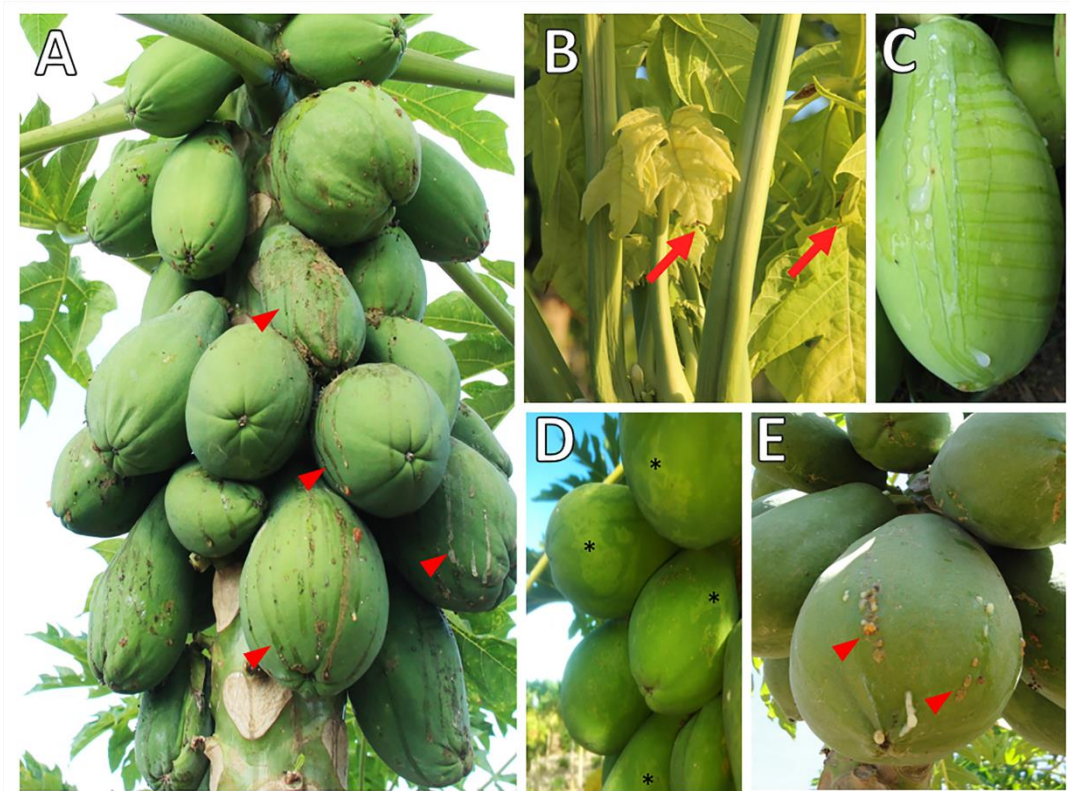
Family	Genus	Virus species
Bunyaviridae	<i>Tospovirus</i>	<i>Tomato spotted wilt virus</i> , TSWV
	<i>Tenuivirus</i>	<i>Papaya mild yellow leaf virus</i> , PMYLV
Geminiviridae	<i>Begomovirus</i>	<i>Papaya leaf curl virus</i> , PaLCuV
		<i>Papaya leaf crumple virus</i> , PaLCrV
		<i>Chilli leaf curl virus</i> , ChiLCuV
		<i>Tomato leaf curl New Delhi virus</i> , ToLCuNDV
		<i>Croton yellow vein mosaic virus</i> , CYVMV
Potyviridae	<i>Potyvirus</i>	<i>Papaya ringspot virus</i> , PRSV-P
		<i>Papaya leaf distortion mosaic virus</i> , PLDMV
		<i>Zucchini yellow mosaic virus</i> , ZYMV
Rhabdoviridae	<i>Rhabdovirus</i>	<i>Papaya apical necrosis virus</i> , PANV
		<i>Papaya droopy necrosis virus</i> , PDNV
Tombusviridae ¹	<i>Carmovirus</i> ¹	<i>Papaya lethal yellowing virus</i> , PLYV
Alphaflexiviridae	<i>Potexvirus</i>	<i>Papaya mosaic virus</i> , PapMV
NE ²	NE ²	<i>Papaya meleira virus</i> ² (PMeV ^a + PMeV-2 ^b)

795 ¹⁻ Molecular research indicates homology with the family *Sobemoviridae* and
796 genus *Sobemovirus*.797 ²⁻ Not established. Molecular characterization of virus genome is in progress; a-
798 tentatively classified in *Totivirus* genus; b- tentatively classified in *Umbravirus*
799 genus.

800

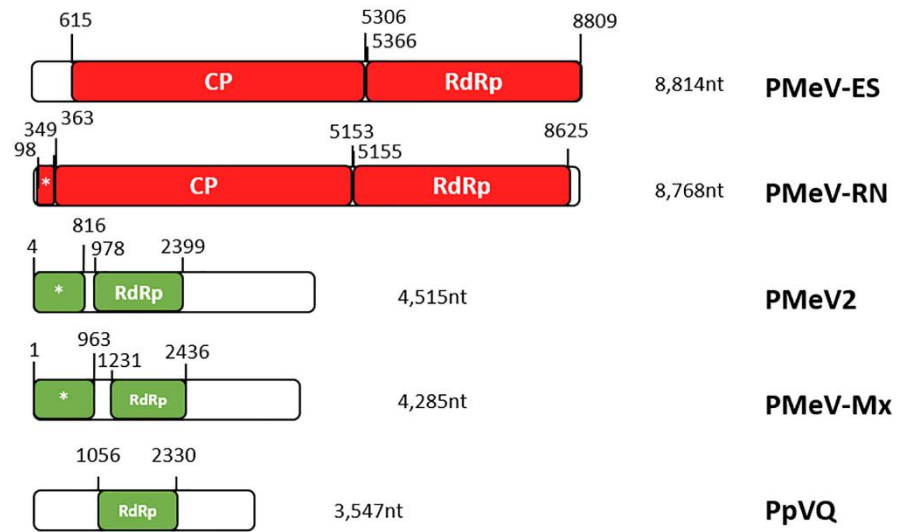
801

802 **FIGURES**
 803
 804
 805

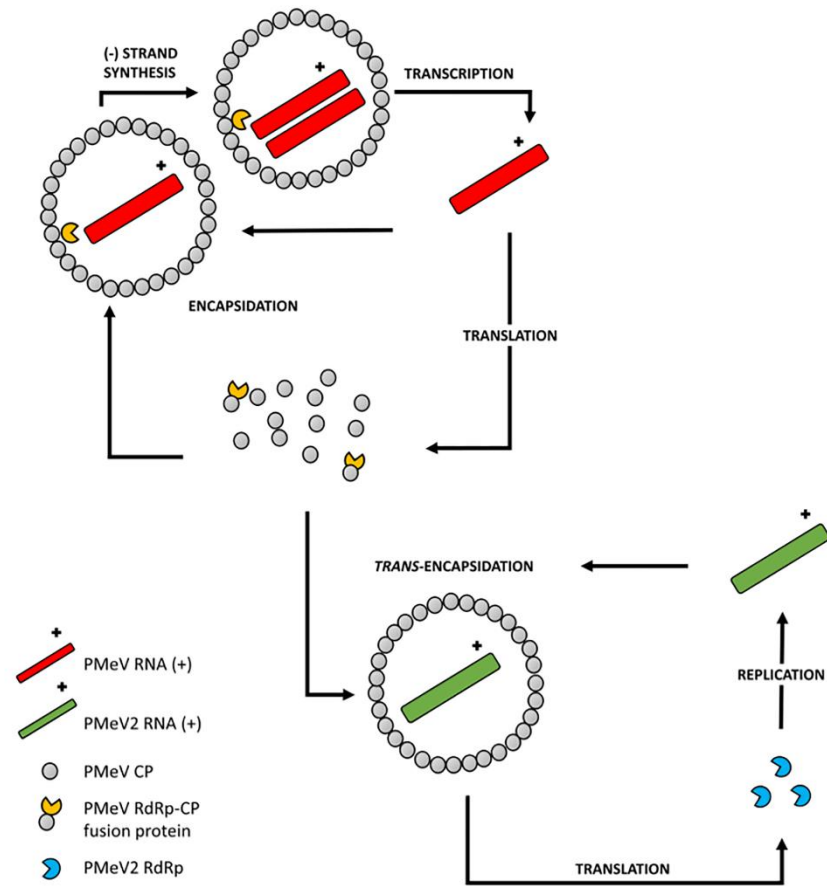


806
 807 Figure 1. Papaya sticky disease (PSD) symptoms. (A) Papaya tree with green
 808 fruits presenting an exudation of fluid latex on their surface which darkens after
 809 oxidation by atmospheric exposure resulting in a sticky aspect (red arrowhead).
 810 (B) This exudation also results in the appearance of small necrotic lesions on the
 811 edges of young leaves (red arrow). (C) Watery, fluid, and translucent latex of an
 812 infected fruit after wound with a scalpel. (D) Irregular light-green and yellowish
 813 areas in green fruit (black asterisk). (E) Papaya fruit from symptomatic Mexican
 814 plant (cv. Maradol).
 815

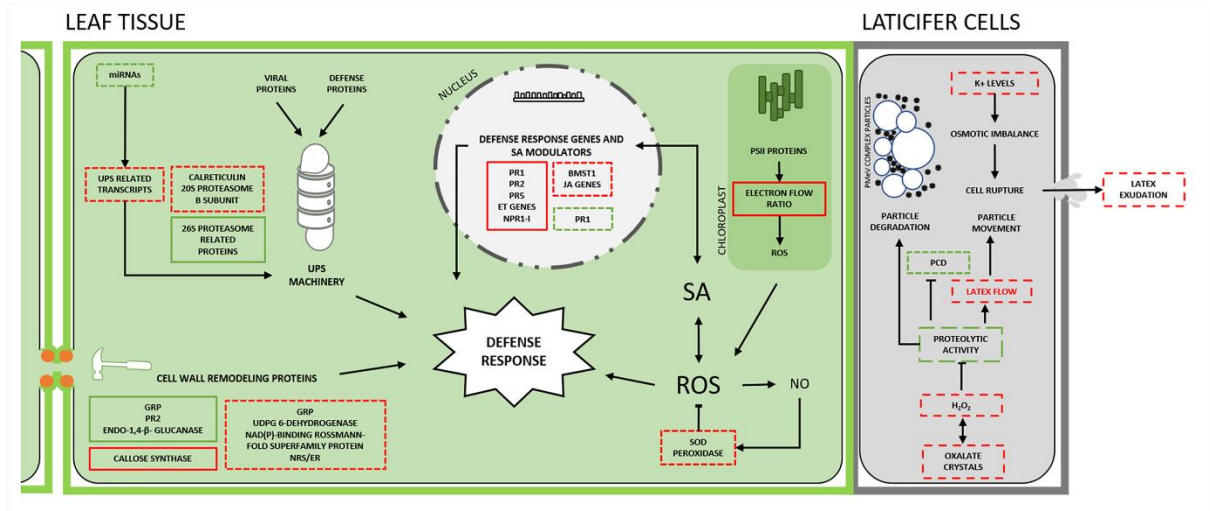
A



B



817 Figure 2. Current isolates of PMeV and PMeV2 and proposed model for
818 interactions between PMeV complex. (A) Genomic organization of PMeV (red) and
819 PMeV2 (green) isolates showing their ORFs and their putative encoded proteins.
820 NCBI accession numbers: PMeV-ES (KT921784); PMeV-RN (KT013296); PMeV2
821 (KT921785); PMeV-Mx (KF214786.1); PpVQ (KP165407). Hypothetical proteins
822 are indicated with an asterisk. (B) PSD in Brazil occurs during a double infection,
823 by PMeV, a toti-like virus, and PMeV2, an umbra-like virus. A possible scenario for
824 PMeV and PMeV2 interplay is illustrated here. PMeV can complete its replication
825 cycle in the host cell without PMeV2. Like an umbravirus, PMeV2 is a capsidless
826 ssRNA virus and is not found alone and uses PMeV CP for encapsidation. A -1
827 ribosomal frameshifting produces the RdRp-CP fusion protein.
828



829
 830 Figure 3. Papaya and PMeV complex interaction. In pre-flowering plants, a
 831 multilayer immune system triggered by PMeV complex infection results in a pre-
 832 flowering tolerance that is partially disabled in post-flowering. See the text (Papaya
 833 and PMeV complex interaction) for details and further references. SA, salicylic
 834 acid; *PR1*, *PR2* and *PR5* are pathogenesis-related protein genes; *BSMT1*, benzoic
 835 acid/SA carboxyl methyltransferase; *NPR1-I*, non-expressor of pathogenesis-
 836 related protein 1; ET, ethylene; JA, jasmonate; GRP, glycine-rich protein; *NRS/ER*,
 837 nucleotide-rhamnose synthase/epimerase-reductase; UPS, ubiquitin/26S
 838 proteasome system; PCD, programmed cell death. ROS, reactive oxygen species;
 839 NO, nitric oxide; SOD, superoxide dismutase; PSII, photosystem II. Dashed box:
 840 post-flowering events (PSD); solid box: pre-flowering events; red: induced or
 841 partially induced processes; green: repressed or partially repressed; black arrows:
 842 direction or order of the cellular event; blocked arrow: inhibition of the cellular
 843 event. Viral icosahedral particles and vesicles are represented in laticifer cells.
 844



845

846

847

848

849

850

851

852

853

Figure 4. The roguing of infected plants. (A) An agricultural technician specialized in recognizing plants with papaya ringspot and papaya sticky disease symptoms, known in Portuguese as 'mosaiqueiro', performs the roguing using a machete. Until now, this is the only management applied to control the PSD. (B) If appropriate agricultural practices were not carried out, the disease spread the whole crop and brought about total yield losses.

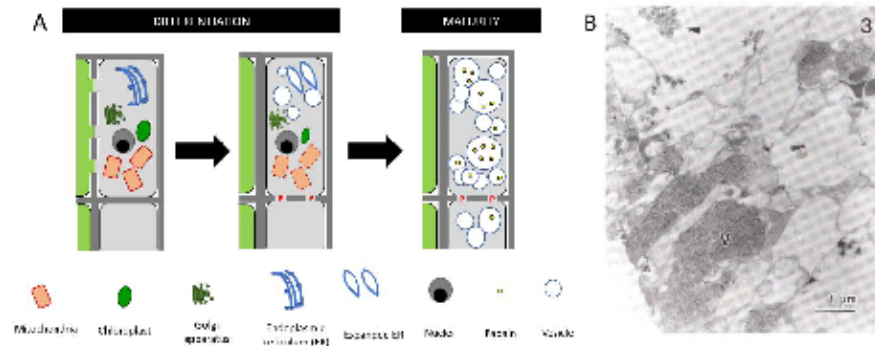


Figure S1. *Carica papaya* laticifers and PMeV complex viral particles. Xylem and phloem are complex tissues that form channels in the plant. Likewise, laticifers correspond to a system of additional channels, but comprised exclusively of living cells. Laticifers are specialized in synthesis and accumulation of latex which varies in biochemical composition depending on the plant species (Hagel et al. 2008). Stored under pressure, this latex is exuded on wounding being an important defense response against pathogens. In *C. papaya*, laticifers are articulated, anastomosed (Hagel et al. 2008) and found in all papaya organs. In the primary growing stem, laticifers localize in parenchyma region between xylem and phloem (Fisher 1980). They are also found in roots, but seem to septate their walls, becoming isolated cells at maturity (Rao et al. 2013). In the immature fruit, laticifers form an anastomosed network throughout the parenchyma, being more numerous and smaller in the fruit periphery. In the ripe fruit, they occur throughout the mesocarp tissue in a parallel arrangement to the vascular bundles (Fisher 1980). Differentiating laticifers have numerous well-developed and active mitochondria, ribosomes, and endoplasmic reticulum (ER). As development progresses, organelles are gradually degenerated, ER expands and splits into fragments, and the autophagy of the cytoplasm by the vacuole becomes evident. In their cell walls, perforations are produced in different places of contact with adjacent laticifers. Reaching maturity, laticifers become filled with vesicles containing proteases, organelles disappear, but the plasma membrane remains intact (Zeng et al. 1994). Some authors report that they rarely find nuclei (Evert 2006; Kitajima et al. 1993) while others report that *C. papaya* laticifers are multinucleated (Fisher 1980). ER and polyribosomes are involved in papain synthesis which is temporally stored in ER-derived vesicles and then in vesicles containing other latex components (Kitajima et al. 1993). A schematic diagram was organized summarizing those findings (Panel A). To date, there is no information on the cellular communication of *C. papaya* laticifers with surrounding cells. PMeV complex particles are visualized within laticifers from fruits and leaves but not in other papaya tissue. Figure B shows electron micrograph of thin sections of latex vessel from PSD fruit. Isometric particles appeared in two patterns: scattered randomly among latex vesicles (arrowheads) or forming aggregates of different sizes (V). Reprinted from Kitajima et al. (1993). P – perforation. Structures outlined with dashed lines are degenerating.

856 **THESIS OBJECTIVE**

857

858

859 **GENERAL OBJECTIVE**

860 To understand the papaya sticky disease pathosystem at host-pathogen interaction and
861 pathogen dispersion level, and develop a diagnosis methodology to contribute to disease
862 management.

863

864

865 **SPECIFIC OBJECTIVES**

866 • To localize papaya meleira virus (PMeV) and papaya meleira virus 2
867 (PMeV2) RNA in *Carica papaya* tissues assessing their preferential site of
868 infection during somatic embryogenesis in papaya (Manuscript #2);

869 • To identify interactions between PMeV ORF1 and plant proteins, finding
870 important players in the pre-flowering tolerance mechanism, mainly affecting
871 PMeV complex replication (Manuscript #3);

872 • To validate a method to detect PMeV complex in samples collected from
873 Brazilian orchards (Manuscript #4);

874 • To open an important discussion for directing new research to understand
875 the vectors of PMeV complex and the use of new management practices in
876 papaya orchards (Manuscript #5).

877

878 **MANUSCRIPT #2. LATICIFERS OF PAPAYA STICKY DISEASED PLANTS ARE**
879 **THE PREFERENTIAL INFECTION SITE OF PAPAYA MELEIRA VIRUS (PMeV), A**
880 **TOTI-LIKE VIRUS AND UMBRAVIRUS-LIKE ASSOCIATED RNA, PAPAYA MELEIRA**
881 **VIRUS 2 (PMeV2)**

882
883 Manuscript in preparation for *Archives of Virology journal* (ISSN 0304-8608; IF 2.574,
884 2021; Qualis B1 Biotecnologia, 2013-2016).

885
886
887 **Laticifers of papaya sticky diseased plants are the preferential infection site of**
888 **papaya meleira virus (PMeV), a toti-like virus and umbravirus-like associated RNA,**
889 **papaya meleira virus 2 (PMeV2)**

890
891
892 **Marlonni Maurastoni**¹, Tathiana F. Sá-Antunes¹, Emanuel F. Abreu², Diva M. A. Dusi²,
893 Ana C. M. M. Gomes², Francisco J. L. Aragão², Simone G. Ribeiro², Francisco M.
894 Zerbini³, Anna E. Whitfield⁴ and Patricia M. B. Fernandes¹

895
896 ¹Núcleo de Biotecnologia, Universidade Federal do Espírito Santo, Vitória,
897 Espírito Santo, Brazil;

898 ²Embrapa Recursos Genéticos e Biotecnologia, Brasília, DF, 70770-900, Brazil

899 ³Dep. de Fitopatologia/BIOAGRO, Universidade Federal de Viçosa, 36570-900, Viçosa,
900 Minas Gerais, Brazil.

901 ⁴Department of Entomology and Plant Pathology, North Carolina State University, 840
902 Main Campus Drive, Raleigh, NC 27606, USA

ABSTRACT

903
904
905
906
907
908
909
910
911
912
913
914
915
916
917
918
919
920
921
922
923
924
925
926
927

Papaya sticky disease (PSD) has affected production and caused the destruction of several orchards in Brazil, Mexico, and Australia. PSD is associated with a viral complex comprised of papaya meleira virus (PMeV), a totivirus-like, and papaya meleira virus 2 (PMeV2), a umbravirus-like associated RNA. In Brazil, both PMeV and PMeV2 are separately packaged by capsid protein coded by PMeV. Asymptomatic plants are detected with PMeV while symptoms can be visualized only after flowering and infection by PMeV2. Spontaneous exudation of aqueous latex from fruits and necrosis at the edges of young leaves are PSD symptoms caused by an osmotic imbalance in laticifer cells. Electron microscopy studies have shown that viral particles are localized in these cells. Here we aim to understand the distribution of both viral RNAs throughout the papaya tissues. *In situ* hybridization targeting both PMeV and PMeV2 RNA shows a preference of both viruses to laticifers in PSD plants. PMeV accumulates in laticifers cells of the main vein, while PMeV2 can infect both the main vein and mesophyll laticifers. To confirm the preference for these cells, we took advantage of a non-laticifer cell producing stages of papaya development using somatic embryogenesis to further characterize PMeV tissue tropism. The results show the PMeV complex is detected in embryogenic calli and somatic-embryogenesis regenerated plants, but not in callus tissue. No plasmodesmata were visualized in *Carica papaya* laticifers, suggesting an uncommon strategy for PMeV entry in these cells.

Keywords: laticifers; tissue culture; plasmodesmata; virus particle

928

929 **INTRODUCTION**

930

931

932 Papaya sticky disease (PSD) has been a causing the destruction of papaya (*Carica*
933 *papaya* L.) orchards in Brazil (NAKAGAWA *et al.*, 1987), Mexico (PEREZ-BRITO *et al.*,
934 2012) and Australia (PATHANIA *et al.*, 2019), countries in which it was officially reported.
935 In Brazil, PSD is associated with a viral complex that comprises papaya meleira virus
936 (PMeV) and papaya meleira virus 2 (PMeV2). PMeV has a dsRNA genome in a typical
937 arrangement of the *Totiviridae* family, while PMeV2 has an ssRNA genome and it has
938 been grouped in the class I umbravirus-like associated RNAs (ulaRNA) (LIU *et al.*, 2021).
939 Both PMeV and PMeV2 are separately encapsidated in particles assembled by PMeV
940 capsid protein (ANTUNES *et al.*, 2016).

941 In PSD plants, isometric viral particles of approximately 42 nm in diameter are visualized
942 only in laticifers. Viral particles are not visualized in any other plant tissue e.g. epidermis,
943 parenchyma, fibers, xylem, and phloem vessels of PSD or asymptomatic plants
944 (KITAJIMA *et al.*, 1993; MAGAÑA-ÁLVAREZ *et al.*, 2016; RODRIGUES *et al.*, 2009).
945 Also, leaf dip preparations made from leaves or fruits of diseased plants only rarely show
946 similar particles (KITAJIMA *et al.*, 1993). The infection in these unusual cells leads to the
947 main PSD symptoms, the spontaneous exudation of fluid latex from green fruits. In
948 contact with air, the oozed latex oxidizes, darkens, and marks the fruit, reducing its
949 commercial value (ABREU *et al.*, 2015; ANTUNES *et al.*, 2020; VENTURA *et al.*, 2004).
950 These symptoms are visualized only after flowering possibly due to a depletion of
951 tolerance mechanisms signalized by salicylic acid (MADROÑERO *et al.*, 2018). Although
952 viral particles are not visualized in asymptomatic plants, sensitive diagnostic techniques
953 e.g., RT-PCR, show that it is not uncommon to detect PMeV and PMeV2 in these plants
954 (ANTUNES *et al.*, 2016; MAURASTONI *et al.*, 2020). Therefore, the non-visualization of
955 viral particles in infected asymptomatic plants but its visualization in symptomatic plants
956 support a correlation of virus accumulation and symptom onset.

957 In *C. papaya*, laticifers are distributed as an articulated and anastomosed channel through
958 all organs of the plant. In the primary growing stem, they are found among parenchyma
959 cells located between the primary xylem and phloem, probably derived from the fascicular
960 cambium (FISHER, 1980). During differentiation, laticifer cells undergo autophagy that
961 results in the complete elimination of their organelles, including the nucleus. The active
962 endoplasmic reticulum swells and fragments producing several vesicles containing
963 proteases. Upon reaching maturity, the tonoplast disappears remaining only the plasma
964 membrane which surrounds a lumen filled with vesicles (ZENG *et al.*, 1994).

965 Plasmodesmata are important cellular communications that allow the transport of
966 molecules through the symplast. In latex-bearing plants such as *Papaver somniferum* L.,
967 plasmodesmata connect laticifers cells to the phloem cells, where there is an exchange
968 of enzymes and mRNAs (FACCHINI; DE LUCA, 2008). On the other hand,
969 plasmodesmata of *Hevea brasiliensis* laticifers are active only during cell differentiation.
970 At maturity, these cells are symplastically isolated from the surrounding cells exchanging
971 molecules with the apoplast through membrane proteins (DE FAY *et al.*, 1989). There is
972 still a lack of information on the cellular communication of *C. papaya* laticifers with other
973 cells. Therefore, the mechanism of import and export of molecules, mRNAs, and viral
974 RNAs to these tissues remains unknown. More importantly, is still unknown if mature
975 papaya laticifers are metabolic active or rely on adjacent cells to support its metabolism,

976 PMeV complex movement within the plant is still unknown, but a hypothesis has been
977 raised based on the biochemical and physiological changes presented by laticifers of
978 diseased plants. The latex of PSD plants is more fluid due to an imbalance of potassium
979 ions and an increase in water content which possibly leads to cell disruption
980 (RODRIGUES *et al.*, 2009). There is a lack of information regarding long-distance
981 transport, cytoplasmic movements, or vesicle traffic in laticifers (PICKARD, 2008). Thus,
982 the rupture and subsequent latex drainage could be used by the PMeV complex as an
983 unusual transport mechanism through the plant (ANTUNES *et al.*, 2020; RODRIGUES *et*
984 *al.*, 2009).

985 To date, electron microscopy studies have only detected viral particles in laticifers cells.
986 However, there is no information regarding RNA localization in papaya tissues. Given that
987 some viruses are known to be limited by a cell type, e.g. phloem tissue, we hypothesize
988 that the PMeV complex is limited to laticifers. Here we show using in situ hybridization
989 that PMeV and PMeV2 RNA accumulates preferentially in the laticifers of infected leaves
990 in PSD plants. Using somatic embryogenesis (SE) as a non-vascular cell culture system,
991 we show that PMeV complex infection is reestablished in cells where laticifers are
992 differentiated. As no plasmodesma are visualized in laticifers of papaya, we speculate an
993 alternative route for the PMeV complex to reach laticifer cells.

994

995

996

997 **METHODS**

998

999

1000 **PCR amplification and cloning**

1001

1002

1003 To obtain the probe for in situ hybridization experiments, cDNA was synthesized from the
1004 total RNA extracted from plants with symptoms using the High-Capacity cDNA Reverse
1005 Transcription kit (Invitrogen, Carlsbad, USA). DNA fragments were amplified from cDNA
1006 samples using the Platinum[®] Taq DNA Polymerase High Fidelity enzyme (Invitrogen,
1007 Carlsbad, USA) and PMeV primer pair (F: 5' CTTGGTTAGGCATAACTGTAGGT 3'; R: 5'
1008 CACGGACTCTTAGAAACGTCTATC 3') or PMeV2 primer pair (F: 5'
1009 CGCCAAGTGGGATAAGTTTAGA 3'; R: 5' CGATTTGAGCACAAGGGTTAATG 3'). PCR
1010 fragments were cloned into pGEM[®]-T (Promega, Madison, USA) generating plasmids
1011 containing fragments of PMeV (pGEM[®]-T-PMeV-ES-2446-2816) and PMeV2 (pGEM[®]-
1012 T-PMeV2-1430-2244). Numbers in the plasmid names represent the region in the
1013 genome of each virus target by the probe (NCBI accession number: KT921784
1014 KT921785).

1015

1016

1017

1018 ***In situ* Hybridization**

1019

1020

1021 The plant material was selected from papayas trees growing in farms in the north of
1022 Espirito Santo state, Brazil. Samples were grouped into two conditions: symptomatic and
1023 asymptomatic. Each condition consisted of 6 plants from which the most expanded green
1024 leaf (second pair) was collected. From these leaves, three 1cm² segments from 3 different
1025 regions of the central rib (close to the petiole, middle of the leaf, and close to the leaf tip)
1026 were removed and immediately fixed in 4% (w/v) paraformaldehyde 0.01M phosphate
1027 buffer pH 7.2, dehydrated in an ethanol series and embedded in Paraplast® plus (Sigma,
1028 San Luis, MO). Specimens were cut into 10 µm sections and placed onto slides treated
1029 with 100 µg/mL of poly-L-lysine (Sigma, San Luis, MO). The Paraplast® was removed
1030 with HistoChoice® (Sigma, San Luis, MO) series.

1031 The plasmids pGEM®-T-PMeV-ES-2446-2816 and pGEM®-T-PMeV2-1430-2244 were
1032 linearized using restriction enzymes NcoI or Sall (Promega, Madison, WI). Sense and
1033 anti-sense probes were labeled with the Roche® Dig RNA Labeling kit (SP6/T7), following
1034 the manufacturers' instructions, and hydrolyzed to 150–200 bp fragments.
1035 Prehybridization was carried out in 0.05 M Tris–HCl pH 7.5 buffer containing 1 µg/mL
1036 proteinase K in a humid chamber at 37°C for 10 min. Hybridization was carried out
1037 overnight in a humid chamber at 42°C, in 10 mM Tris–HCl pH 7.5 buffer containing 300
1038 mM NaCl, 50% formamide (deionized), 1 mM EDTA pH 8, 1 X Denhardt's solution, 10%
1039 dextran sulfate, 600 ng/mL tRNA and 600 ng/mL of the RNA probe.. Detection was
1040 performed following the instructions of the Roche® Dig Detection kit, using anti-DIG
1041 conjugated alkaline phosphatase and NBT/BCIP as substrates. Sections were mounted
1042 in glycerol 50% (v/v) and regions of the main vein and mesophyll were observed under
1043 Leica DMRX or Zeiss-Axiophot light microscopes. Treatment with 10 mg/ml of RNase A
1044 was performed after visualization to ensure the hybridization signals were genuine. This
1045 experiment was performed three times and at least 10 regions of the main vein and

1046 mesophyll of each section in a total of 18 sections were analyzed for each plant group
1047 (see results section).

1048

1049

1050

1051 **PMeV complex monitoring during somatic embryogenesis**

1052

1053

1054 Somatic embryogenesis tissue culture media and culture conditions were performed
1055 according to KOEHLER *et al.* (2013). Four 2-month-old plants growing in a greenhouse
1056 were inoculated with latex tapped from infected plants (ABREU *et al.*, 2012). The
1057 diagnosis was made on young leaves 30 days after inoculation. New emerged leaves
1058 were removed and used as explants for somatic embryogenesis. The experiment was set
1059 up on 15 Petri dishes per plant, each dish containing 4 leaf disks (1cm² each).

1060 Leaf disks were inoculated in an induction medium. Monthly for three months, friable
1061 embryogenic calli (FEC) were transferred to a fresh tissue culture medium containing half
1062 of the 2,4-D concentration of the previous medium. FEC exhibiting somatic embryo
1063 clusters were transferred to a maturation medium with conditions described by Koheler
1064 *et al.*, 2013. During 3 months, somatic embryos in the mature cotyledonary stage were
1065 isolated and placed on germination medium (Koheler *et al.*, 2013). After germination,
1066 seedlings were transferred to the regeneration medium (Koheler *et al.*, 2013) in glass
1067 flasks (14cm x 8 cm) containing 50 ml of culture medium. Each month the seedlings were
1068 transferred to a new fresh medium until they reach an approximate 8-10 cm height.

1069 The monitoring of the PMeV complex was performed in 3 different stages of somatic
1070 embryogenesis: (i) three-month-old calli, (ii) calli exhibiting somatic embryo in mature
1071 cotyledonary stage, and (iii) regenerated seedlings. The diagnosis of PMeV complex was
1072 performed according to ANTUNES *et al.* (2016).

1073

1074

1075

1076 Plasmodesmata identification

1077

1078

1079 Plasmodesmata were identified by staining papaya tissue with an aniline blue reagent.
1080 Semi-thin sections of the leaf main vein (12 μm) obtained from fixed material and included
1081 in paraffin were immersed in a solution of aniline blue 0.1% (w/v) in 1M glycine (pH 9.5).
1082 Sections were incubated for 5 min in the dark under gentle agitation and then washed in
1083 deionized water for 5 min. Slides were mounted in deionized water and visualized under
1084 a fluorescence microscope (NIKON® Ti-Eclipse) using an excitation filter: bandpass (BP)
1085 365/12 nm; emission: long pass (LP) 397 nm. The images were photographed and
1086 analyzed with the aid of the Nis-Elements AR 4.20.00 software. At least 10 regions of the
1087 main vein of 18 sections were observed.

1088

1089

1090

1091 RESULTS

1092

1093

**1094 PMeV and PMeV2 RNA accumulates preferentially in the laticifers of infected leaves
1095 in PSD plants**

1096

1097 After diagnosis, symptomatic and asymptomatic plants were grouped in (i) asymptomatic
1098 and positive for PMeV only (ii) asymptomatic and positive for PMeV complex, and (iii)
1099 symptomatic and positive for PMeV complex. *In situ* hybridization assays using semi-thin
1100 sections of *C. papaya* leaves were performed to localize the PMeV and PMeV2 RNA in
1101 papaya tissues. The main vein and mesophyll regions of the second pair of leaves were
1102 analyzed (Figure 1 and 2). The results show that in group iii PMeV RNA is restricted to
1103 the laticifers of the main vein. Both sense and antisense strands were detected in this
1104 cell. These results corroborate those discovered by Rodrigues (2006) who detected the
1105 PMeV dsRNA in the layers with the parenchyma, xylem, vascular cambium, and phloem.

1106 On the other hand, the sense RNA of PMeV2 is restricted to the laticifers of the main vein
1107 as well as mesophyll. The PMeV2 antisense RNA was not detected in the analyzed
1108 material. RNA of both viruses was not detected in any other tissue of diseased plants or
1109 the laticifers of plants in the groups i and ii. Curiously, in all groups, a hybridization signal
1110 is visualized in non-identified structures (Figure S1). These structures are present inside
1111 cells surrounded by parenchyma. In transversal sections of the main vein, they are found
1112 between phloem bundles and forming a ring near to collenchyma cells. In longitudinal
1113 sections, this ring is found as parenchymatic rays. These structures are also visualized in
1114 the transitioning parenchyma between the main vein and mesophyll (Figure S1).

1115

1116

1117

1118 **PMeV complex is detected in embryogenic calli and somatic embryogenesis-**
1119 **regenerated plants**

1120

1121 To monitor the presence of the PMeV complex in a system comprised of partially
1122 undifferentiated cells (i.e., devoid of laticifers), we induced somatic embryogenesis using
1123 the leaf of PMeV complex-infected plants as explants (Figure 3.A). PMeV complex
1124 diagnosis was conducted by RT-PCR in three different SE stages: (i) 3-month-old calli,
1125 (ii) calli exhibiting somatic embryo in mature cotyledonary stage, and (iii) regenerated
1126 seedlings.

1127 The callogenic response was observed in the explants after 30 days in the culture
1128 medium. In the next two months, the callus tissue covered the entire leaf explant (Figure
1129 3.B). During the following months, successive reductions of 2,4-D were made to half the
1130 molarity per month. At this stage, only embryogenic calluses were transferred to the
1131 maturation medium (Figure 3.C). At this time, somatic embryos can be visualized at
1132 different stages of development. Embryos in the mature cotyledonary stage were
1133 removed and transferred to the germination medium. After 2 weeks, embryos germinated
1134 in normal plants (Figure 3.F). Then, seedlings were transferred to flasks where their

1135 growth was monitored for 3 months (Figure 3. G, H, and I). After 3 months of cultivation,
1136 seedlings were 8-10 cm long and their leaves were used for molecular diagnosis.

1137 RT-PCR diagnosis shows that all inoculated explant-donor plants were infected with the
1138 PMeV complex (Table 1). After inducing somatic embryogenesis from inoculated plants,
1139 PMeV and PMeV2 were monitored in 3-month-old calluses and plants regenerated by
1140 SE. PMeV was detected in eight of sixteen calli while none of the analyzed calluses
1141 showed detection for PMeV2. Interestingly, all samples obtained from embryogenic callus
1142 and regenerated plants tested positive for the viral complex.

1143

1144

1145

1146 **No plasmodesmata are visualized in *C. papaya* laticifers**

1147

1148 To identify cellular communications between laticifers and adjacent tissues we used
1149 aniline blue as a fluorescent dye to detect the presence of callose, a polysaccharide well
1150 known to be found in plasmodesmata. It was possible to identify plasmodesmata
1151 associated with parenchymal tissues (Figure 4) and located between sieve tube elements
1152 and between sieve tube/companion cell complex in the phloem (Figure 4.A and B -
1153 arrowheads). No staining was visualized between laticifer cells and adjacent tissues
1154 (Figure 4.B - arrows).

1155

1156

1157

1158 **DISCUSSION**

1159

1160

1161

1162

1163 During the virus cycle, the production of new particles is directly associated with the
1164 replication of their viral RNA (HULL, 2014). In PSD plants viral particles of the PMeV
1165 complex are only seen in laticifers, not in any other cell type (epidermis, parenchyma,
1166 fibers, xylem, and phloem vessels), while no particles have been found in asymptomatic
1167 plants (KITAJIMA *et al.*, 1993; RODRIGUES *et al.*, 1989). Since the discovery of the viral
1168 nature of PSD etiology, the visualization in agarose gel of the viral RNAs extracted from
1169 latex has been used as the simplest procedure to identify infected plants (TAVARES *et*
1170 *al.*, 2004). However, the viral RNA is not always detected by the method above when total
1171 RNA is extracted from latex of asymptomatic plants neither from leaf tissues of
1172 symptomatic plants (data not shown). This suggests that the PMeV complex can
1173 accumulate in the latex of diseased plants, more so than in other green tissues. The
1174 sequencing of the PMeV complex allowed the use of more sensitive techniques for
1175 detection (ABREU *et al.*, 2012; ANTUNES *et al.*, 2016; MAURASTONI *et al.*, 2020) and
1176 changed the diagnosis of false-negative plants as PMeV and PMeV2 could now be
1177 detected in asymptomatic plants (ANTUNES *et al.*, 2016; MAURASTONI *et al.*, 2020).
1178 Taken together, this supports a correlation between increasing virus titer, the
1179 accumulation of virions in laticifer, and the symptom's onset. Supporting this idea, only
1180 diseased plants showed detection by the PMeV complex through *in situ* hybridization.
1181 Both asymptomatic plants with single infection (PMeV) and plants infected with PMeV
1182 complex do not show signs of infection through *in situ* hybridization, suggesting that
1183 additional factors, besides PMeV2 infection, (e.g the development stage when the plants
1184 are infected) lead to virus accumulation in these cells. The depletion of the tolerance
1185 mechanism in post-flowering plants and the biochemical and physiological modifications
1186 directly associated with laticifers could be important for this process (MADROÑERO *et*
1187 *al.*, 2018; RODRIGUES *et al.*, 2009; RODRIGUES *et al.*, 2012; SOARES *et al.*, 2016).

1188 The vascular system is the main route used by viruses to systemically infect a plant. The
1189 phloem, for example, is the most advantageous conduit as it leads to almost all cells and
1190 organs (SEO; KIM, 2016). Although some viruses can reach phloem cells, several
1191 mechanisms limit their ability to escape from it, as seen during potato leafroll virus (PLRV)
1192 and citrus tristeza virus (CTV) infection (BENDIX; LEWIS, 2018). Similar to phloem cells,
1193 papaya laticifers are distributed among all tissues and organs of the papaya plant

1194 (FISHER, 1980), but their role in exchanging molecules with surrounding cells still needs
1195 to be addressed. Here, we observed a preferential infection of both viruses in laticifers
1196 which suggests that PMeV complex accumulation is limited to laticifers. PMeV and
1197 PMeV2 also present a differential distribution throughout the leaf of diseased plants. Both
1198 positive and negative strands of PMeV RNA are detected only in laticifers of the main
1199 vein, while PMeV2 positive strand is detected in the main vein and by itself in mesophyll
1200 laticifers. PMeV2 has been grouped in class I of umbravirus-like associated RNAs, which
1201 are coat protein-dependent subviral RNA replicons related to umbraviruses (LIU *et al.*,
1202 2021). As they do not encode a capsid protein, umbraviruses need an auxiliary virus
1203 responsible for packing their RNA to be transmitted by a vector, however when
1204 mechanically inoculated they can establish systemic infection (TALIANSKY; ROBINSON,
1205 2003). The fact that PMeV2 is found alone in mesophyll laticifers suggests that it is
1206 capable of infecting tissue independent of its auxiliary virus. The reason that PMeV is not
1207 detected in other mesophyll cells or how PMeV2 reached these cells remains
1208 inconclusive. In *Hevea brasiliensis*, laticifers that originated from primary meristematic
1209 zones have a different morphology and transcriptome profile from the ones that originated
1210 from the cambium, with the former associated with defense against biotic stresses and
1211 the latter to abiotic stresses (TAN *et al.*, 2017). This supports the idea that laticifers from
1212 mesophyll and main vein could have different physiology which in turn will affect the
1213 distribution of the PMeV complex through the leaf.

1214 The preference of PMeV complex for laticifer cells was also evaluated using somatic
1215 embryogenesis as a non-laticifer cell system. Ultrastructural analysis showed that *C.*
1216 *papaya* callus consists of partially differentiated cells containing numerous lipid bodies.
1217 Laticifers are observed in somatic embryos regenerated from the callus and no laticifers
1218 are observed in all the callogenic tissue (YAMAMOTO; TABATA, 1989). In this work, we
1219 used infected leaves as explants and followed the same material until the regeneration of
1220 in vitro plants. Monitoring of the PMeV complex during somatic embryogenesis showed
1221 that embryogenic calluses and SE-regenerated plants were infected with the viral
1222 complex. However, in 3-month old callus only few samples were detected with PMeV,
1223 while none were detected with PMeV2. The non-detection in this material could be
1224 attributed to the low viral titer in these cells supporting the idea that the system could not

1225 support virus replication at the same extent as laticifers. The ability of the PMeV complex
1226 to infect plants regenerated from SE raises questions about how PMeV can move from
1227 the infected callogenic tissue to the differentiating embryo. In indirect somatic
1228 embryogenesis, embryos originate from pro-embryogenic complexes. Pro-embryogenic
1229 complexes are compact structures, formed by an aggregation of cells with high similarity
1230 to meristematic cells (FEHÉR, 2015). Histochemical analyzes of the indirect SE process
1231 in *C. papaya* show that pro-embryogenic complexes are delimited by cell walls with high
1232 deposition of callose (β -1,3-glucan) (KOEHLER, 2004). This thickening collapses
1233 plasmodesmata keeping them isolated from the other callus cells (FERNANDO *et al.*,
1234 2001). As a result, there is a restriction to symplastic transport, preventing the
1235 physiological influence of external cells on the embryogenic pathway of the complex's
1236 cells. In this work, somatic embryos are produced through indirect SE, as can be observed
1237 by the formation of embryogenic calluses, where there is a production of pro-embryogenic
1238 complexes. In addition to the level of cell organization, the somatic embryo has laticifers
1239 that are not visualized in the rest of the callus (YAMAMOTO; TABATA, 1989). Therefore,
1240 it is likely that, in embryogenic callus, the PMeV complex infects somatic embryos and
1241 accumulates in laticifers. The visualization of particles in embryogenic calluses of *C.*
1242 *papaya* could confirm this hypothesis.

1243 Plasmodesmata are fundamental nanochannels connecting the plant cell symplast which
1244 permit the passage of several small molecules, including ions, hormones, nucleic acids,
1245 and photosynthates. Viruses exploit these structures for their intercellular movement
1246 mainly in the form of ribonucleoprotein complexes and interacting with several proteins
1247 present in the plasmodesmata site (HULL, 2014; KUMAR *et al.*, 2015). It has been pointed
1248 out that the lacking or the dynamics of the plasmodesmata network in some cells is
1249 detrimental for the symplastic exclusion and cell differentiation, which is the case of the
1250 apical meristem cells. However, the mechanisms that exclude some viruses or viroids in
1251 this structure are not fully understood (BRADAMANTE *et al.*, 2021). Here,
1252 plasmodesmata were identified mainly between sieve tube elements and between sieve
1253 tube/companion cell complexes present in the phloem, but not between papaya laticifers
1254 and adjacent tissues. Staining with aniline blue showed that in *Hevea brasiliensis* there
1255 are no plasmodesmata between the laticifers and adjacent parenchyma cells. Similarly,

1256 laticifers of poinsettia lack cellular communication at maturity (FINERAN, 1983).
1257 Interestingly, in these plants, laticifers are visualized containing occluded plasmodesmata
1258 resulted from cell differentiation (DE FAY *et al.*, 1989) which supports the hypothesis that
1259 this cell type is independently programmed (JOHNSON *et al.*, 2021). In the absence of
1260 plasmodesmata, the most favorable moment for the PMeV complex to reach laticifer cells
1261 would occur in young organs containing initial cells from laticifers that initiated their cell
1262 differentiation. Supporting this idea, it has been pointed out that PMeV has a persistent
1263 lifestyle (ANTUNES *et al.*, 2016). Despite the PMeV complex infecting papaya
1264 systemically, there are no ORFs capable of encoding typical viral movement proteins.
1265 Most persistent plant viruses have a dsRNA genome and encode only one RdRp and one
1266 CP, without the MP essential for systemic infection (ROOSSINCK, 2010; ROOSSINCK,
1267 2013). Therefore, there is no cell-to-cell movement or virus transport within the plant,
1268 except when the cell divides (BOCCARDO *et al.*, 1987), an event characteristic of plant
1269 meristematic cells. Papaya laticifers are articulated, a class of laticifers originated from
1270 multiple initials that later in their development become a multinucleate structure through
1271 cell fusion (JOHNSON *et al.*, 2021). Therefore, it is reasonable to imagine that PMeV
1272 infects laticifers initials earlier in its differentiation, being able to reach all organs through
1273 the further cytoplasm fusion of adjacent laticifers.

1274 Taken together, we show that laticifers of the main vein are the preferential site of PMeV
1275 complex accumulation and PMeV2 alone can infect laticifers of the mesophyll. No
1276 plasmodesmata were visualized in mature laticifers of the main vein leading to the
1277 assumption that the PMeV complex reaches mature laticifers early in its differential
1278 through infection of laticifer initials. Supporting this idea, we show using somatic
1279 embryogenesis as a non-laticifer tissue system that PMeV complex can infect somatic
1280 embryos as well as regenerated plants.

1281

1282 **REFERENCES**

- 1283
- 1284
- 1285 ABREU, P. M. V.; ANTUNES, T. F. S.; MAGAÑA-ÁLVAREZ, A.; PÉREZ-BRITO, D.;
 1286 TAPIA-TUSSELL, R.; VENTURA, J. A.; FERNANDES, A. A. R.; FERNANDES, P. M. B.
 1287 A current overview of the Papaya meleira virus, an unusual plant virus. **Viruses**, 7, n. 4,
 1288 p. 1853-1870, 2015.
- 1289 ABREU, P. M. V.; PICCIN, J. G.; RODRIGUES, S. P.; BUSS, D. S.; VENTURA, J. A.;
 1290 FERNANDES, P. M. B. Molecular diagnosis of Papaya meleira virus (PMeV) from leaf
 1291 samples of *Carica papaya* L. using conventional and real-time RT-PCR. **Journal of**
 1292 **Virological Methods**, 180, n. 1, p. 11-17, 2012/03/01/ 2012.
- 1293 ANTUNES, T. F. S.; AMARAL, R. J. V.; VENTURA, J. A.; GODINHO, M. T.; AMARAL, J.
 1294 G.; SOUZA, F. O.; ZERBINI, P. A.; ZERBINI, F. M.; FERNANDES, P. M. B. The dsRNA
 1295 Virus Papaya Meleira Virus and an ssRNA Virus are Associated with Papaya Sticky
 1296 Disease. **PloS One**, 11, p. e0155240, 2016.
- 1297 ANTUNES, T. F. S.; MAURASTONI, M.; MADROÑERO, L. J.; FUENTES, G.;
 1298 SANTAMARÍA, J. M.; VENTURA, J. A.; ABREU, E. F.; FERNANDES, A. A. R.;
 1299 FERNANDES, P. M. B. Battle of Three: The Curious Case of Papaya Sticky Disease.
 1300 **Plant Disease**, 104, n. 11, p. 2754-2763, 2020.
- 1301 BENDIX, C.; LEWIS, J. D. The enemy within: phloem-limited pathogens. **Molecular Plant**
 1302 **Pathology**, 19, n. 1, p. 238-254, 2018.
- 1303 BOCCARDO, G.; LISA, V.; LUISONI, E.; MILNE, R. G. Cryptic plant viruses. **Advances**
 1304 **in Virus Research**, 32, p. 171-214, 1987.
- 1305 BRADAMANTE, G.; MITTELSTEN SCHEID, O.; INCARBONE, M. Under siege: virus
 1306 control in plant meristems and progeny. **The Plant Cell**, 33, n. 8, p. 2523-2537, 2021.
- 1307 DE FAY, E.; SANIER, C.; HEBANT, C. The distribution of plasmodesmata in the phloem
 1308 of *Hevea brasiliensis* in relation to laticifer loading. **Protoplasma**, 149, n. 2, p. 155-162,
 1309 1989/06/01 1989.
- 1310 FACCHINI, P. J.; DE LUCA, V. Opium poppy and Madagascar periwinkle: model non-
 1311 model systems to investigate alkaloid biosynthesis in plants. **The Plant Journal**, 54, n.
 1312 4, p. 763-784, 2008.
- 1313 FERNANDO, J. A.; MELO, M.; SOARES, M. K.; APPEZZATO-DA-GLÓRIA, B. Anatomy
 1314 of somatic embryogenesis in *Carica papaya* L. **Brazilian Archives of Biology and**
 1315 **Technology**, 44, p. 247-255, 2001.
- 1316 FEHÉR, A. Somatic embryogenesis - stress-induced remodeling of plant cell fate.
 1317 **Biochimica et Biophysica Acta - Gene Regulatory Mechanisms**, 2015.

- 1318 FINERAN, B. A. Differentiation of Non-articulated Laticifers in Poinsettia (*Euphorbia*
1319 *pulcherrima* Willd.). **Annals of Botany**, 52, n. 3, p. 279-293, 1983.
- 1320 FISHER, J. B. The vegetative and reproductive structure of papaya (*Carica papaya*).
1321 **Lyonia**, 1, n. 4, p. 191-208, 1980.
- 1322 GAMBINO, G.; DI MATTEO, D.; GRIBAUDO, I. Elimination of Grapevine fanleaf virus
1323 from three *Vitis vinifera* cultivars by somatic embryogenesis. **European Journal of Plant**
1324 **Pathology**, 123, n. 1, p. 57-60, 2009/01/01 2009.
- 1325 GAMBINO, G.; VALLANIA, R.; GRIBAUDO, I. In situ localization of Grapevine fanleaf
1326 virus and phloem-restricted viruses in embryogenic callus of *Vitis vinifera*. **European**
1327 **journal of plant pathology**, 127, n. 4, p. 557-570, 2010.
- 1328 HULL, R. Chapter 10 - Movement of Viruses Within Plants. *In*: HULL, R. (Ed.). **Plant**
1329 **Virology (Fifth Edition)**. Boston: Academic Press, 2014. p. 531-603.
- 1330 JOHNSON, A. R.; MOGHE, G. D.; FRANK, M. H. Growing a glue factory: Open questions
1331 in laticifer development. **Current Opinion in Plant Biology**, 64, p. 102096, 2021/12/01/
1332 2021.
- 1333 KITAJIMA, E. W.; RODRIGUES, C. H.; SILVEIRA, J. S.; ALVES, F.; VENTURA, J. A.;
1334 ARAGÃO, F. J. L.; OLIVEIRA, L. H. R. Association of isometric viruslike particles,
1335 restricted to laticifers, with "meleira" (sticky disease) of papaya (*Carica papaya*).
1336 **Fitopatologia Brasileira**, 18, p. 118, 1993.
1337
- 1338 KOEHLER, A. D. EMBRIOGÊNESE SOMÁTICA EM MAMOEIRO (*Carica papaya* L.):
1339 ANATOMIA, HISTOQUÍMICA E INFLUÊNCIA DE ACC, AVG E STS E DE PULSOS DE
1340 2,4-D. 2004. Universidade Federal de Viçosa, 2004.
- 1341 KOEHLER, A. D.; CARVALHO, C. R.; ABREU, I. S.; CLARINDO, W. R. Somatic
1342 embryogenesis from leaf explants of hermaphrodite *Carica papaya*: a new approach for
1343 clonal propagation. **African Journal of Biotechnology**, 12, n. 18, 2013.
- 1344 KUMAR, D.; KUMAR, R.; HYUN, T. K.; KIM, J.-Y. Cell-to-cell movement of viruses via
1345 plasmodesmata. **Journal of Plant Research**, 128, n. 1, p. 37-47, 2015/01/01 2015.
- 1346 LIU, J.; CARINO, E.; BERA, S.; GAO, F.; MAY, J. P.; SIMON, A. E. Structural Analysis
1347 and Whole Genome Mapping of a New Type of Plant Virus Subviral RNA: Umbravirus-
1348 Like Associated RNAs. **Viruses**, 13, n. 4, p. 646, 2021.
- 1349 MADROÑERO, J.; RODRIGUES, S. P.; ANTUNES, T. F. S.; ABREU, P. M. V.;
1350 VENTURA, J. A.; FERNANDES, A. A. R.; FERNANDES, P. M. B. Transcriptome analysis
1351 provides insights into the delayed sticky disease symptoms in *Carica papaya*. **Plant Cell**
1352 **Reports**, 37, n. 7, p. 967-980, 2018/07/01 2018.
- 1353 MAGAÑA-ÁLVAREZ, A.; VENCIONECK DUTRA, J. C.; CARNEIRO, T.; PÉREZ-BRITO,
1354 D.; TAPIA-TUSSELL, R.; VENTURA, J. A.; HIGUERA-CIAPARA, I.; FERNANDES, P. M.
1355 B.; FERNANDES, A. A. R. Physical Characteristics of the Leaves and Latex of Papaya

- 1356 Plants Infected with the Papaya meleira virus. **International Journal of Molecular**
1357 **Sciences**, 17, p. 574, 2016.
- 1358 MAURASTONI, M.; ANTUNES, T. F. S.; OLIVEIRA, S. A.; SANTOS, A. M. C.; VENTURA,
1359 J. A.; FERNANDES, P. M. B. A multiplex RT-PCR method to detect papaya meleira virus
1360 complex in adult pre-flowering plants. **Archives of Virology**, 165, n. 5, p. 1211-1214,
1361 2020/05/01 2020.
- 1362 NAKAGAWA, J.; TAKAYAMA, Y.; SUZUKAMA, Y. Exudação de látex pelo mamoeiro.
1363 Estudo de ocorrência em Teixeira de Freitas, BA. *In*: Congresso Brasileiro de Fruticultura,
1364 1987, **9**. p. 555-559.
- 1365 PATHANIA, N.; VALERIANA JUSTO; PABLITO MAGDALITA; FE DE LA CUEVA;
1366 LORNA HERRADURA; AIRA WAJE; ADELFA LOBRES; ARCANGEL CUETO; NATALIE
1367 DILLON; LYNTON VAWDREY; LOUISE HUCKS; DONNA CHAMBERS; GRACE SUN;
1368 CHEESMAN, J. Integrated disease management strategies for the productive, profitable
1369 and sustainable production of high quality papaya fruit in the southern Philippines and
1370 Australia (FR2019-89). ACIAR. Australia: Australian Centre for International Agricultural
1371 Research (ACIAR) 2019: 64 p. 2019.
- 1372 PELAH, D.; ALTMAN, A.; CZOSNEK, H. Tomato yellow leaf curl virus DNA in callus
1373 cultures derived from infected tomato leaves. **Plant Cell, Tissue and Organ Culture**, 39,
1374 n. 1, p. 37-42, 1994/10/01 1994.
- 1375 PEREZ-BRITO, D.; TAPIA-TUSSELL, R.; CORTES-VELAZQUEZ, A.; QUIJANO-
1376 RAMAYO, A.; NEXTICAPAN-GARCEZ, A.; MARTÍN-MEX, R. First report of papaya
1377 meleira virus (PMeV) in Mexico. **African Journal of Biotechnology**, 11, p. 13564-13570,
1378 2012.
- 1379 PICKARD, W. F. Laticifers and secretory ducts: two other tube systems in plants. **New**
1380 **Phytologist**, 177, n. 4, p. 877-888, 2008.
- 1381 RODRIGUES, C.; VENTURA, J.; MAFFIA, L. Distribuição e transmissão da meleira em
1382 pomares de mamão no Espírito Santo. **Fitopatologia Brasileira**, 14, p. 118, 1989.
- 1383 RODRIGUES, S. P.; DA CUNHA, M.; VENTURA, J. A.; FERNANDES, P. M. B. Effects
1384 of the Papaya meleira virus on papaya latex structure and composition. **Plant Cell**
1385 **Reports**, 28, p. 861-871, 2009.
- 1386 RODRIGUES, S. P.; VENTURA, J. A.; AGUILAR, C.; NAKAYASU, E. S.; CHOI, H.;
1387 SOBREIRA, T. J. P.; NOHARA, L. L.; WERMELINGER, L. S.; ALMEIDA, I. C.; ZINGALI,
1388 R. B.; FERNANDES, P. M. B. Label-free quantitative proteomics reveals differentially
1389 regulated proteins in the latex of sticky diseased *Carica papaya* L. plants. **Journal of**
1390 **Proteomics**, 75, p. 3191-3198, 2012.
- 1391 ROOSSINCK, M. J. Lifestyles of plant viruses. **Philosophical transactions of the Royal**
1392 **Society of London. Series B, Biological sciences**, 365, n. 1548, p. 1899-1905, 2010.
- 1393 ROOSSINCK, M. J. Plant virus ecology. **PLoS Pathog**, 9, n. 5, p. e1003304, 2013.

- 1394 SEO, J.-K.; KIM, K.-H. Long-Distance Movement of Viruses in Plants. *In*: WANG, A. e
1395 ZHOU, X. (Ed.). **Current Research Topics in Plant Virology**. Cham: Springer
1396 International Publishing, 2016. p. 153-172.
- 1397 SOARES, E.; WERTH, E. G.; MADROÑERO, L. J.; VENTURA, J. A.; RODRIGUES, S.
1398 P.; HICKS, L. M.; FERNANDES, P. M. B. Label-free quantitative proteomic analysis of
1399 pre-flowering PMeV-infected *Carica papaya* L. **Journal of Proteomics**, 151, p. 275-283,
1400 2016.
- 1401 TALIANSKY, M. E.; ROBINSON, D. J. Molecular biology of umbraviruses: phantom
1402 warriors. **Journal of General Virology**, 84, n. 8, p. 1951-1960, 2003.
- 1403 TAN, D.; HU, X.; FU, L.; KUMPEANGKEAW, A.; DING, Z.; SUN, X.; ZHANG, J.
1404 Comparative morphology and transcriptome analysis reveals distinct functions of the
1405 primary and secondary laticifer cells in the rubber tree. **Scientific Reports**, 7, n. 1, p.
1406 3126, 2017/06/09 2017.
- 1407 TAVARES, E. T.; TATAGIBA, J. S.; VENTURA, J. A.; SOUZA JR, M. T. Dois novos
1408 sistemas de diagnose precoce da meleira do mamoeiro. **Fitopatologia Brasileira**, 29,
1409 n. 5, p. 563-566, 2004.
- 1410 VENTURA, J. A.; COSTA, H.; TATAGIBA, J. D. S. Papaya Diseases and Integrated
1411 Control. *In*: NAQVI, S. A. M. H. (Ed.). **Diseases of Fruits and Vegetables: Volume II:
1412 Diagnosis and Management**. Dordrecht: Springer Netherlands, 2004. p. 201-268.
- 1413 YAMAMOTO, H.; TABATA, M. Correlation of papain-like enzyme production with laticifer
1414 formation in somatic embryos of papaya. **Plant Cell Rep**, 8, n. 4, p. 251-254, Apr 1989.
- 1415 ZENG, Y.; JI, B.; YU, B. Laticifer ultrastructural and immunocytochemical studies of
1416 papain in *Carica papaya*. **Acta Botanica Sinica**, 36, n. 7, p. 497-501, 1994.
- 1417

1418 **TABLES**

1419

1420 Table 1. Results of RT-PCR diagnosis monitoring PMeV complex
 1421 during somatic embryogenesis in *Carica papaya*

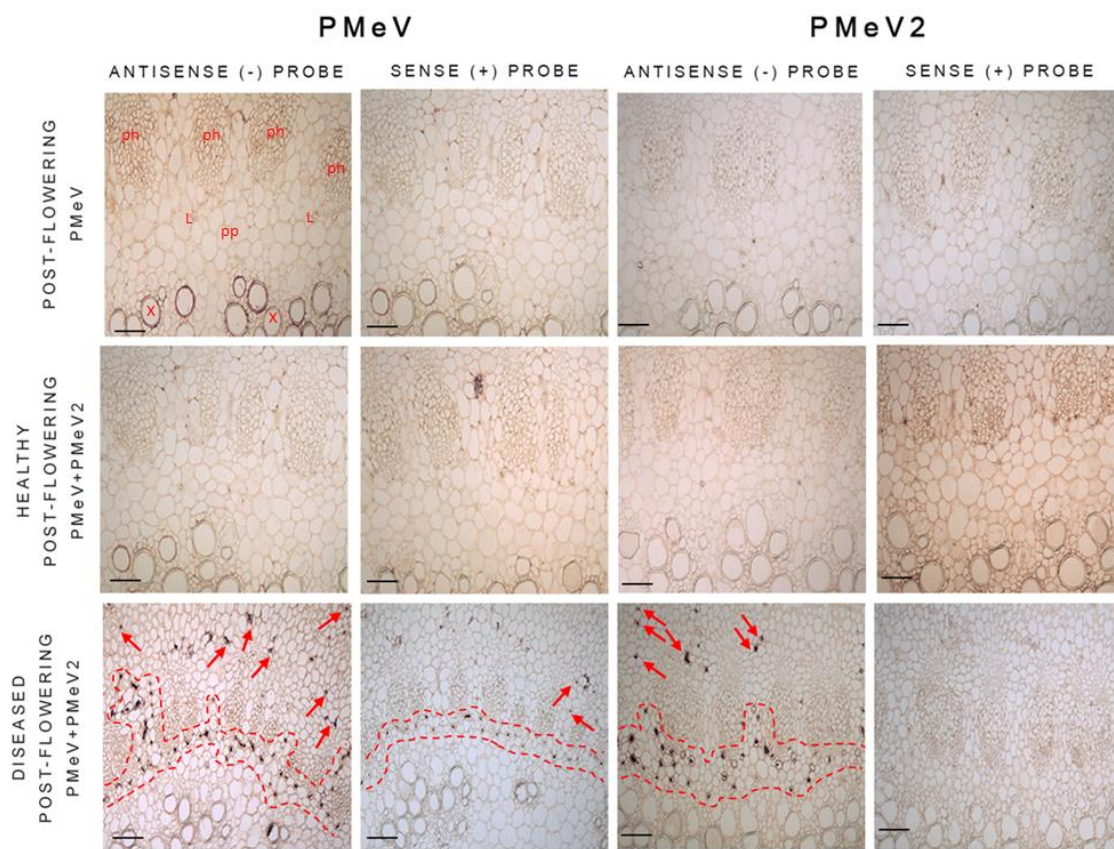
Plant material	No. infected/total	
	PMeV	PMeV2
Donor-plant	4/4	4/4
3-month-old calli	8/16	0/16
Embryogenic calli	6/6	6/6
SE-regenerated plants	16/16	16/16

1422

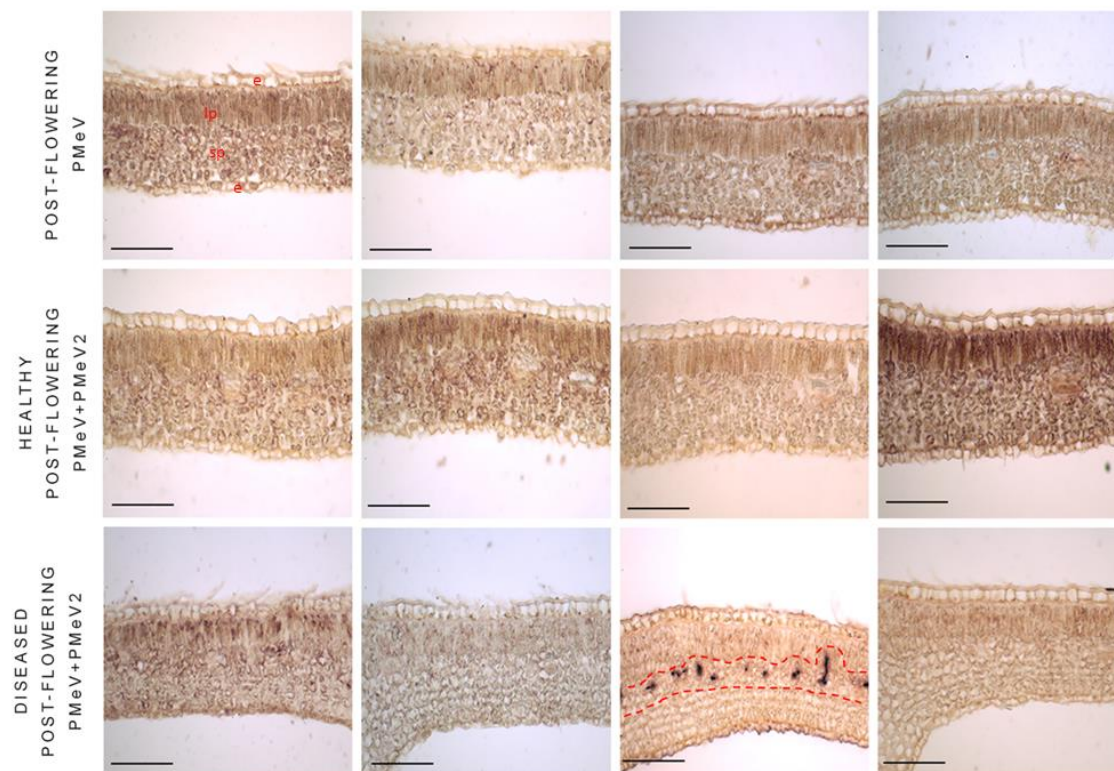
1423 **FIGURES**

1424

A

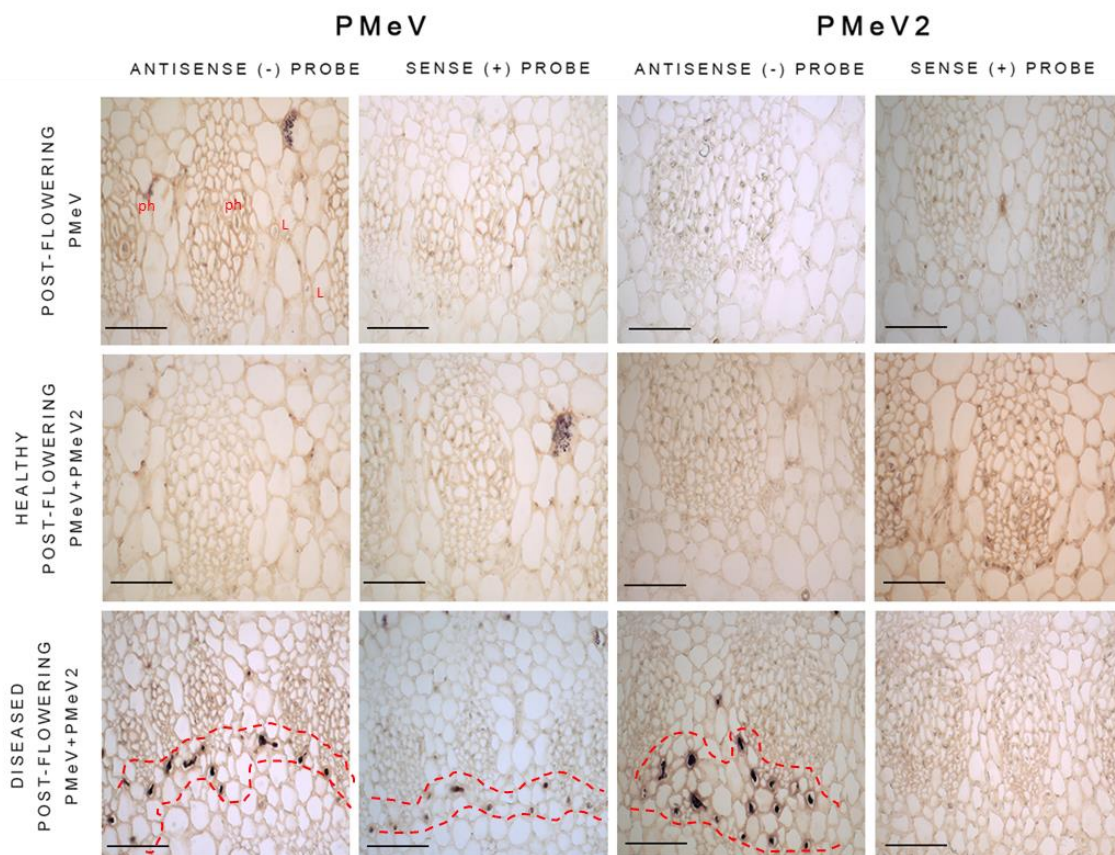


B

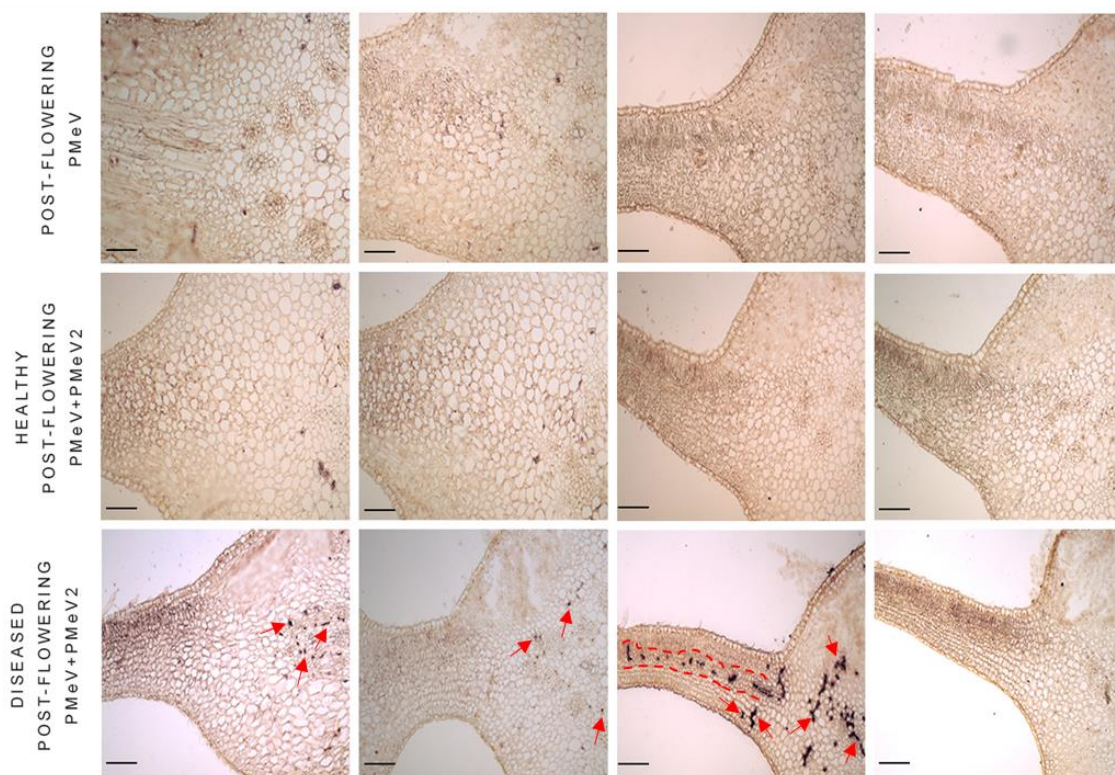


1426 Figure 1. PMeV complex localization in the main vein and mesophyll laticifers cells of *C. papaya*
1427 by *in situ* hybridization. Cross sections of main vein (**A**) and mesophyll (**B**) obtained from infected
1428 leaves were hybridized with a specific probe for PMeV and PMeV2 sense and antisense strand.
1429 Red arrows and dashed lines representing laticifers where the signal was visualized. ph: phloem;
1430 L: laticifer; x: xylem; pp: parenchyma; e: epidermis; lp: lacunar parenchyma; sp: spongy
1431 parechyma.
1432
1433

A

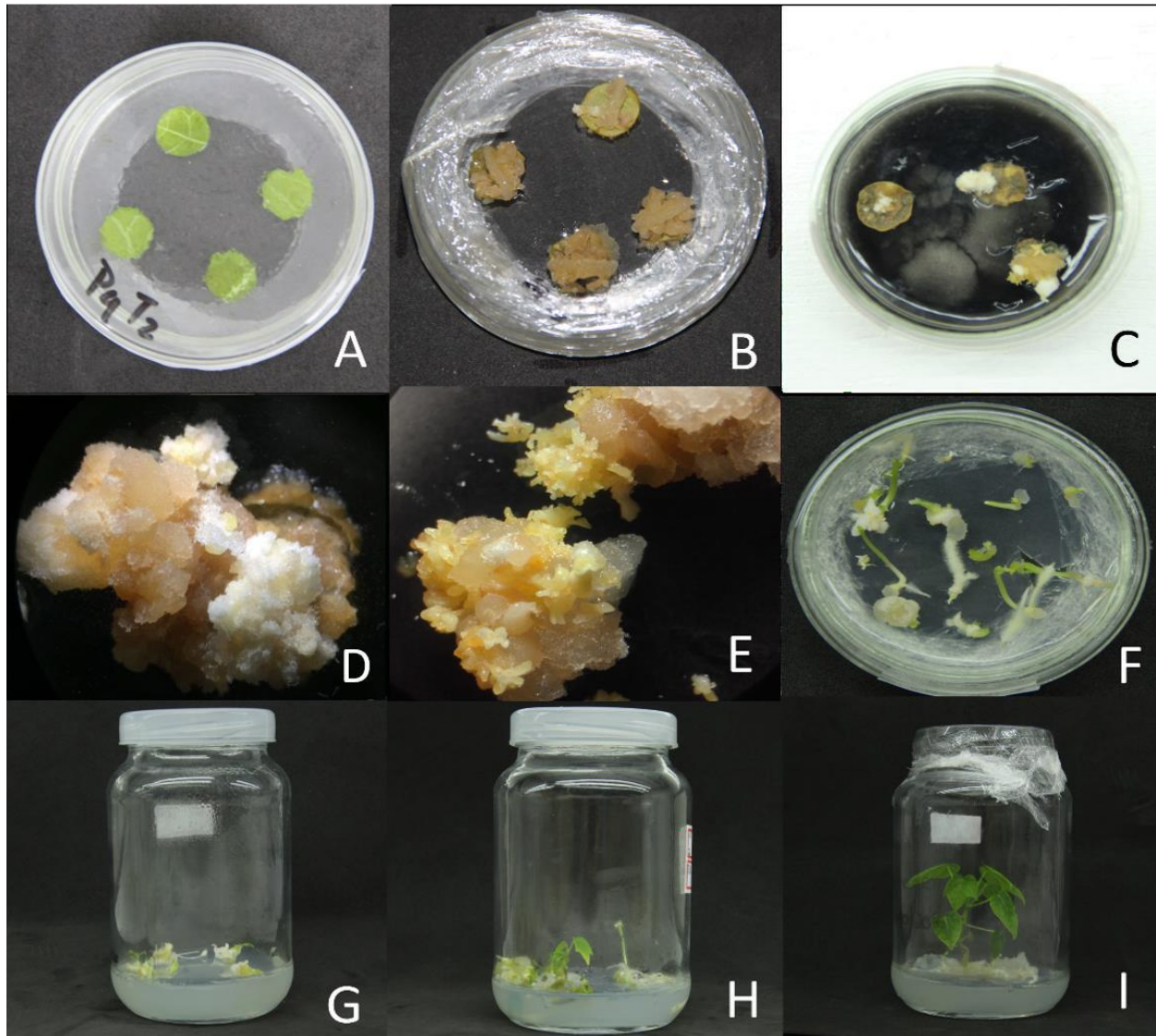


B



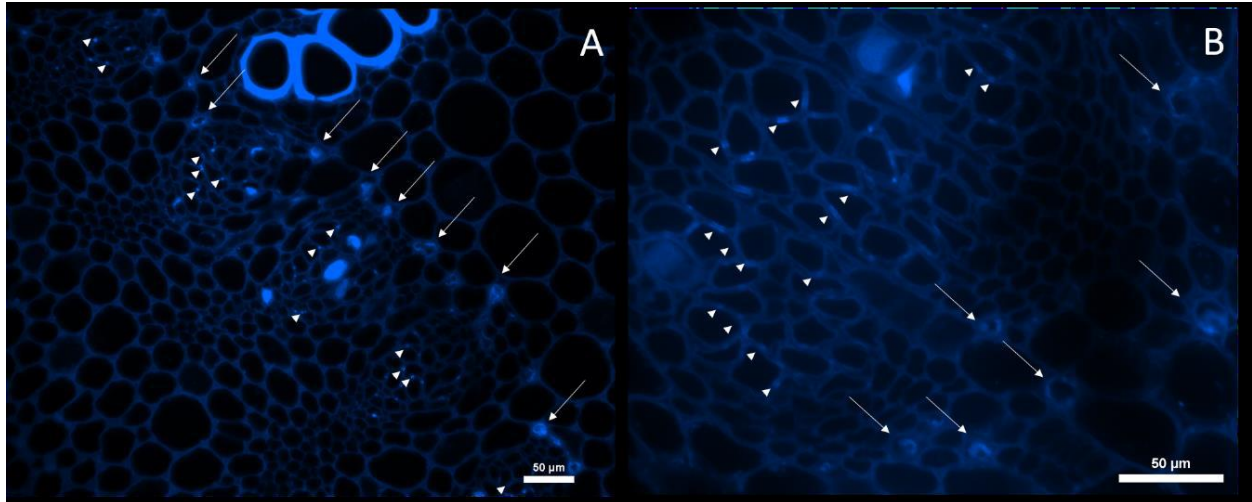
1435
1436
1437
1438
1439
1440
1441

Figure 2. PMeV complex localization in the main vein and mesophyll laticifers cells of *C. papaya* by *in situ* hybridization. Cross sections obtained from infected leaves were hybridized with a specific probe for PMeV and PMeV2 sense and antisense strand. **A.** Detail of phloem bundles of the main vein. **B.** Transitioning region of main vein to mesophyll. Red arrows and dashed lines representing laticifers where the signal was visualized. ph: phloem; L: laticifer.



1442
1443
1444
1445
1446
1447
1448
1449
1450
1451

Figure 3. Development stages of somatic embryogenesis in *Carica papaya*. **A.** Establishment of ES, from infected leaf discs grown in semi-solid medium supplemented with 2,4-D- at 1st day of cultivation. **B.** Callus proliferation in 45 days of cultivation. **C.** Proliferation of embryogenic calluses in semi-solid medium supplemented with activated carbon. **D.** Non-embryogenic callus. **E.** Embryogenic callus. **F.** Somatic embryos germinating in germination medium after 2 weeks of cultivation. **G-I.** The sequential growth process of papaya seedlings obtained by ES *in vitro*. **I.** Seedlings regenerated in basal MS medium, without the addition of growth regulators. 3-month-old callus (not shown), somatic embryogenic callus (E), and regenerated plants (I) were used for monitoring PMeV complex.



1452

1453 Figure 4. Identification of plasmodesmata in vascular tissue cells of *C. papaya* by aniline blue
1454 staining. Cross-sections obtained from leaves were observed under a fluorescence microscope.
1455 **A** and **B**. Visualization of plasmodesmata between phloem cells. No plasmodesmata are
1456 visualized between laticifers and adjacent cells. White arrowheads: plasmodesmata stained with
1457 aniline blue; white arrows: laticifers.

1458

1459 **SUPPLEMENTARY MATERIAL**

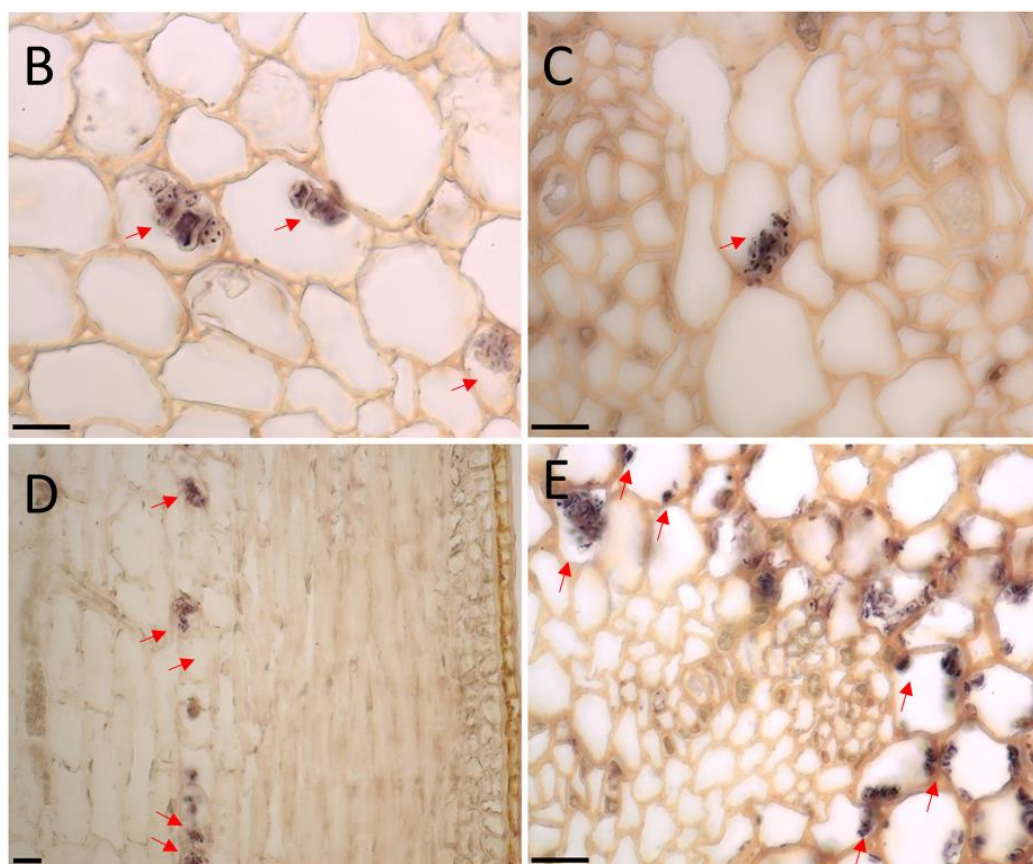
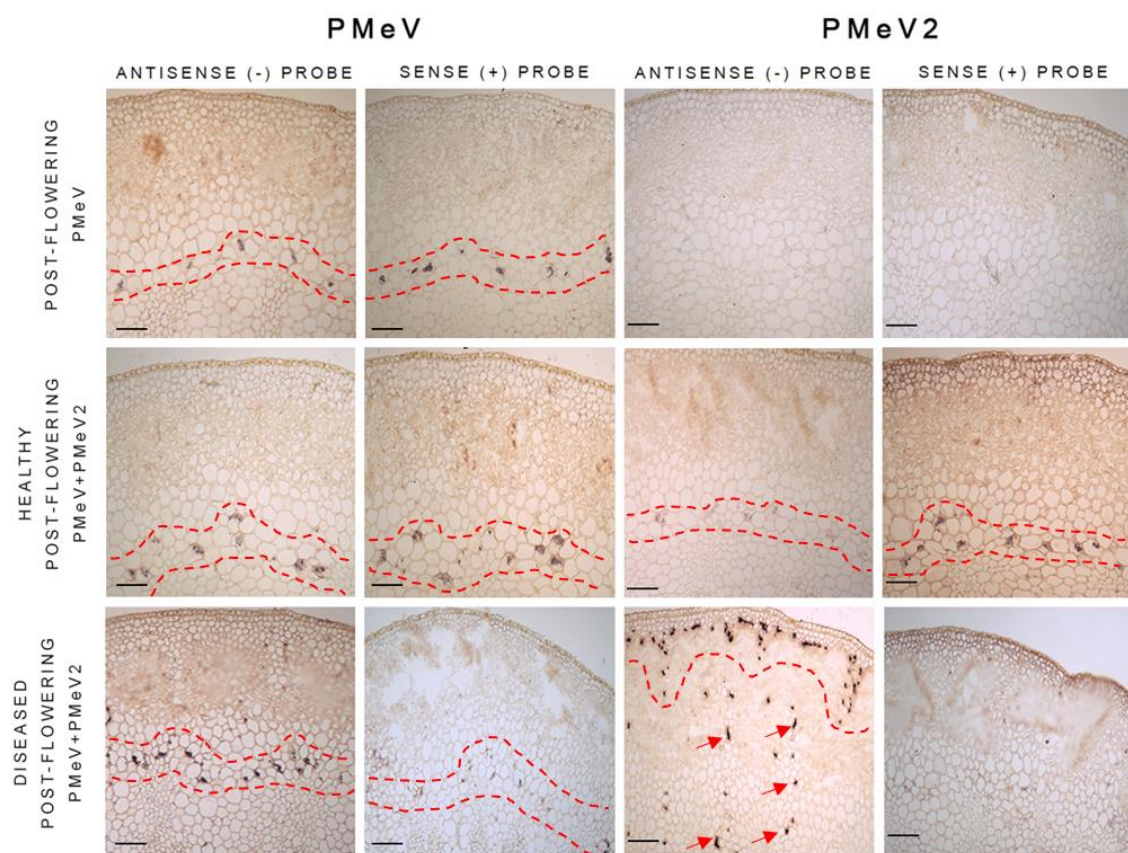
1460

1461 Figure S1. Hybridization signal observed in structures that resemble plastids. **A.** Signal is
1462 distributed as a ring near to the epidermis in cross sections of the main vein. **B.** Detail of
1463 parenchyma cells near to the epidermis. **C.** Detail in parenchyma cells between two
1464 phloem bundles. **D.** Longitudinal section of the parenchyma near to the main vein
1465 collenchyma. **E.** Transversal section of the transition between main vein to mesophyll.

1466

1467

A



1469 **MANUSCRIPT #3. A CAPSID PROTEIN FRAGMENT OF PAPAYA MELEIRA**
1470 **VIRUS (PMeV), A TOTI-LIKE VIRUS FOUND IN PAPAYA LATEX INTERACTS WITH**
1471 **THE 50S RIBOSOMAL PROTEIN L17**

1472

1473 Manuscript in preparation for *Molecular Plant Pathology* (ISSN 1464-6722; IF 5.663, 2021;
1474 Qualis A1 Biotecnologia 2013-2016)

1475

1476

1477 **A capsid protein fragment of papaya meleira virus (PMeV), a toti-like virus found in**
1478 **papaya latex interacts with the 50S ribosomal protein L17**

1479

1480

1481 **Marlonni Maurastoni**¹, Tathiana F. Sá-Antunes¹, Emanuel F. Abreu², Angela Mehta²,
1482 Marcio M. Sanches², W. Fontes³, Fabiano T. Cruz¹, Alexandre M. C. Santos¹, Francisco
1483 J. L. Aragão², Elliot W. Kitajima⁴, Simone G. Ribeiro², Francisco M. Zerbini⁵, Anna E.
1484 Whitfield⁶ and Patricia M. B. Fernandes¹

1485

1486 ¹Núcleo de Biotecnologia, Universidade Federal do Espírito Santo, Vitória, Espírito Santo,
1487 Brazil;

1488 ²Embrapa Recursos Genéticos e Biotecnologia, Brasília, DF, 70770-900, Brazil

1489 ³Toxinology Laboratory, Department of Physiological Sciences, University of Brasilia,
1490 Brasilia/DF, Brazil, 70.910-900

1491 ⁴Escola Superior de Agricultura Luiz de Queiroz, Universidade de São Paulo, CEP,
1492 Piracicaba, SP, 13418-400, Brazil

1493 ⁵Dep. de Fitopatologia/BIOAGRO, Universidade Federal de Viçosa, 36570-900, Viçosa,
1494 Minas Gerais, Brazil.

1495 ⁶Department of Entomology and Plant Pathology, North Carolina State University, 840
1496 Main Campus Drive, Raleigh, NC 27606, USA

1497

ABSTRACT

1498

1499

1500

1501 An unusual trans-encapsidation phenomenon is observed in the PMeV complex, the
1502 association of a totivirus-like and a umbravirus-like associated RNA (ulaRNA), papaya
1503 meleira virus (PMeV), and papaya meleira virus 2 (PMeV2), respectively. Both viruses are
1504 encapsidated by particles produced by PMeV coat protein (CP) which is a translation
1505 product of the putative PMeV ORF1, predicted to encode a polypeptide of 177kDa. In
1506 previous work, purification from papaya latex by sucrose gradient followed by mass
1507 spectrometry analysis identified nine peptide fragments accounting for 8% of the PMeV
1508 ORF1 predicted amino acid sequence (125 of 1563 aa) and encompassing the central
1509 region of the putative protein (from aa 356 to 785). However, the structural proteins of
1510 PMeV capsid remain unknown. In this work, an additional purification step, a cesium
1511 chloride gradient, resulted in obtaining high- and low-density fractions that both enriched
1512 for viral particles with similar morphology as visualized by transmission electron
1513 microscopy. The separation of these fractions by SDS-PAGE revealed the presence of
1514 two major polypeptides with a molecular mass of ~40kDa and ~55kDa. Peptide mass
1515 fingerprint analysis of both bands revealed overlapping peptides that match with the PMeV
1516 ORF1 increasing its coverage to the N-terminal side. To identify interactions between
1517 PMeV capsid protein and plant proteins, a yeast two-hybrid assay identified several
1518 *Arabidopsis* proteins potentially interacting with a fragment of these polypeptides. A PPI
1519 network using differentially accumulated proteins of PMeV complex host (*Carica papaya*)
1520 and PMeV CP fragment-interacting protein shows the 50S ribosomal protein L17 family
1521 protein (RPL17) as an important player potentially associated with modulated translation-
1522 related proteins. The AtRPL17 co-localizes with PMeV CP fragment when transiently
1523 expressed and shows interaction with PMeV CP fragment in vivo by BiFC and yeast two-
1524 hybrid. We speculate that the interaction of capsid protein with RPL17 could be an
1525 important player in the totivirus-like virus-plant interactions.

1526

1527 Keywords: totivirus; protein-protein interaction; coat protein.

1528

1529

1530 **INTRODUCTION**

1531

1532

1533 Additional functions have been reported for coat proteins (CP) of plant viruses in addition
1534 to protection of the viral genome. The multifunctional nature of a CP is observed in its
1535 roles as participating in the virus cell-to-cell and systemic movement, component of
1536 genome transcription and replication complex, modulating host defense pathways, and
1537 processing host mRNA (A. CALLAWAY *et al.*, 2001; BOL, 2008; HERRANZ *et al.*, 2017;
1538 VAIRA *et al.*, 2018). Dimers of a single CP are the building blocks of icosahedral capsids,
1539 mainly found among dsRNA viruses which usually need the enclosed structure to avoid
1540 host cell defense mechanisms. This T = 1 capsid, comprised of 120 subunits of 60
1541 asymmetrical polypeptides, are found in members of the families *Reoviridae*,
1542 *Picobirnaviridae*, and *Cystoviridae*, and in the mycoviruses of the families *Totiviridae*,
1543 *Partitiviridae*, and *Megabirnaviridae* (LUQUE *et al.*, 2018).

1544 Most of our knowledge regarding non-structural functions of totiviruses capsids relies on
1545 *Saccharomyces cerevisiae L-A virus* (ScV-L-A), the type species of the genus *Totivirus*
1546 (family *Totiviridae*). A remarkable function is performed by this virus and its host cell. To
1547 avoid viral RNA degradation by host exoribonuclease, ScV-L-A decaps the 7-
1548 methylguanosine 5'-monophosphate (m7GMP) from host mRNA hijacking it for its RNAs.
1549 This enzymatic activity is performed by the segment Gln139-Ser182 of ScV-LA capsid
1550 (FUJIMURA; ESTEBAN, 2011). To date, only a few totiviruses have been found infecting
1551 plants (AKINYEMI *et al.*, 2018; GUO *et al.*, 2016; ZHANG *et al.*, 2021). Our main
1552 understanding of how plants respond to totiviruses comes from the papaya sticky disease
1553 (PSD) pathosystem which has been studied at the biochemical and molecular level
1554 (ABREU *et al.*, 2015; MADROÑERO *et al.*, 2018; RODRIGUES *et al.*, 2011; RODRIGUES
1555 *et al.*, 2012; SÁ ANTUNES; *et al.*, 2020; SOARES *et al.*, 2016). Proteomic and
1556 transcriptomic analysis of infected *Carica papaya* plants shows a tolerance mechanism to
1557 symptoms before flowering, mainly related to changes in hormone-responsive genes,
1558 protein turnover, and chloroplast-related proteins. Although we know the effect of infection

1559 on the accumulation of proteins and transcripts, there is still a lack of information about
1560 the key aspects of the plant-virus interaction and data on the viral protein-plant protein
1561 interactions, which hinders the development of more effective strategies to control PSD.

1562 The PSD is associated with the PMeV complex which is comprised of papaya meleira
1563 virus (PMeV), a toti-like dsRNA virus, and papaya meleira virus 2 (PMeV2), a umbravirus-
1564 like associated RNA (ulaRNA) ssRNA virus (LIU *et al.*, 2021). Similar to the virus-virus
1565 interaction between the dsRNA yadokari virus 1 (YkV1) and the positive-sense single-
1566 stranded [(+) ssRNA] yadonushi virus 1 (YnV1) (DAS *et al.*, 2021), a trans-encapsidation
1567 phenomenon is observed between the PMeV complex as they are both encapsidated in
1568 particles formed by PMeV CP. The full-length PMeV ORF1 is predicted to encode a
1569 polypeptide of 1563 aa which is 20-26% identical to analogous proteins found in
1570 mycoviruses, but these putative proteins have no significant matches in protein
1571 databases. The PMeV CP is known to be part of the predicted PMeV ORF1 polypeptide
1572 (ANTUNES *et al.*, 2016). Although the precise PMeV CP sequence remains unknown,
1573 virus purification from papaya latex by sucrose gradient followed by mass spectrometry
1574 analysis identified nine peptide fragments accounting for 8% of the PMeV ORF1 predicted
1575 amino acid sequence (125 of 1563 aa) encompassing the central region of the putative
1576 protein (from aa 356 to 785) (ANTUNES *et al.*, 2016).

1577 We report herein that PMeV capsid, coded by PMeV ORF1, contains two major
1578 polypeptides with overlapping sequences. We sought to identify *Arabidopsis* proteins that
1579 interact with two fragments of PMeV ORF1 by using a yeast two-hybrid (Y2H) assay which
1580 identified 28 interacting proteins mostly targeted to the chloroplast. We also built a protein-
1581 protein interaction (PPI) network showing that PMeV capsid can be indirectly responsible
1582 for the modulation of several proteins during pre- and post-flowering stages of infected
1583 papaya plants. We speculate that one of these proteins, a 50S ribosomal protein L17
1584 family protein (RPL17) can be an important target to modulate virus infection.

1585

1586

1587

1588 **METHODS**

1589

1590

1591 **Virus purification and polypeptide composition**

1592

1593

1594 Sucrose gradient purification was performed according to (ANTUNES *et al.*, 2016).
1595 Additional purification was performed by layering all the three fractions collected from the
1596 sucrose gradient onto a 50% (w/w) CsCl gradient and centrifuged for 18 h at 145,000 g.
1597 Fractions were collected and centrifuged again for 3.5 h at 35,000 g. The final pellet was
1598 resuspended in 0.01M borate buffer pH 9.0. To visualize viral particles, viral preparations
1599 were negatively stained in 2% (w/v) potassium phosphotungstate, pH 6.8, and observed
1600 in a JEOL JEM-1011 transmission electron microscope (TEM).

1601 To determine the composition of structural proteins, preparations of CsCl purified virions
1602 were applied to a 15% (w/v) polyacrylamide gel after boiling in Laemmli buffer (LAEMMLI,
1603 1970). Following electrophoresis, the gel was stained overnight with 0.1% (w/v)
1604 Coomassie blue and destained for 1 h to visualize the separated proteins. The molecular
1605 mass of the proteins was estimated from the measurement of electrophoretic mobilities
1606 (WEBER; OSBORN, 1969). Polypeptides p40 and p55 obtained in the gel from M fraction
1607 were subjected to in situ digestion according to Shevchenko *et al.* (2006) and subsequent
1608 mass spectrometry analysis using a Bruker Autoflex II TOF/TOF instrument (Bruker
1609 Daltonics, Bremen, Germany). Samples were resuspended in acetonitrile/water (1:1, v/v)
1610 containing TFA 0.1% (v/v), and 1 μ L of sample was applied to a stainless-steel plate with
1611 1 μ L of HCCA (10 mg/mL). The data were analyzed using MASCOT software (Matrix
1612 Sciences, Chicago, IL, USA). The search parameters used were: type of search as peptide
1613 mass fingerprint, enzyme as trypsin, fixed modification as carbamidomethyl (C), variable
1614 modification as oxidation (M), mass values as monoisotopic, protein mass as unrestricted,
1615 peptide mass tolerance as \pm 200 ppm, peptide charge state as 1+ and max missed
1616 cleavages as 1. Search results with significant MASCOT scores (>90) were taken into
1617 consideration to identify the peptides matching with the predicted PMeV ORF1. To avoid
1618 missing any proteins during viral preparation, crude virion preparations of M fraction

1619 obtained after the sucrose gradient were subjected to protein extraction according to
1620 Carmo *et al.* (2013) and its peptides were identified as described above.

1621

1622

1623

1624 **Secondary structure prediction**

1625

1626

1627 The secondary structure prediction was done with five different prediction tools Frag1D,
1628 Porter 5.0, PsiPred, RaptorX, and SOMPA and a consensus structure was generated
1629 using the combined results.

1630

1631

1632

1633 **Cloning of PMeV ORF1 and AtRPL17**

1634

1635

1636 To generate a PMeV ORF1 clone, total RNA was extracted from 100 µl of a pool of latex
1637 obtained from PSD plants using TRIzol® reagent (Thermo Fisher Scientific, Waltham, MA,
1638 USA), according to the manufacturer's protocol. One microgram of total RNA was treated
1639 with DNase I (Thermo Fisher Scientific, Waltham, MA, USA) and used for cDNA synthesis
1640 using Superscript III Reverse Transcriptase and the sequence-specific reverse primer
1641 according to the manufacturer's instructions. PCR was performed using Platinum High
1642 Fidelity DNA Polymerase (Invitrogen, Waltham, MA, USA) and specific primers following
1643 the manufacturer's instructions in a Mastercycler Thermocycler (Eppendorf, Hamburg,
1644 Germany). PCR amplicon was visualized on 1% agarose gel, excised, and purified using
1645 PureLink™ Quick Gel Extraction Kit (Thermo Fisher Scientific, Waltham, MA, USA). The
1646 amplicon was cloned into Gateway™ pDONR™221 Vector and the whole clone was
1647 submitted to Sanger sequencing. The clone was named pDONR™221-PMeVORF1. To
1648 generate PMeV ORF1 fragments, a total of 10 primers pairs were designed based on the
1649 pDONR™221-PMeVORF1 sequence. AtRPL17 full-length gene was amplified from a

1650 pGADT7 plasmid recovered from an *Arabidopsis* cDNA library in yeast. The plasmid was
1651 sequenced and compared against the NCBI database. Amplicons from both PMeV ORF1
1652 fragments and *AtRPL17* were cloned into pENTR-D/TOPO then recombined to yeast and
1653 plant expression vectors using Gateway cloning techniques. Primers used in this work are
1654 listed in the supplementary material (Supplementary materials Table S1).

1655

1656

1657

1658 **Binary interactions and library screening using yeast two-hybrid assay**

1659

1660

1661 A yeast two-hybrid system (Y2H) was used to test binary interactions between PMeV
1662 ORF1 fragments. We recombined a pENTR-D/TOPO clone containing a PMeV ORF1
1663 fragment with the pDESTGADT7 and pDESTGBKT7 destination vectors to generate a
1664 protein fused to the GAL4 activating domain (AD) and -binding domain (BD). Briefly, the
1665 yeast reporter strain Y2HGold (Takara Bio Inc., Kusatsu, Shiga, Japan) was co-
1666 transformed with both AD- and BD- plasmids according to the manufacturer's instruction.
1667 Co-transformants were selected by culture on double dropout media (DDO), i.e. synthetic
1668 defined minimal media (SD) lacking leucine and tryptophan (SD/-L/-W). Positive
1669 interactions were selected by culture on quadruple dropout media, i.e. SD lacking leucine,
1670 tryptophan, adenine, and histidine, (SD/-L/-W/-H/-A/-). We co-transformed plasmids
1671 containing GAL4 DNA-BD fused with murine p53 (pGBKT7-p53) plus GAL4 AD fused with
1672 SV40 large T-antigen (pGADT7-T) as positive control and GAL4 BD fused with lamin
1673 (pGBKT7-Lam) plus pGADT7-T as a negative control. We also tested the autoactivation
1674 of each fragment by co-transforming BD and AD plasmids with empty plasmids. An
1675 overnight culture of all co-transformants was normalized to OD₆₀₀ 2, spotted in DDO and
1676 QDO/X/A (QDO media supplemented with Aureobasidin A and the chromogenic substrate
1677 X-alpha-gal) plates, and kept at 30°C for 4 days. The entire experiment was performed
1678 three times.

1679 Yeast two-hybrid library screening was performed using the Matchmaker® Mate & Plate
1680 Two-Hybrid System (Takara Bio Inc., Kusatsu, Shiga, Japan). To choose the bait, we
1681 performed an expression assay in yeast following the manufacturer's instructions.
1682 Plasmids containing the fragments fused to GAL4 BD were transformed in the yeast strain
1683 Y2HGold according to the manufacturer's protocol and spread on single dropout media
1684 (SDO), i. e. SD lacking tryptophan (SD/-W). Protein expression was induced by growing
1685 the positive transformants on YPD media. Yeast proteins were extracted according to
1686 Kushnirov (2000) and normalized to the equivalent of 2-3 OD₆₀₀ units. The expression of
1687 fused proteins was verified by SDS-PAGE and Western blotting assay using mouse anti-
1688 myc monoclonal antibody (Invitrogen, Waltham, Massachusetts) at 2: 10,000 dilution
1689 followed by incubation with a goat anti-mouse IgG (H+L)-HRP Conjugated (Biorad,
1690 Hercules, California) at 1: 10,000 dilution according to standard protocols.

1691 A normalized cDNA *Arabidopsis* library fused to GAL4 AD in the yeast strain Y187 (Mate
1692 & Plate™ Library - Takara Bio Inc., Kusatsu, Shiga, Japan) was used to mate with
1693 Y2HGold containing the ORF1 fragment 4 fused to GAL4 BD. Cells were initially screened
1694 on 60 150mm plates containing DDO/X/A media. Then, 306 blue colonies were patched
1695 on QDO/X/A media and QDO/X/A media supplement with 2.5mM and 5mM of 3-Amino-
1696 1,2,4-triazole (3-AT). Plasmids from colonies picked from all media were extracted from
1697 yeast, recovered in *Escherichia coli*, sequenced, and identified.

1698 A total of 28 unique plasmids were transformed in yeast with an empty GAL4 BD plasmid
1699 and fragment 4 AD-containing plasmid to test autoactivation and interaction, respectively.
1700 Given that most of our peptides obtained in the mass spectrometry analysis covered the
1701 fragment 2, we took advantage of the interaction between fragment 4 and fragment 2 (see
1702 results section) and also tested the 28 unique plasmids interaction with fragment 2.
1703 Positive interactors were spotted in DDO, QDO/X/A, and QDO/X/A supplemented with
1704 0mM, 1mM, 2.5mM, and 5mM of 3-AT media. The interaction of pGBKT7-p53 and
1705 pGADT7-T was used as positive control and pGBKT7-Lam and pGADT7-T as a negative
1706 control. The experiment was performed three times.

1707

1708

1709

1710 Protein-protein interaction network

1711

1712

1713 A protein-protein interaction network was constructed with differentially modulated
1714 proteins of PMeV complex-infected papaya at 4- and 7-months post-germination
1715 (SOARES et al., 2016), and PMeV ORF1 fragment 2 and 4-interacting proteins. Biomart
1716 (<https://phytozome.jgi.doe.gov/biomart/>) was used to obtain *Arabidopsis* orthologues from
1717 the Phytozome database (<http://phytozome.jgi.doe.gov/>) in April 2021. Sequences were
1718 uploaded on String (SZKLARCZYK et al., 2018) and an interaction network of high
1719 confidence level was exported to Cytoscape (SHANNON et al., 2003).

1720

1721

1722

1723 Transient expression and detection of protein interaction in *Nicotiana benthamiana*

1724

1725

1726 To identify the interaction of PMeV capsid protein and RPL17 in vivo, we first aimed to
1727 localize RPL17 and PMeV fragment 2 in plant cells fusing proteins to red or green
1728 fluorescent proteins. For EGFP fusions, we used the binary plasmids pSITE-2CA and
1729 pSITE-2NB and for RFP fusions we used pSITE-4CA and pSITE-4NB. “-CA” or “-NB”
1730 indicates that the plasmid allows cloning of fluorescent protein fused to the N-terminus
1731 and C-terminus of the desired protein, respectively (CHAKRABARTY et al., 2007). For the
1732 bimolecular fluorescence complementation (BiFC) assay, we recombined *AtRPL17* and
1733 ORF1 fragment 2 into the BiFC vectors (pSITE-nen, pSITE-cen, pSITE-nec, pSITE-cec)
1734 as fusions either the C- or N-terminal sequence of both halves of the eYFP gene (MARTIN
1735 et al., 2009). As a negative control, we challenged fragment 2 with Glutathione S-
1736 transferase (GST) fusions to YFP halves. A positive interaction was considered if the
1737 fluorescence was above the observed as for the negative control and if at least 50 cells
1738 with similar localization signal for the interaction were visualized. For *Agrobacterium*-
1739 mediated expression, an overnight culture of *A. tumefaciens* cells containing the plasmids

1740 was inoculated in a fresh media containing the appropriated antibiotics and brought to
1741 standard concentration ($OD_{600}=0.5-1.0$) in 10mM MES buffer, pH 5.6, containing 10mM
1742 $MgCl_2$. The culture was incubated for at least 2 h at 28°C with no agitation in the presence
1743 of 200 μ M acetosyringone (Sigma-Aldrich, St. Louis, MO, USA).

1744 Agroinfiltration was performed using 1 ml syringes without a needle on the abaxial side of
1745 *N. benthamiana* leaves wild type or transgenic expressing the histone 2B protein fused to
1746 RFP (MARTIN *et al.*, 2009). Leaves were analyzed for five days after agroinfiltration.
1747 Transient expression and localization of fluorescent fusion proteins, EGFP, RFP, or YFP
1748 in leaf cells of *N. benthamiana* were visualized using BioTek ® Cytation 5 image reader.
1749 Images were analyzed in Gen5 version 3.04 Microplate reader and imager software. This
1750 experiment was performed three times, with a least two leaves per infiltration treatment.

1751

1752

1753

1754 RESULTS

1755

1756

1757 **PMeV capsid is composed of two major polypeptides with overlapping sequences**

1758

1759

1760 To determine the composition of PMeV capsid, virus particles were purified using sucrose
1761 gradient centrifugation followed by a CsCl isopycnic gradient purification. Three
1762 opalescent zones, as reported by Antunes *et al.* (2016), were visible in the sucrose
1763 gradient. The additional purification in the CsCl gradient yielded bands for the top and
1764 bottom fraction, while the middle fraction appeared as a zone (Figure 1.A). The presence
1765 of nucleic acid in these bands was confirmed through RNA extraction from each fraction
1766 (Figure 1.B). Fraction B contained a single band of the approximate size of PMeV. RNAs
1767 extracted from fraction M present a band of the approximated size of PMeV2 and a smear
1768 above this band. The presence of PMeV and PMeV2 was also confirmed by visualization
1769 of viral particles by transmission electron microscopy (Figure 1.C). Fraction M contained

1770 a higher number of particles compared to fraction B, which shows a fibrillary material
1771 associated with them. No nucleic acid or viral particle was obtained for the top fraction.
1772 Purified virions from both B and M fractions showed two major polypeptides after SDS-
1773 PAGE with a molecular mass of approximately 55kDa and 40kDa, named p55 and p40
1774 (Figure 1.D). Mass spectrometry analysis from both p40 and p50 shows an accumulation
1775 of overlapping peptides extending from aa 287 to 731 (Figure 3.E). Three additional minor
1776 bands of higher molecular mass, named p68, p85, and p100, and several minor bands
1777 below p40 were also visualized, but no matches with PMeV or PMeV2 sequences were
1778 obtained for these polypeptides.

1779

1780

1781

1782 **PMeV ORF1 predicted protein is mostly composed of alpha-helix**

1783

1784

1785 A consensus sequence based on the secondary structure prediction of five prediction tools
1786 was built for PMeV ORF1 (Figure 2). PMeV ORF1 has 34 alpha helixes, 39 beta-sheets,
1787 and 11 non-consensus structures, which account for 22.3 %, 11.3 %, and 3.3 % of the
1788 whole sequence, respectively. Three low complexity regions extending from aa 105 to
1789 125, 214 to 227, and 1260 to 1270 are also found in the sequence. No other domains are
1790 found in protein database.

1791

1792

1793

1794 **A central region of the PMeV complex capsid protein interacts with a PMeV ORF1**
1795 **fragment (aa 961-1200)**

1796

1797

1798

1799 To determine dimerization regions on PMeV capsid protein, we tested binary interactions
1800 of the full length and five non-overlapping fragments of PMeV ORF1 using a yeast two-
1801 hybrid system (Takara®) (Figure 3.A). ORF1 fragments for expression in yeast were
1802 selected based on secondary structure (no disruption of predicted alpha-helix or beta
1803 strands, i.e., the fragments start and end at random coil regions), and peptide coverage
1804 of the polypeptide obtained from purified particles. The five non-overlapping fragments
1805 tested were named CP1 (aa 1 to 320), CP2 (aa 321 to 670), CP3 (aa 671-960), CP4 (aa
1806 961-1200), and CP5 (aa 1201-1563). Binary interactions were identified between CP2 and
1807 CP4, CP3 and CP4, and a self-interaction for CP4. No interaction was identified for the
1808 full-length protein, CP1 or CP5.

1809

1810

1811

1812 ***Arabidopsis* library screening using 961-1200 ORF1 fragment identified 28 plant**
1813 **interacting proteins**

1814

1815

1816 A commercial *Arabidopsis* cDNA library (Mate & Plate™ Library - Takara Bio Inc., Kusatsu,
1817 Shiga, Japan) was used to identify host proteins interacting with PMeV ORF1 fragments.

1818 The best candidate to use as bait was determined after testing the expression of each
1819 fragment fused to the GAL4-binding domain (Figure 4.B). Although most of the peptides
1820 identified from the mass spectrometry assay obtained from the major polypeptides match
1821 with CP2, this fragment showed a lower level of expression when compared to CP4.

1822 Moreover, given that CP4 interacts with CP2 in our binary yeast two-hybrid assay, we
1823 decided to use CP4 as bait and validate the interactors with both fragments. Using a
1824 GAL4-based yeast two-hybrid system, independent yeast transformants were screened
1825 using CP4 as bait. Three hundred six colonies, 36 and 48 were screened from QDO/X/A
1826 supplement with 0mM, 2.5mM, and 5mM of 3-AT, respectively. From 48 colonies
1827 sequenced, 28 represented unique sequences that also interact with CP2 (Table 1;
1828 Supplementary Materials Figure S1). A functional categorization analysis shows that most
1829 proteins are targeted to the chloroplast and have protein binding and catalytic activity (data
1830 not shown).

1831

1832

1833

1834

1835 **CP2 putatively associates with translation-related proteins differentially modulated**
1836 **in pre-flowering papaya**

1837

1838 *Arabidopsis* orthologues were obtained from a list of differentially accumulated proteins of
1839 pre-and post-flowering PMeV complex-infected *C. papaya* and submitted to protein-
1840 protein interaction (PPI) analysis. From 130 differential accumulated proteins at pre-
1841 flowering, it was possible to retrieve 101 orthologues in *Arabidopsis* (Supplementary
1842 Materials Table S2), while at post-flowering 123 *Arabidopsis* proteins were obtained from
1843 160 differential accumulated proteins (Supplementary Materials Table S3). Two PPI
1844 networks were built including the 28 CP2 and CP4-interacting proteins (Figure 4 and
1845 Supplementary Materials Table S4 and S5). In both networks, *AtRPL17* appears
1846 consistently predicted to interact with several modulated proteins, mainly translation-
1847 related proteins.

1848

1849

1850

1851

1852 **CP2 and *AtRPL17* co-localize and interact in *Nicotiana benthamiana* cells**

1853

1854 To identify the interaction of PMeV capsid and *AtRPL17* we first determine the localization
1855 of CP2 and *AtRPL17* in plant tissue fusing GFP to the protein C- and N-terminus. CP2 is
1856 detected at the nucleus and cytoplasm; no frequent fluorescent signals were detected
1857 when GFP was fused to the N-terminal end of CP2. In the cytoplasm, punctate fluorescent
1858 signals are observed in epidermal cells (Figure 5.A). GFP::*AtRPL17* was observed at
1859 nucleus and chloroplasts (Figure 5.A). Co-localization of RFP::*AtRPL17* and CP2::GFP
1860 was observed as punctate signals (Figure 5.B). No changes in the localization of *AtRPL17*
1861 or CP2 were observed when proteins were co-infiltrated. BiFC assays showed that both

1862 proteins do not interact in the nucleus as observed by the agroinfiltration with the
1863 transgenic *N. benthamiana* expressing RFP fused to the histone protein 2B (Figure 5.C
1864 and D).

1865

1866

1867

1868 **DISCUSSION**

1869

1870 Viruses tentatively classified in the *Totiviridae* family are found infecting a plethora of
1871 organisms: filamentous fungi, yeast, parasitic protozoa, mollusks, arthropods
1872 (including mosquitoes, ants, shrimps, and planthoppers), and plants (DE LIMA *et al.*,
1873 2019). Our knowledge of interactions between totiviruses and plants is still very scarce,
1874 as the best-studied totiviruses are found infecting fungi. However, the papaya sticky
1875 disease pathosystem has been studied at the transcriptome and proteome level which
1876 revealed that papaya plants present a delay in the appearance of the symptoms until
1877 flowering due to a multilayered tolerance mechanism (ANTUNES *et al.*, 2020,
1878 MADRONERO *et al.*, 2018). Even though, key aspects of the viral protein-plant protein
1879 interactions in this pathosystem are still unknown, which hinders the development of
1880 more effective strategies to control PSD. In this scenario, capsid proteins are an
1881 important target of study as they possess a multifunctional nature (A. CALLAWAY *et al.*
1882 *et al.*, 2001; BOL, 2008; HERRANZ *et al.*, 2017; VAIRA *et al.*, 2018).

1883 Here we show that the capsid of PMeV, a totivirus-like virus, is mainly composed of
1884 two major polypeptides with overlapping sequences matching with PMeV ORF1. A
1885 central region of these polypeptides, named here as CP2, interacts with 28 proteins
1886 mostly targeted to the chloroplast. One of these proteins, the 50S ribosomal protein
1887 L17 family protein (RPL17), co-localizes and interact with CP2 in *Nicotiana*
1888 *benthamiana* cells and putatively associates with translation-related proteins
1889 differentially modulated in pre-flowering papaya.

1890

1891 It has been pointed out that PMeV complex viral structural proteins could be originated
1892 from self-cleavage or cleavage by papaya latex proteases of the PMeV ORF1
1893 translated product (ANTUNES *et al.*, 2016; ANTUNES *et al.*, 2020). The first analysis
1894 to identify the nature of PMeV coat protein applied trypsin digestion to the crude
1895 sucrose-purified virions followed by mass spectrometry analysis identifying peptides
1896 matching with the predicted PMeV ORF1 sequence (ANTUNES *et al.*, 2016). The

1897 polypeptide coded by PMeV ORF1 is predicted to be 177kDa, which is unusual
1898 because most totiviruses coat proteins range in molecular mass from 70-100kDa (DE
1899 LIMA *et al.*, 2019). The additional CsCl purification followed by SDS-PAGE led us to
1900 identify the polypeptides of PMeV complex viral preparations. Both particles from M
1901 and B fractions presented the same banding profile on SDS-PAGE giving another
1902 support to the transcapsidation between these viruses. Interestingly peptide mass
1903 fingerprinting of the major polypeptides identified in CsCl preparations, p40 and p55,
1904 shows overlapping peptides supporting the idea that the capsid is composed of two
1905 proteins with slightly different compositions. The presence of two major components in
1906 virus purification is also visualized in the prototype of the genus *Victorvirus* (family
1907 *Totiviridae*), *Helminthosporium victoriae* virus 190S (HvV190S). Only one ORF1 is
1908 predicted for HvV190S but SDS-PAGE of purified virions shows three forms of the CP
1909 p88, p83, and p78, named after their relative molecular weights (GHABRIAL; HAVENS,
1910 1992). Interestingly, p83 and p78 are products of the proteolytic processing of p88
1911 although no protease-like protein is coded by HvV190S (HUANG *et al.*, 1997). The
1912 presence of two carboxy-terminal proteins making a viral capsid is also found in the
1913 Yado-nushi virus 1 (YkV1) a virus tentatively classified in the *Totiviridae* family (ZHANG
1914 *et al.*, 2016). Proteins of 177kDa were not observed in our CsCl virus preparations but
1915 in our sucrose purification, even polypeptides with higher molecular mass are
1916 visualized (data not shown). This could indicate that a polyprotein is coded by PMeV
1917 but is not present in the assembled capsid. In this case, the ORF1 translation product
1918 may be separated into different polypeptides, which is not an uncommon phenomenon
1919 among viruses in the family *Totiviridae*. Totiviruses in the proposed Artivirus clade,
1920 possess 2A-like sequences in their genomes which mediates a skipping effect of the
1921 ribosome resulting in an apparent co-translation cleavage of polyproteins, therefore
1922 lacking the need of a protease. Pseudo 2A-sites are found in Giardivirus clade but their
1923 amino acid composition makes them unlikely to produce a skipping effect (DE LIMA *et*
1924 *al.*, 2019). No 2A-like sequences or pseudo 2A-sites are found in the PMeV ORF1,
1925 which suggests another strategy for ORF1 polyprotein processing. Another possibility
1926 is that the bands from both p40 and p50 contain more than one protein. Peptides
1927 obtained from p40 and p50 matching with PMeV ORF1 span a region with predicted
1928 molecular mass higher than their correspondent band. More sensible separation

1929 methods as liquid chromatography or two-dimensional gel electrophoresis could give
1930 additional information.

1931 It is noteworthy that PMeV complex is, hitherto, the only viruses described to inhabit
1932 papaya laticifer cells, a physical and chemical defense barrier against pathogens. In
1933 previous work, we showed that laticifers are the preferred site for PMeV complex
1934 accumulation (Manuscript #2). It is during laticifer differentiation that papaya proteases
1935 are accumulated. Early laticifer cells undergo autophagy of their well-developed
1936 organelles, but later in differentiation, their endoplasmic reticulum split in fragments
1937 and initiates the production and accumulation of proteases which are stored within
1938 vesicles of the mature laticifer (ANTUNES *et al.*, 2020; ZENG *et al.*, 1994). Diseased
1939 plants, however, present a reduction in the accumulation and activity of proteases,
1940 mainly cysteine proteases, which is likely to be caused by oxidation of the enzyme
1941 active site by hydrogen peroxide, a reactive oxygen species present in high levels in
1942 disease latex. This assumption is credited to promote (i) a reduction in latex
1943 coagulation facilitating virus flow through the laticifers and (ii) a delay in programmed
1944 cell death which has been attributed to PMeV infection (RODRIGUES *et al.*, 2009).
1945 Several viruses encode their own proteases which are necessary for post-translational
1946 modifications of their polyproteins to ensure that proteins can travel together to the viral
1947 assembly site, to ensure the proper time for the initiation of folding and assembly, and
1948 to control the concentration of key viral proteins (BABÉ; CRAIK, 1997). However, the
1949 ones that do not encode a protease rely on their host counterparts for protein
1950 processing, as seen with two members of the *Totiviridae* family. A specific host cysteine
1951 protease act as the protein responsible for separate capsid and replicase polyprotein
1952 of Giardiavirus (GLV) and Leishmania RNA virus (LRV) (LAGUNAS-RANGEL *et al.*,
1953 2021; YU *et al.*, 1995). Here, we identified 28 Arabidopsis proteins interacting with two
1954 fragments of PMeV ORF1. One of these proteins, a cysteine protease, has homologs
1955 identified in papaya green tissues and latex (RODRIGUES *et al.*, 2011; RODRIGUES
1956 *et al.*, 2012; SOARES *et al.*, 2016), which supports the idea that cysteine proteases
1957 are important players during PMeV complex infection of papaya. Using Y2H, no
1958 dimerization or expression was detected for the full-length ORF1. Besides yeast, the
1959 full-length ORF1 protein is undetectable when expressed in *N. benthamiana*, sf9
1960 insect, and *E. coli* cells (data not shown), indicating that a highly specific environment

1961 is necessary for its correct expression and processing. Indeed, using transmission
1962 electron microscopy, Kitajima et al. (1993) analyzed different tissues and organs of
1963 asymptomatic and symptomatic papaya tissues looking for PMeV complex capsids that
1964 were not observed in any other symptomatic papaya tissue, but laticifers. Papaya latex
1965 is mainly composed of lipids, phenols, alkaloids, sugars, and oxalate crystals,
1966 polyisoprenes, and mostly proteins (RODRIGUES *et al.*, 2009). In papaya latex,
1967 cysteine proteases are only activated upon latex exudation (MOUTIM *et al.*, 1999),
1968 which is a spontaneous event in diseased plants. Taken together, PMeV could take
1969 advantage of the young active laticifer cells for translation of its ORF1 polypeptide
1970 which could be processed upon interaction with papaya cysteine proteases during the
1971 spontaneous exudation. Although proteins identified in latex (RODRIGUES *et al.*,
1972 2011; RODRIGUES *et al.*, 2012), are also found in other papaya green tissues
1973 (SOARES *et al.*, 2016), their accumulation level associated with physiological changes
1974 in laticifer cells might be important for PMeV ORF1 correct expression, processing, and
1975 interaction with cellular factors.

1976 The dimerization assay using yeast two-hybrid revealed that CP4 dimerizes and
1977 interacts with the other two fragments of PMeV ORF1, CP2 and CP3. Peptides
1978 corresponding to CP4 were not obtained in our CsCl purification, but in protein extracts
1979 of sucrose purified virions (data not shown), which supports the idea that CP4 is not
1980 part of the capsid but it could assist the virus in different moments of the infection
1981 through the interaction with plant factors. The yeast two-hybrid screening with
1982 *Arabidopsis* library identified 28 proteins interacting with both CP2 and CP4. To choose
1983 a protein that could play an important role in the PMeV complex-papaya pathosystem,
1984 we built a PPI network using *Arabidopsis* orthologs of *C. papaya* proteins modulated
1985 during PMeV infection at 4- and 7 months post-germination (mpg). The 50S ribosomal
1986 protein L17 (RPL17) appeared in both scenarios as putatively associated with 4 up-
1987 accumulated proteins and 1 down-accumulated protein at 4mpg and 3 up-accumulated
1988 proteins and 1 down-accumulated protein at 7 mpg. It is interesting to note that at 4
1989 mpg, RPL17 is associated with several down-accumulated proteins related to the
1990 regulation of protein synthesis and ribosome biogenesis, which includes ribosomal
1991 protein S13A (RPS13A, AT4G00100), eukaryotic translation initiation factor 3E (EIF3E,
1992 AT3G57290), poly(A) binding protein 2 (PAB8, AT1G49760), fibrillarlin 2 (FIB2,

1993 AT4G25630) and NOP56-like pre-RNA processing ribonucleoprotein (NOP56-like,
1994 AT3G05060). Ribosomal proteins have been reported to directly affect several
1995 processes during virus infections, either with a pro- or antiviral activity (LI, 2019;
1996 MILLER *et al.*, 2021). A proviral function is observed in the translational transactivation
1997 of *Cauliflower mosaic virus* (CaMV) in which RPL18 of *Arabidopsis thaliana* interacts
1998 with P6 of CaMV in a complex comprised of RPs including L18, L24, and eIF3
1999 (BUREAU *et al.*, 2004). On the other hand, it has been shown that RPL10 is an
2000 important player in the antiviral defense pathway in plants. The phosphorylation of
2001 RPL10 by its specific partner, the geminiviral nuclear shuttle protein-interacting kinase,
2002 redirects it to the nucleus to modulate viral infection (CARVALHO *et al.*, 2008). The
2003 fact that translation-regulating proteins are down-accumulated at 4 mpg gives support
2004 to the tolerance mechanism presented by papaya plants at pre-flowering and the
2005 interaction of RPL17 with PMeV complex capsid protein could be detrimental to this
2006 process.

2007 Despite modulation of translation could be an important mechanism used by PMeV
2008 complex or hosts to regulate virus levels, several other cellular mechanisms could be
2009 altered due to the interaction of plant proteins with the PMeV capsid protein. Our results
2010 point to other processes including polyprotein and RNA processing, cell wall
2011 modification, gene expression regulation, and reactive oxygen species detoxification
2012 that have been identified as modulated in our previous transcriptome and proteome
2013 analysis of PMeV complex-infected papaya. Thus, the identification of binding partners
2014 of PMeV CP provided a framework for a better understanding of the response of plants
2015 against totiviruses and potentially identified new targets for the development of more
2016 effective strategies to control PSD.

2017

2018 **REFERENCES**

2019

2020

2021 A. CALLAWAY; D. GIESMAN-COOKMEYER; E. T. GILLOCK; T. L. SIT, A.; LOMMEL,
2022 S. A. THE MULTIFUNCTIONAL CAPSID PROTEINS OF PLANT RNA VIRUSES.
2023 **Annual Review of Phytopathology**, 39, n. 1, p. 419-460, 2001.

2024 ABREU, P. M. V.; ANTUNES, T. F. S.; MAGAÑA-ÁLVAREZ, A.; PÉREZ-BRITO, D.;
2025 TAPIA-TUSSELL, R.; VENTURA, J. A.; FERNANDES, A. A. R.; FERNANDES, P. M.
2026 B. A current overview of the Papaya meleira virus, an unusual plant virus. **Viruses**, 7,
2027 n. 4, p. 1853-1870, 2015.

2028 AKINYEMI, I. A.; WANG, F.; CHANG, Z.-X.; WU, Q. Genome characterization of the
2029 newly identified maize-associated totivirus Anhui. **Archives of Virology**, 163, n. 10, p.
2030 2929-2931, 2018/10/01 2018.

2031 ANTUNES, T. F. S.; AMARAL, R. J. V.; VENTURA, J. A.; GODINHO, M. T.; AMARAL,
2032 J. G.; SOUZA, F. O.; ZERBINI, P. A.; ZERBINI, F. M.; FERNANDES, P. M. B. The
2033 dsRNA Virus Papaya Meleira Virus and an ssRNA Virus are Associated with Papaya
2034 Sticky Disease. **PloS One**, 11, p. e0155240, 2016.

2035 ANTUNES, T. F. S.; MAURASTONI, M.; MADROÑERO, L. J.; FUENTES, G.;
2036 SANTAMARÍA, J. M.; VENTURA, J. A.; ABREU, E. F.; FERNANDES, A. A. R.;
2037 FERNANDES, P. M. B. Battle of Three: The Curious Case of Papaya Sticky Disease.
2038 **Plant Disease**, 104, n. 11, p. 2754-2763, 2020.

2039 BABÉ, L. M.; CRAIK, C. S. Viral Proteases: Evolution of Diverse Structural Motifs to
2040 Optimize Function. **Cell**, 91, n. 4, p. 427-430, 1997.

2041 BOL, J. F. Role of Capsid Proteins. *In*: FOSTER, G. D.; JOHANSEN, I. E., *et al* (Ed.).
2042 **Plant Virology Protocols: From Viral Sequence to Protein Function**. Totowa, NJ:
2043 Humana Press, 2008. p. 21-31.

2044 BUREAU, M.; LEH, V.; HAAS, M.; GELDREICH, A.; RYABOVA, L.; YOT, P.; KELLER,
2045 M. P6 protein of Cauliflower mosaic virus, a translation reinitiator, interacts with
2046 ribosomal protein L13 from *Arabidopsis thaliana*. **Journal of General Virology**, 85, n.
2047 12, p. 3765-3775, 2004.

2048 CARMO, L. S. T.; RESENDE, R. O.; SILVA, L. P.; RIBEIRO, S. G.; MEHTA, A.
2049 Identification of host proteins modulated by the virulence factor AC2 of Tomato
2050 chlorotic mottle virus in *Nicotiana benthamiana*. **Proteomics**, 13, n. 12-13, p. 1947-
2051 1960, 2013.

2052 CARVALHO, C. M.; SANTOS, A. A.; PIRES, S. R.; ROCHA, C. S.; SARAIVA, D. I.;
2053 MACHADO, J. P. B.; MATTOS, E. C.; FIETTO, L. G.; FONTES, E. P. B. Regulated
2054 nuclear trafficking of rpL10A mediated by NIK1 represents a defense strategy of plant
2055 cells against virus. **PLOS Pathogens**, 4, n. 12, p. e1000247, 2008.

- 2056 CHAKRABARTY, R.; BANERJEE, R.; CHUNG, S.-M.; FARMAN, M.; CITOVSKY, V.;
2057 HOGENHOUT, S. A.; TZFIRA, T.; GOODIN, M. pSITE vectors for stable integration or
2058 transient expression of autofluorescent protein fusions in plants: probing *Nicotiana*
2059 *benthamiana*-virus interactions. **Molecular Plant-Microbe Interactions**, 20, n. 7, p.
2060 740-750, 2007.
- 2061 DE LIMA, J. G. S.; TEIXEIRA, D. G.; FREITAS, T. T.; LIMA, J. P. M. S.; LANZA, D. C.
2062 F. Evolutionary origin of 2A-like sequences in *Totiviridae* genomes. **Virus Research**,
2063 259, p. 1-9, 2019/01/02/ 2019.
- 2064 FUJIMURA, T.; ESTEBAN, R. Cap-snatching mechanism in yeast L-A double-stranded
2065 RNA virus. **Proceedings of the National Academy of Sciences**, 108, n. 43, p. 17667-
2066 17671, 2011.
- 2067 GHABRIAL, S. A.; HAVENS, W. M. The *Helminthosporium victoriae* 190S mycovirus
2068 has two forms distinguishable by capsid protein composition and phosphorylation
2069 state. **Virology**, 188, n. 2, p. 657-665, 1992/06/01/ 1992.
- 2070 GHOSH, S.; KANAKALA, S.; LEBEDEV, G.; KONTSEDALOV, S.; SILVERMAN, D.;
2071 ALON, T.; MOR, N.; SELA, N.; LURIA, N.; DOMBROVSKY, A.; MAWASSI, M.; HAVIV,
2072 S.; CZOSNEK, H.; GHANIM, M.; SIMON, A. E. Transmission of a new polerovirus
2073 infecting pepper by the whitefly *Bemisia tabaci*. **Journal of Virology**, 93, n. 15, p.
2074 e00488-00419, 2019.
- 2075 GUO, L.; YANG, X.; WU, W.; TAN, G.; FANG, S.; ZHANG, S.; LI, F. Identification and
2076 molecular characterization of *Panax notoginseng* virus A, which may represent an
2077 undescribed novel species of the genus *Totivirus*, family *Totiviridae*. **Archives of**
2078 **Virology**, 161, n. 3, p. 731-734, 2016/03/01 2016.
- 2079 HERRANZ, M. C.; PALLAS, V.; APARICIO, F. Multifunctional Roles for the N-Terminal
2080 Basic Motif of Alfalfa mosaic virus Coat Protein: Nucleolar/Cytoplasmic Shuttling,
2081 Modulation of RNA-Binding Activity, and Virion Formation. *Molecular Plant-Microbe*
2082 *Interactions*®, 25, n. 8, p. 1093-1103, 2012.
- 2083 HUANG, S.; SOLDEVILA, A. I.; WEBB, B. A.; GHABRIAL, S. A. Expression, Assembly,
2084 and Proteolytic Processing of *Helminthosporium victoriae* 190S Totivirus Capsid
2085 Protein in Insect Cells. **Virology**, 234, n. 1, p. 130-137, 1997/07/21/ 1997.
- 2086 KITAJIMA, E. W.; RODRIGUES, C. H.; SILVEIRA, J. S.; ALVES, F.; VENTURA, J. A.;
2087 ARAGÃO, F. J. L.; OLIVEIRA, L. H. R. Association of isometric viruslike particles,
2088 restricted to lacticifers, with "meleira" (sticky disease) of papaya (*Carica papaya*).
2089 **Fitopatologia Brasileira**, 18, p. 118, 1993.
- 2090 KUSHNIROV, V. V. Rapid and reliable protein extraction from yeast. *Yeast*, 16, n. 9,
2091 p. 857-860, 2000.
- 2092 LAGUNAS-RANGEL, F. A.; KAMEYAMA-KAWABE, L. Y.; BERMÚDEZ-CRUZ, R. M.
2093 Giardiavirus: an update. **Parasitology Research**, 120, n. 6, p. 1943-1948, 2021/06/01
2094 2021.

- 2095 LAEMMLI, U. K. Cleavage of Structural Proteins during the Assembly of the Head of
2096 Bacteriophage T4. **Nature**, 227, n. 5259, p. 680-685, 1970/08/01 1970.
- 2097 LI, S. Regulation of Ribosomal Proteins on Viral Infection. **Cells**, 8, n. 5, p. 508, 2019.
- 2098 LUQUE, D.; MATA, C. P.; SUZUKI, N.; GHABRIAL, S. A.; CASTÓN, J. R. Capsid
2099 structure of dsRNA fungal viruses. **Viruses**, 10, n. 9, p. 481, 2018.
- 2100 MADROÑERO, J.; RODRIGUES, S. P.; ANTUNES, T. F. S.; ABREU, P. M. V.;
2101 VENTURA, J. A.; FERNANDES, A. A. R.; FERNANDES, P. M. B. Transcriptome
2102 analysis provides insights into the delayed sticky disease symptoms in *Carica papaya*.
2103 **Plant Cell Reports**, 37, n. 7, p. 967-980, 2018/07/01 2018.
- 2104 MARTIN, K.; KOPPERUD, K.; CHAKRABARTY, R.; BANERJEE, R.; BROOKS, R.;
2105 GOODIN, M. M. Transient expression in *Nicotiana benthamiana* fluorescent marker
2106 lines provides enhanced definition of protein localization, movement and interactions
2107 in planta. **The Plant Journal**, 59, n. 1, p. 150-162, 2009.
- 2108 MATA, C. P.; LUQUE, D.; GÓMEZ-BLANCO, J.; RODRÍGUEZ, J. M.; GONZÁLEZ, J.
2109 M.; SUZUKI, N.; GHABRIAL, S. A.; CARRASCOSA, J. L.; TRUS, B. L.; CASTÓN, J.
2110 R. Acquisition of functions on the outer capsid surface during evolution of double-
2111 stranded RNA fungal viruses. **PLOS Pathogens**, 13, n. 12, p. e1006755, 2017.
- 2112 MILLER, C. M.; SELVAM, S.; FUCHS, G. Fatal attraction: The roles of ribosomal
2113 proteins in the viral life cycle. **WIREs RNA**, 12, n. 2, p. e1613, 2021.
- 2114 MOUTIM, V.; SILVA, L. G.; LOPES, M. T. P.; FERNANDES, G. W.; SALAS, C. E.
2115 Spontaneous processing of peptides during coagulation of latex from *Carica papaya*.
2116 **Plant Science**, 142, n. 2, p. 115-121, 1999/03/29/ 1999.
- 2117 RODRIGUES, S. P.; DA CUNHA, M.; VENTURA, J. A.; FERNANDES, P. M. B. Effects
2118 of the Papaya meleira virus on papaya latex structure and composition. **Plant Cell**
2119 **Reports**, 28, p. 861-871, 2009.
- 2120 RODRIGUES, S. P.; VENTURA, J. A.; AGUILAR, C.; NAKAYASU, E. S.; ALMEIDA, I.
2121 C.; FERNANDES, P.; ZINGALI, R. B. Proteomic analysis of papaya (*Carica papaya* L.)
2122 displaying typical sticky disease symptoms. **Proteomics**, 11, n. 13, p. 2592-2602,
2123 2011.
- 2124 RODRIGUES, S. P.; VENTURA, J. A.; AGUILAR, C.; NAKAYASU, E. S.; CHOI, H.;
2125 SOBREIRA, T. J. P.; NOHARA, L. L.; WERMELINGER, L. S.; ALMEIDA, I. C.;
2126 ZINGALI, R. B.; FERNANDES, P. M. B. Label-free quantitative proteomics reveals
2127 differentially regulated proteins in the latex of sticky diseased *Carica papaya* L. plants.
2128 **Journal of Proteomics**, 75, p. 3191-3198, 2012.
- 2129 SHANNON, P.; MARKIEL, A.; OZIER, O.; BALIGA, N. S.; WANG, J. T.; RAMAGE, D.;
2130 AMIN, N.; SCHWIKOWSKI, B.; IDEKER, T. Cytoscape: A Software Environment for
2131 Integrated Models of Biomolecular Interaction Networks. **Genome Research**, 13, n.
2132 11, p. 2498-2504, November 1, 2003 2003.

- 2133 SHEVCHENKO, A.; TOMAS, H.; HAVLI, J.; OLSEN, J. V.; MANN, M. In-gel digestion
2134 for mass spectrometric characterization of proteins and proteomes. **Nature Protocols**,
2135 1, n. 6, p. 2856-2860, 2006/12/01 2006.
- 2136 SOARES, E.; WERTH, E. G.; MADROÑERO, L. J.; VENTURA, J. A.; RODRIGUES,
2137 S. P.; HICKS, L. M.; FERNANDES, P. M. B. Label-free quantitative proteomic analysis
2138 of pre-flowering PMeV-infected *Carica papaya* L. **Journal of Proteomics**, 151, p. 275-
2139 283, 2016.
- 2140 SZKLARCZYK, D.; GABLE, A. L.; LYON, D.; JUNGE, A.; WYDER, S.; HUERTA-
2141 CEPAS, J.; SIMONOVIC, M.; DONCHEVA, N. T.; MORRIS, J. H.; BORK, P.; JENSEN,
2142 L. J.; MERING, CHRISTIAN V. STRING v11: protein–protein association networks with
2143 increased coverage, supporting functional discovery in genome-wide experimental
2144 datasets. **Nucleic Acids Research**, 47, n. D1, p. D607-D613, 2018.
- 2145 VAIRA, A. M.; LIM, H. S.; BAUCHAN, G.; GULBRONSON, C. J.; MIOZZI, L.; VINALS,
2146 N.; NATILLA, A.; HAMMOND, J. The interaction of Lolium latent virus major coat
2147 protein with ankyrin repeat protein NbANKr redirects it to chloroplasts and modulates
2148 virus infection. **Journal of General Virology**, 99, n. 5, p. 730-742, 2018.
- 2149 WEBER, K.; OSBORN, M. The Reliability of Molecular Weight Determinations by
2150 Dodecyl Sulfate-Polyacrylamide Gel Electrophoresis. **Journal of Biological**
2151 **Chemistry**, 244, n. 16, p. 4406-4412, 1969.
- 2152 YU, D.; WANG, C. C.; WANG, A. L. Maturation of giardiavirus capsid protein involves
2153 posttranslational proteolytic processing by a cysteine protease. **Journal of Virology**,
2154 69, n. 5, p. 2825-2830, 1995.
- 2155 ZENG, Y.; JI, B.; YU, B. Laticifer ultrastructural and immunocytochemical studies of
2156 papain in *Carica papaya*. **Acta Botanica Sinica**, 36, n. 7, p. 497-501, 1994.
- 2157 ZHANG, Z. Y.; HUANG, H.; HAN, X. X.; LI, R.; WU, L. P.; WU, L. Identification and
2158 molecular characterization of tea-oil camellia-associated totivirus 1. **Archives of**
2159 **Virology**, 2021/04/17 2021.
- 2160 ZHANG, R.; HISANO, S.; TANI, A.; KONDO, H.; KANEMATSU, S.; SUZUKI, N. A
2161 capsidless ssRNA virus hosted by an unrelated dsRNA virus. **Nature Microbiology**,
2162 1, p. 15001, Jan 11 2016

TABLES

Table 1. Yeast-two-hybrid-derived clones obtained from a screening using PMeV ORF1 fragment 4 as bait

Clone No.	Growth media	NCBI or TAIR Description	TAIR accession	Gene ontology information
1	QXA	Beta-1,4-N-acetylglucosaminyltransferase family protein (AT3G01620), mRNA	AT3G01620	Located in Golgi apparatus
2	QXA	Zinc finger protein 2 (ZFP2), mRNA	AT5G57520	Located in nucleus
3	QXA	DHHC-type zinc finger family protein (AT2G40990), partial mRNA	AT2G40990	Is active in Golgi apparatus and endoplasmic reticulum
4	QXA	Polynucleotide adenylyltransferase family protein (AT5G23690), mRNA	AT5G23690	Involved in RNA processing
5	QXA	Transmembrane protein (AT2G35750)	AT2G35750	Located in mitochondrion
6	QXA	Inorganic carbon transport protein-like protein (NdhL), mRNA	AT1G70760.1	Located in chloroplast, chloroplast thylakoid membrane, thylakoid membrane

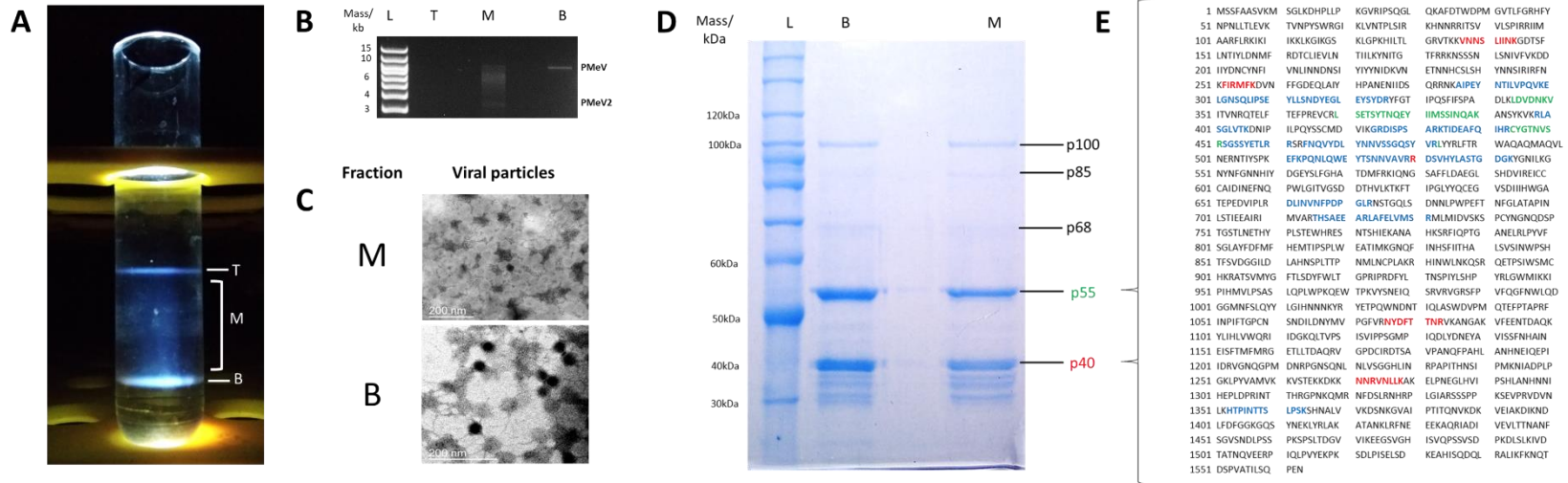
7	QXA 2.5mM	Cytochrome c oxidase assembly protein CtaG / Cox11 family (AT1G02410), mRNA	AT1G02410	Is located in chloroplast, integral component of mitochondrial membrane, mitochondrion
8	QXA 2.5mM	Pectin lyase-like superfamily protein (AT1G04680), mRNA	AT1G04680	Located in extracellular region
9	QXA 2.5mM	Plastid developmental protein DAG (MORF9), mRNA	AT1G11430	Located in chloroplast, chloroplast envelope, chloroplast stroma
10	QXA 2.5mM	Plant/protein (AT1G13990), mRNA	AT1G13990	Located in chloroplast
11	QXA 2.5mM	Peroxidase CB (PRXCB), mRNA	AT3G49120	Located in Golgi apparatus, apoplast, cell wall, cytosol, extracellular region, plant-type cell wall, plant-type vacuole, secretory vesicle
12	QXA 2.5mM	RmlC-like cupins superfamily protein (AT1G03890), mRNA	AT1G03890	Located in extracellular region
13	QXA 2.5mM	RNA polymerase transcriptional regulation mediator-like protein (MED6), mRNA	AT3G21350	Located in nucleus
14	QXA 2.5 mM	Chloroplast ribosomal protein S3	ATCG00800.1	Located in chloroplast, chloroplast envelope, chloroplast nucleoid, chloroplast stroma, plastid

15	QXA 2.5 mM	Chloroplast GRX 12, GRXS12	AT2G20270	Located in chloroplast, chloroplast stroma, mitochondrion
16	QXA 5mM	DNAJ heat shock family protein (AT2G22360), mRNA	AT2G22360	Located in chloroplast, chloroplast envelope, chloroplast thylakoid membrane, cytoplasm, vacuole
17	QXA 5mM	Ribosomal protein L17 family protein (AT3G54210), mRNA	AT3G54210	Located in chloroplast, chloroplast envelope, chloroplast stroma, cytosol
18	QXA 5mM	Sec14p-like phosphatidylinositol transfer family protein (AT1G72160), mRNA	AT1G72160	Located in plasma membrane
19	QXA 5mM	GDSL-like Lipase/Acylhydrolase superfamily protein (AT5G45670), mRNA	AT5G45670	Located in extracellular region
20	QXA 5mM	Chaperone protein dnaJ-like protein (AT5G06130), mRNA	AT5G06130	Located in chloroplast membrane, mitochondrion
21	QXA 5mM	GPI-anchored protein (AT3G18050), mRNA	AT3G18050	Located in anchored component of membrane, chloroplast
22	QXA 5mM	Pyrimidin 4 (PYR4), mRNA	AT4G22930	Located in chloroplast, cytosol, mitochondrion

23	QXA 5mM	Pectinacetyl esterase family protein (AT4G19420), mRNA	AT4G19420	Located in extracellular region
24	QXA 5mM	Double Clp-N motif protein (AT4G12060), mRNA	AT4G12060	Located in chloroplast, chloroplast envelope, chloroplast stroma, cytosol, plastid stroma
25	QXA 5mM	PEBP (phosphatidylethanolamine-binding protein) family protein (FT), mRNA	AT1G65480	Located in cytoplasm nucleus
26	QXA 5mM	Clone RAFL09-89-G08 (R19778) putative cellulose synthase catalytic subunit (RSW1) (At4g32410), mRNA	AT4G32410.1	Located in Golgi apparatus, endosome, plasma membrane, trans-Golgi network
27	QXA 5mM	mRNA for plastid protein, complete cds, clone: RAFL15-06-D14	AT1G32580.1	Located in chloroplast, mitochondrion, nucleus
28	QXA 5mM	Papain family cysteine protease (AT4G16190), mRNA	AT4G16190	Located in extracellular region, lytic vacuole, plant-type vacuole, vacuole

2164
2165
2166

FIGURES



2167
2168
2169
2170
2171
2172
2173
2174

Figure 1. Characterization of PMeV complex capsid protein polypeptide composition. **a** The three opalescent fractions obtained after ultracentrifugation at 145,000 g for 18 h at 4°C in a 50 % (w/v) CsCl isopycnic gradient. T- Top fraction. M- middle fraction. B- Bottom fraction. **b** Agarose gel electrophoresis of total RNA extracted from the fractions. Twenty micrograms of each fraction were submitted for phenol: chloroform (1:1) extraction and RNA was loaded in gel. L- 1kb plus DNA ladder Invitrogen®. **c** Transmission electron microscope images of viral particles from the M and B fractions, as shown in figure a. No particles were visualized for fraction T. **d** Coomassie blue-stained SDS-PAGE of fractions collected from M and B. Viral particles were boiled for 3 min in loading buffer and 40µg of protein was loaded in the gel. L- Benchmark™ protein ladder Invitrogen®. **e**. Deduced amino acid sequence of ORF1 highlighting the positions of the peptides identified from the p40 and p55 bands

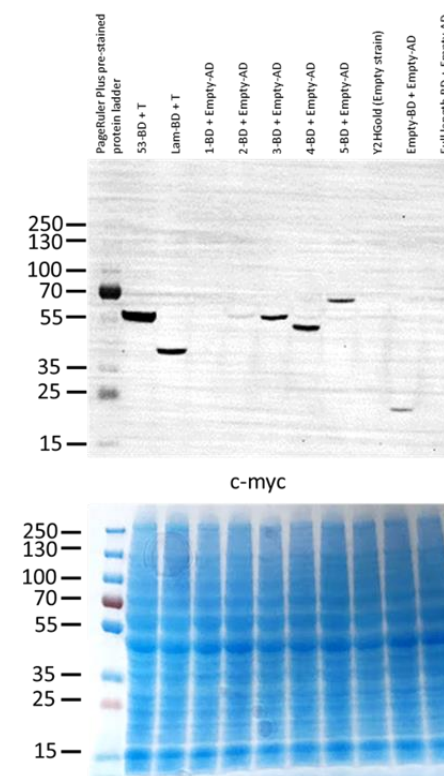
2175 extracted from the M fraction lane. Peptides identified from p40 and p55 bands are highlighted in red and green, respectively. Overlapping peptides



2177 Figure 2. A consensus secondary structure of the PMeV ORF1. The alpha-helix, beta-strand,
2178 and random coil segments are represented schematically as rectangles, arrows, and lines,
2179 respectively. All secondary-structure predictions were made with five different software (see
2180 Methods). GenBank accession number for PMeV ORF1: AMU19319.1.

A

ORF1 fragment	Range (aa)	No. amino acids	Approximated size (kDa)	Yeast Growth in QDO/X/A						
				BD	AD					
					1	2	3	4	5	6
CP1	1-320	320	35.2	1						
CP2	321-670	350	38.5	2						
CP3	671-960	290	31.9	3						
CP4	961-1200	240	26.4	4						
CP5	1201-1563	363	39.9	5						
Full length	1-1563	1563	177	6						

B

2181

2182

2183

2184

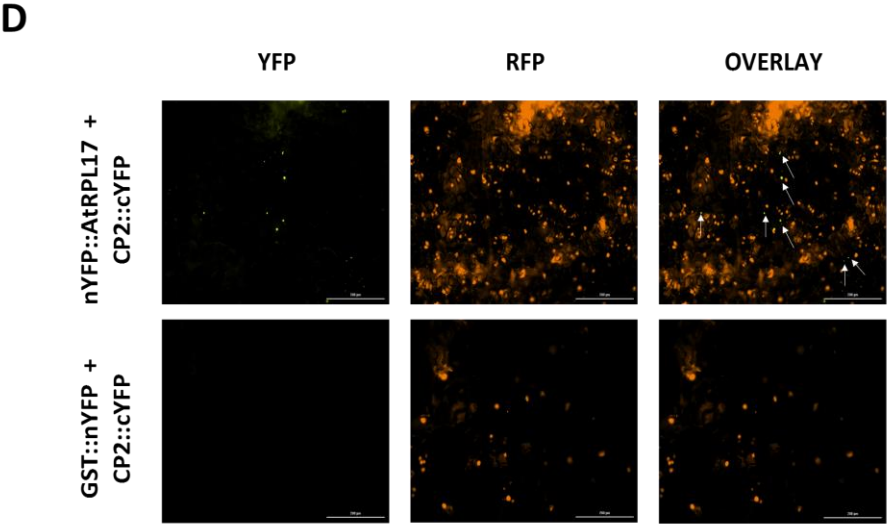
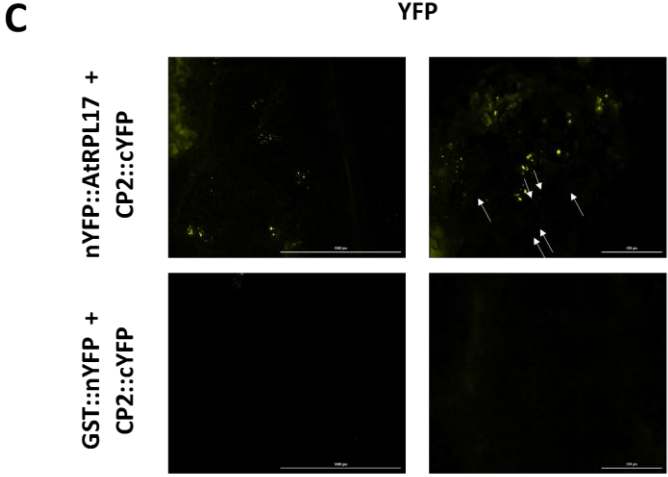
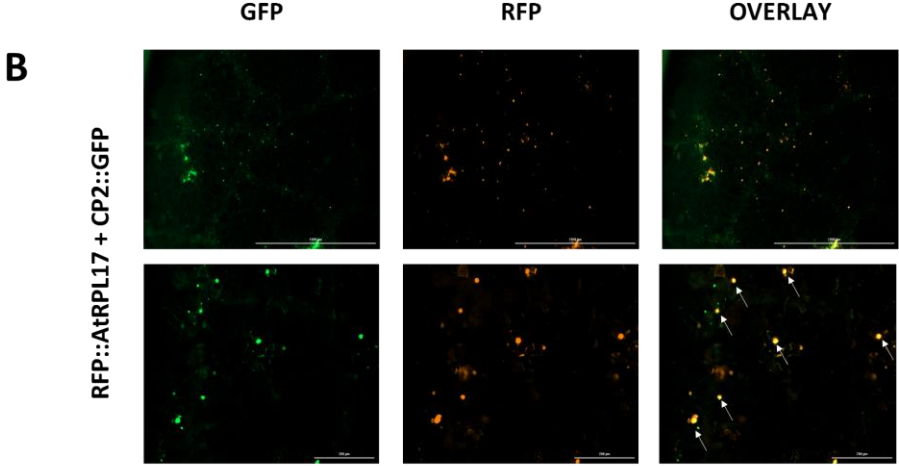
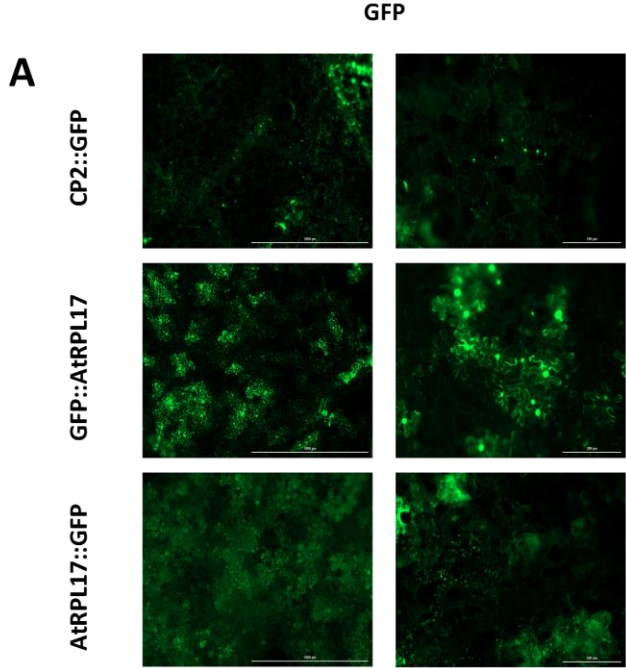
2185

2186

2187

Figure 3. Summary of yeast two-hybrid assays to map dimerization fragments in PMeV ORF1 and detection of 5 fragments of PMeV ORF1. **a** Each fragment was fused either to GAL4 Binding domain (BD) or GAL4 Activation domain (AD) in pDESTGBKT7 and pDESTGADT7, respectively, and transformed in yeast strain Y2HGold (Takara®). Positive interactors were selected in QDO/X/A media. **b** Expression was verified by SDS-PAGE of yeast crude protein extracts and western blotting using an anti-c-myc antibody. The c-myc tag is fused to the expressed protein. 1 to 5-BD represents each fragment of PMeV ORF1 fused to GAL4 BD. GAL4 DNA-BD fused with murine p53, GAL4 BD fused with Lamin were used as a positive control. Untransformed yeast and yeast transformed with pDEST-BGKT7 plasmids were used as a negative control.

2191 an infected plant at **(a)** pre-flowering stage (4 months post-germination – 4MPG) and **(b)** post-
2192 flowering stage (7 months post-germination – 7MPG). Red nodes are up-accumulated
2193 proteins; green nodes are down-accumulated proteins; gray nodes are PMeV CP2 and CP4-
2194 interacting proteins.



2196 Figure 5. Transient expression of *AtRPL17* and CP2, and their interaction in *Nicotiana benthamiana*. **a** Localization of *AtRPL17* and CP2 proteins
2197 expressed as fusions to a green fluorescent protein (GFP) in leaf epidermal cells of *N. benthamiana*. The fusion proteins CP2::GFP,
2198 *AtRPL17*::GFP, and GFP::*AtRPL17* were expressed and visualized at 2 days post infiltration. The right column represents an image in higher
2199 magnification. **b** Co-localization of *AtRPL17* and CP2 expressed as fusions to (GFP) or red fluorescent protein (RFP) in *N.*
2200 *benthamiana* epidermal leaf cells. First column, GFP channel; Second column, RFP channel; Third column, Overlay of GFP and RFP channels.
2201 The fusion proteins RFP::*AtRPL17* were expressed along with GFP::CP2. Lower row represents an image in higher magnification. **c and d** PMeV
2202 CP2-*AtRPL17* interaction in vivo by bimolecular fluorescence complementation (BiFC) in wild type (**c**) and transgenic *N. benthamiana* expressing
2203 RFP::H2B as a nuclear marker (**d**). Fusion proteins nYFP::*AtRPL17* or GST::nYFP were expressed along with CP2::cYFP by agroinfiltrating the
2204 encoding plasmids into leaves of *N. benthamiana*. The reconstitution of the yellow fluorescence was visualized 2 days post infiltration. Fusion
2205 protein combinations expressed in each sample are indicated at the left of the corresponding row of images. Scale bars are represented in the
2206 figures. White arrows: co-localization or interaction signals.

2207

2208

2209

2210 **SUPPLEMENTARY MATERIAL**

2211

2212 Supplementary Material 1

2213 Table S1. List of primers used to generate the clones in this study.

2214 Table S2. Arabidopsis orthologs obtained from proteins differentially accumulated in
2215 infected papaya leaf at 4 months post-germination.

2216 Table S3. Arabidopsis orthologs obtained from proteins differentially accumulated in
2217 infected papaya leaf at 7 months post-germination.

2218 Table S4. Arabidopsis orthologs obtained from proteins differentially accumulated in
2219 infected papaya leaf (at 4 months post-germination) used retrieved the protein-protein
2220 interaction network of CP2 and CP4-interacting proteins.

2221 Table S5. Arabidopsis orthologs obtained from proteins differentially accumulated in
2222 infected papaya leaf (at 7 months post-germination) used retrieved the protein-protein
2223 interaction network of CP2 and CP4-interacting proteins.

2224 Link to access supplementary tables

2225 <https://1drv.ms/x/s!ApYzPMWzGjw8gdlc6kRIIdNDYfjzQ?e=oLaeJL>

2226

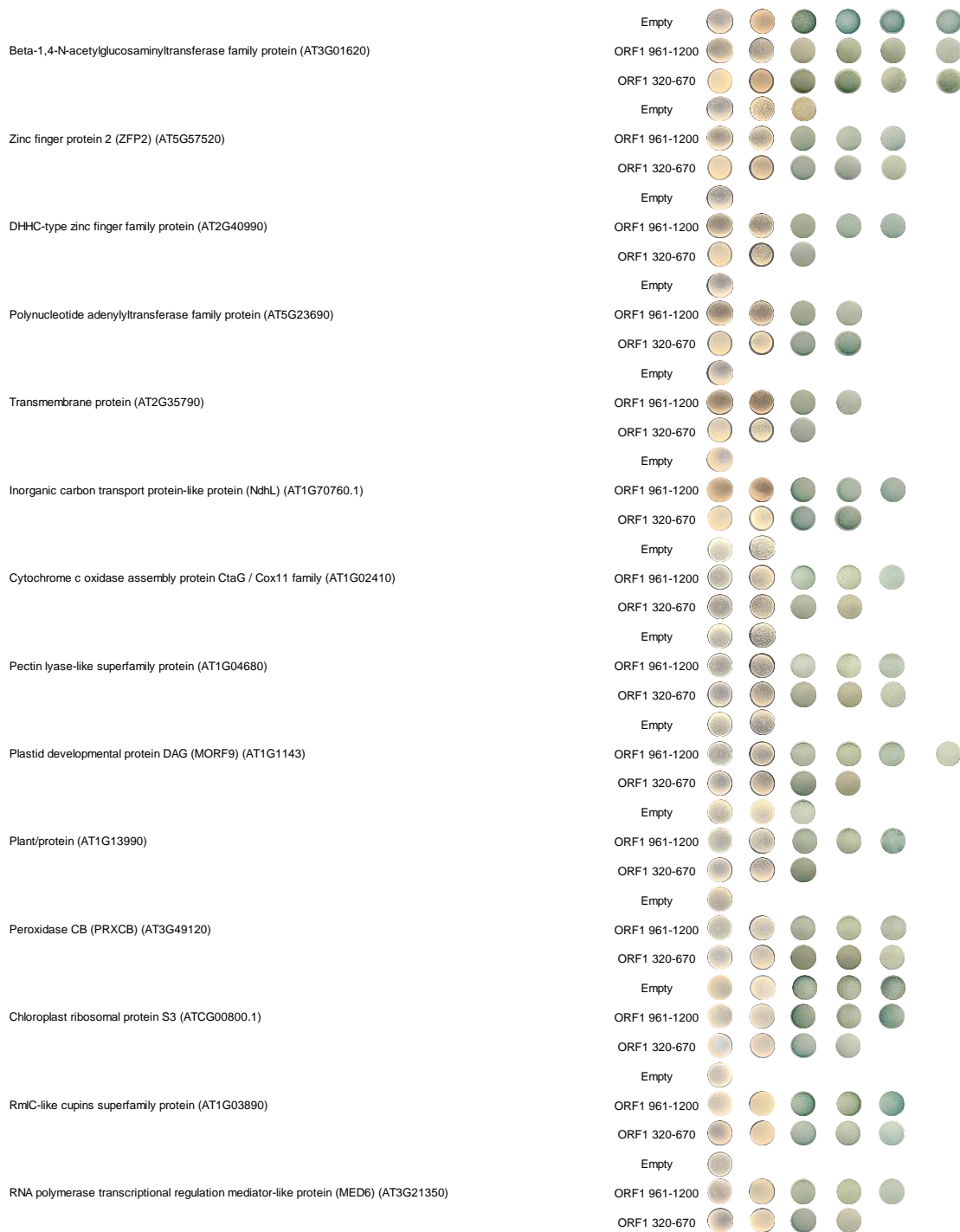
2227 Figure S1. Spot plating showing the validation of genuine positives interacting CP2 and
2228 CP4. After overnight growth, cultures were normalized to $OD_{600}=2$, and 20uL was
2229 spotted in nine different selective media. To test the autoactivation of baits, yeast
2230 transformed only with the BD-fused protein were spotted in SDO, SDO/X, and SDO/X/A
2231 media. Yeast co-transformed with bait and empty-AD plasmids were spotted in DDO,
2232 DDO/X, DDO/X/A, QDO, QDO/X, and QDO/X/A. None of the tested baits, except the
2233 positive control, shows growth in QDO/X and QDO/X/A media. The growth in these
2234 media depends on the activation of reporter genes.

2235

p-AD	p-BD	Yeast Growth					
		DDO	QDO	QDOXA + 3-AT			
				0 mM	1 mM	2.5 mM	5 mM
T	53						
T	Lam						
	Empty						
DNAJ heat shock family protein (AT2G22360)	ORF1 961-1200						
	ORF1 320-670						
	Empty						
Ribosomal protein L17 family protein (AT3G54210)	ORF1 961-1200						
	ORF1 320-670						
	Empty						
Sec14p-like phosphatidylinositol transfer family protein (AT1G72160)	ORF1 961-1200						
	ORF1 320-670						
	Empty						
GDSL-like Lipase/Acylhydrolase superfamily protein (AT5G45670)	ORF1 961-1200						
	ORF1 320-670						
	Empty						
Chloroplast GRX 12, GRXS12 (AT2G20270)	ORF1 961-1200						
	ORF1 320-670						
	Empty						
Chaperone protein dnaJ-like protein (AT5G06130)	ORF1 961-1200						
	ORF1 320-670						
	Empty						
GPI-anchored protein (AT3G18050)	ORF1 961-1200						
	ORF1 320-670						
	Empty						
Pyrimidin 4 (PYR4) (AT4G22930)	ORF1 961-1200						
	ORF1 320-670						
	Empty						
Pectinacetyltransferase family protein (AT4G19420)	ORF1 961-1200						
	ORF1 320-670						
	Empty						
Double Clp-N motif protein (AT4G12060)	ORF1 961-1200						
	ORF1 320-670						
	Empty						
PEBP (phosphatidylethanolamine-binding protein) family protein (FT) (AT1G6548)	ORF1 961-1200						
	ORF1 320-670						
	Empty						
Clone RAFL09-89-G08 (R19778) putative cellulose synthase catalytic subunit (RSW1) (At4g32410)	ORF1 961-1200						
	ORF1 320-670						
	Empty						
mRNA for plastid protein, complete cds, clone: RAFL15-06-D14 (AT1G32580.1)	ORF1 961-1200						
	ORF1 320-670						
	Empty						
Papain family cysteine protease (AT4G16190)	ORF1 961-1200						
	ORF1 320-670						

2236

2237



2238

2239

2240

2241

2242

2243 **MANUSCRIPT #4. A MULTIPLEX RT-PCR METHOD TO DETECT PAPAYA**
2244 **MELEIRA VIRUS COMPLEX IN ADULT PRE-FLOWERING PLANTS**

2245

2246

2247 Paper published in the *Archives of Virology journal* (ISSN 0304-8608; IF 2.574, 2021;
2248 Qualis B1 Biotecnologia, 2013-2016). <https://doi.org/10.1007/s00705-020-04588-5>

2249

2250

2251 **A multiplex RT-PCR method to detect papaya meleira virus complex in adult**
2252 **pre-flowering plants**

2253

2254

2255 **Marlonni Maurastoni^a**, Tathiana F. Sá-Antunes^a, Scarlett A. Oliveira^a, Alexandre M.
2256 C. Santos^a, José A. Ventura^{a,b} and Patricia M. B. Fernandes^{a*}

2257

2258 ^aNúcleo de Biotecnologia, Universidade Federal do Espírito Santo, Vitória, Espírito
2259 Santo, Brazil

2260 ^bInstituto Capixaba de Pesquisa, Assistência Técnica e Extensão Rural, Vitória,
2261 Espírito Santo, Brazil

2262 *Corresponding author: patricia.fernandes@ufes.br

2263

ABSTRACT

2264

2265

2266

2267 Papaya sticky disease (PSD), which can destroy orchards, was first attributed to
2268 papaya meleira virus (PMeV). However, the discovery of papaya meleira virus 2
2269 (PMeV2) associated with PSD plants impose the need to detect this viral complex. We
2270 developed a multiplex RT-PCR (mPCR) technique capable of detecting two viruses in
2271 a single assay from pre-flowering plant samples, which is a useful tool for early
2272 diagnosis of PSD. We also determined the limit of detection (LOD) using asymmetric
2273 plasmid dilutions of both PMeV and PMeV2, which revealed that a higher titer of one
2274 virus prevents detection of the other. Thus, this technique is an alternative method for
2275 detecting PMeV and PMeV2 in a single reaction.

2276

2277 Keywords: papaya sticky disease; *Carica papaya*; virus diagnosis

2278

2279 Officially reported in Brazil and Mexico, papaya sticky disease (PSD) is a severe
2280 disease that can devastate papaya orchards. Initially, the causal agent of PSD was
2281 identified as papaya meleira virus (PMeV), a virus with a double-stranded RNA genome
2282 similar to those of members of the family *Totiviridae* enclosed in a 42-nm-diameter
2283 isometric particle [1, 2]. Later, papaya meleira virus 2 (PMeV2), a single-stranded RNA
2284 virus closely related to members of the genus *Umbravirus*, was also discovered in
2285 association with PSD plants. These viruses have an interesting relationship in mixed
2286 infections, because the PMeV and PMeV2 genomes are separately encapsidated in
2287 particles formed by the PMeV capsid protein [3].

2288 No papaya cultivars have been found that are resistant to PMeV and PMeV2 (PMeV
2289 complex) [4]. Visual identification of diseased plants and their eradication (roguing) is
2290 the only available control method [5]. However, symptoms of PSD appear only after
2291 flowering. Thus, an infected symptomless plant in a field may remain unnoticed for an
2292 extended period, acting as a virus inoculum source [5, 6]. Therefore, development of
2293 diagnostic procedures for early detection is imperative.

2294 Previous reports have described alternative diagnostic methods for PMeV: (i) viewing
2295 in an agarose gel the viral dsRNA band purified from latex [7], (ii) conventional reverse
2296 transcription PCR (RT-PCR) from nucleic acids obtained from latex diluted in
2297 ammonium or sodium citrate [8], and (iii) conventional RT-PCR and quantitative RT-
2298 PCR (qRT-PCR) from small quantities of leaf-purified RNA [9]. Despite these
2299 advances, the discovery of PMeV2 associated with PSD plants [3] requires new
2300 diagnostic methodologies. A method modified from conventional RT-PCR was
2301 described by Antunes et al. [3], who used primers based on sequenced genomes.
2302 However, the methodology requires synthesis of two cDNAs and two PCR reactions,
2303 one for each virus, making it laborious and time-consuming, especially when screening
2304 a large number of samples.

2305 In contrast, the multiplex PCR (mPCR) method is based on a single PCR that can
2306 simultaneously detect different viruses [10]. The method has been used to
2307 simultaneously detect papaya ringspot virus (PRSV-P), papaya leaf distortion mosaic
2308 virus (PLDMV), and papaya mosaic virus (PapMV). These viruses are difficult to
2309 distinguish visually since they cause similar symptoms [11].

2310 The sensitivity or limit of detection (LOD) of a PCR method is an important parameter
2311 used to evaluate the minimum amount of amplicon DNA that can be detected and
2312 quantified [12, 13]. It is commonly determined using total nucleic acids [14, 15], nucleic
2313 acids extracted from viral particles purified from infected plants [16], or plasmids
2314 containing the target [17,18,19]. These templates are quantified, mixed in equimolar
2315 amounts, serially diluted and used as a template for mPCR. However, an equimolar
2316 mix may not be a proper template to determine the LOD. This can lead to misleading
2317 results, as the different viruses in mixed infection do not usually have the same titer in
2318 a host [20,21,22]. Here, we report a mPCR method for simultaneous identification of
2319 PMeV and PMeV2 in pre-flowering papaya plants. Moreover, we propose that an
2320 asymmetric mixture of PMeV and PMeV2 templates is the most appropriate target for
2321 determining the sensitivity of the mPCR method.

2322 A survey was conducted on four groups of plants at different stages on several papaya
2323 production farms in the north of Espírito Santo state, Brazil. For the first group, (i)
2324 papaya seedlings (n = 10) were kept under greenhouse conditions for two months
2325 before leaves were collected. For the other groups, the papaya leaves in the field were
2326 collected from trees (ii) that were in the adult pre-flowering stage (n = 10), (iii) that were
2327 asymptomatic in the post-flowering stage (n = 16), and (iv) that were symptomatic in
2328 the post-flowering stage (n = 6). Leaf samples were taken on the same day from
2329 different papaya plants.

2330 Total RNA was extracted from 100 mg of papaya leaves using TRIzol® Reagent
2331 (Invitrogen, Carlsbad, CA, USA). RNA purity (A_{260}/A_{280}) was assessed using a
2332 NanoDrop® ND2000 spectrophotometer (Thermo Fisher Scientific, Waltham, MA,
2333 USA). The templates used for RT-PCR reactions were obtained from 1 µg of purified
2334 RNA that had been treated with DNase I (Invitrogen, Carlsbad, CA, USA). For the
2335 uniplex PCR reaction, the RNA was incubated at 96 °C for 3 min and 70 °C for 10 min
2336 to denature the dsRNA (PMeV) and ssRNA (PMeV2). For the mPCR reaction, the RNA
2337 was denatured at 96 °C for 3 min. First-strand cDNA synthesis was performed using
2338 random hexamers and Moloney murine leukemia virus (M-MLV) reverse transcriptase
2339 (Invitrogen, Carlsbad, CA, USA).

2340 Two primer pairs were utilized for both uniplex PCR and mPCR diagnosis. The PMeV-
2341 specific primer pair targets the predicted PMeV ORF1 at nucleotide position 2446-2816
2342 (PMeVC1F, 5'CTTGGTTAGGCATAACTGTAGGT3'; PMeVC1R,
2343 5'CACGGACTCTTAGAAACGTCTATC3') [3]. The PMeV2-specific primer pair targets
2344 ORF2 at nucleotide position 1430-2244 (PMeV2F,
2345 5'CGCCAAGTGGGATAAGTTTAGA3'; PMeV2R,
2346 5'CGATTTGAGCACAAGGGTTAATG3') based on an available genomic sequence
2347 (NCBI GenBank no. KT921785). The primers were designed using the PrimerQuest
2348 Tool (<https://www.idtdna.com/PrimerQuest/Home/Index>), and their specificity was
2349 verified using BLAST (<https://www.ncbi.nlm.nih.gov/tools/primer-blast/>). The primers
2350 for PMeV amplify a 370-bp fragment, and those for PMeV2 amplify an 814-bp fragment.

2351 Uniplex and mPCR reactions were performed in a Mastercycler Thermocycler
2352 (Eppendorf, Hamburg, Germany) using Taq DNA Polymerase (Invitrogen, Carlsbad,
2353 CA, USA). To determine the optimal PCR conditions, different annealing temperatures
2354 (52 °C, 54 °C, 56 °C, 58 °C, 60 °C, 62 °C) and concentrations of each specific primer
2355 set (0.5:0.5 µM or 1.5:0.5 µM) were tested.

2356 Following optimization, PCR amplification was performed in a 10-µl volume containing
2357 1.54 µl of PCR mix (1 µl of 10X PCR Buffer -Mg²⁺, 0.3 µl of 50 mM MgCl₂, 0.2 µl of 10
2358 mM dNTP mixture and 0.04 µl of recombinant Taq DNA polymerase [5 U/ µl]), and
2359 deionized water. The uniplex PCR reaction for detection of PMeV or PMeV2 contained
2360 1 µl of PMeV or PMeV2 primers (10 µM), while multiplex PCR reactions were
2361 performed with half the amount of both primers. Both uniplex and mPCR reaction were
2362 performed with 55 ng of cDNA. The PCR mix and primers were manufactured by
2363 Invitrogen, Carlsbad, CA, USA.

2364 The PCR protocol consisted of the following: 94 °C for 3 min followed by 35 cycles of
2365 amplification (94 °C for 45 s, 58 °C for 30 s, 72 °C for 1 min) and a final extension at
2366 72 °C for 10 min. PMeV2 conditions were the same as for PMeV, but the extension
2367 time during the cycles was increased to 1.2 min. The mPCR program was the same as
2368 for the PMeV2 uniplex reaction. PCR amplicons were analyzed by electrophoresis on
2369 1% (w/v) agarose gels stained with ethidium bromide and visualized under UV light.

2370 To assess the LOD of the uniplex and mPCR assays, we generated recombinant
2371 plasmids by ligating the RT-PCR products into the plasmid pGEM®-T Easy Vector
2372 (Promega, Fitchburg, WI, USA). The specificity of PCR was validated by Sanger
2373 sequencing. The plasmid copy number was determined [18], and serial tenfold dilutions
2374 (10^8 - 10^1 copies/ μ l) were used as a template in 10- μ L uniplex PCR mixtures. To
2375 determine the sensitivity of the mPCR, two different assays were performed. In the first
2376 one, equal volumes of each plasmid dilution were used as a template in different PCR
2377 reactions. In the second, different ratios of the PMeV and PMeV2 plasmids were used
2378 (10^8 : 10^3 , 10^8 : 10^2 , and 10^8 : 10^1) to mimic situations in which different viral titers are
2379 present in field samples. All reactions were performed according to the program
2380 described above for mPCR.

2381 To determine the optimal annealing temperature for the PCR reactions, a gradient test
2382 was performed in uniplex and mPCR reactions. No differences in the efficiency of the
2383 reaction were found when different temperatures were tested; therefore, the annealing
2384 temperature was chosen to be 58 °C. This temperature was also used to test different
2385 PMeV and PMeV2 primer ratios in mPCR using cDNA from symptomatic post-flowering
2386 plants. Based on the intensity of amplicons, the 0.5:0.5 μ M primer ratio was used in
2387 further reactions. Moreover, reliable diagnosis of the PMeV complex using current
2388 techniques requires synthesis of a cDNA with two different denaturation temperatures
2389 (one for each virus) [3], and this consumes double the materials and reagents for PCR
2390 detection. We tested these two cDNA samples in the mPCR assay, but only the PMeV
2391 dsRNA denaturation protocol (96 °C for 3 min) gave results that were consistent with
2392 those obtained with the uniplex RT-PCR (data not shown).

2393 The sensitivity test showed that the uniplex RT-PCR assay could detect 10 copies of
2394 PMeV, whereas the LOD for PMeV2 was 100 copies (Online Resource 1). The
2395 sensitivity of the uniplex PCR was compared with that of the mPCR, and they were
2396 found to have equal sensitivity, although the band intensity was weaker at all dilutions
2397 in the mPCR.

2398 To validate the mPCR assay for use in field surveys, samples collected from papaya
2399 plants at stages i, ii, iii, and iv were tested. Forty-two papaya plants were tested, and
2400 the results are summarized in Table 1. In seedlings, all samples were positive for PMeV

2401 but negative for PMeV2. All adult pre-flowering plants tested positive for both PMeV
2402 and PMeV2, although some differences were found between the post-flowering
2403 groups. PMeV2 was detected in 12 out of 16 samples from group iii and in all samples
2404 of group iv, while fewer samples (three in the asymptomatic group and two in the
2405 symptomatic group) tested negative for PMeV. To rule out a false-negative diagnosis,
2406 we perform the uniplex RT-PCR assay with samples that tested negative for one of the
2407 viruses (data not shown). The results for the four samples from group iii that tested
2408 negative for PMeV2 and all seedling samples agreed with the mPCR results. On the
2409 other hand, uniplex RT-PCR confirmed the infection in the remaining samples,
2410 revealing a discrepancy between the results of this experiment and those of the LOD
2411 experiment.

2412 The sensitivity test using an equimolar plasmid ratio demonstrated that PMeV and
2413 PMeV2 detection in the mPCR was not altered when compared to the uniplex PCR
2414 (Online Resource 1). Therefore, it was not clear why some field samples were positive
2415 for PMeV in the uniplex PCR but not in the mPCR assay. One possible reason could
2416 be related to differences in viral titer. The use of equal amounts of PMeV and PMeV2
2417 recombinant plasmids in sensitivity assay may not reflect the actual amounts of these
2418 viruses in the papaya plants. To test this hypothesis, we performed assays with
2419 different PMeV:PMeV2 plasmid copy number ratios ($10^8:10^3$, $10^8:10^2$, and $10^8:10^1$) in
2420 the mPCR. The results showed that when one virus was present at a high titer, the
2421 band intensity for the other virus in the agarose gel was lower (Online Resource 1).

2422 The discovery of a second virus associated with sticky disease in plants indicated the
2423 need for the development of a new diagnostic tool. In this study, an already available
2424 primer pair [3] and a new one were used to develop an mPCR assay to detect PMeV
2425 and PMeV2 in a single reaction and its sensitivity and applicability for use in field
2426 surveys were evaluated.

2427 It is a common practice to use equimolar amounts of PCR templates to determine the
2428 detection limit of an mPCR assay [14, 17,18,19]. Here, we determined the detection
2429 limit when different ratios of templates were used and found that altering the relative
2430 amount of the templates indeed affected the results (Online Resource 1). Although
2431 PMeV was detected more frequently than PMeV2 in pre-flowering papaya plants [23],

2432 this difference was more pronounced at later stages of infection (post-flowering
2433 symptomatic), as both viruses were successfully detected by mPCR in all adult pre-
2434 flowering plants. Amplicons produced by mPCR in the sensitivity test showed lower
2435 band intensity in an agarose gel. The presence of two primer pairs forces competition
2436 between the amplicons by the PCR reagents and thus reduces the yield of either the
2437 amplicons [24]. When templates were used in equal amounts, the reduced yield did
2438 not affect the LOD for both PMeV or PMeV2 amplicon.

2439 In this study, we developed a multiplex PCR method for simultaneous detection of
2440 PMeV and PMeV2 in papaya pre-flowering plants. This method is very useful for early
2441 diagnosis because it can be used to screen simultaneously for both viruses in a large
2442 number of samples. Therefore, this procedure will contribute to a better understanding
2443 of PSD epidemiology and to the development of disease management strategies.

2444 **Acknowledgments:** T.F. Sá Antunes and S. A. Oliveira would like to thank the
2445 *Coordenação de Aperfeiçoamento de Pessoal de Nível Superior, CAPES* (Ministry of
2446 Education of Brazil) and M. Maurastoni the *Fundação de Amparo à Pesquisa do*
2447 *Espírito Santo, FAPES* for their fellowship. P.M.B. Fernandes and José A. Ventura
2448 were granted with the research productivity award from the *Conselho Nacional de*
2449 *Desenvolvimento Científico e Tecnológico (CNPq)*, Grant #304719/2014-5 and
2450 #308631/2016-1, respectively.

2451 **Conflicts of Interest:** The authors declare that they have no conflict of interest.
2452

2453

2454

2455 REFERENCES

2456

2457

2458 1. Maciel-Zambolim E, Kunieda-Alonso S, Matsuoka K, De Carvalho M, Zerbini F
2459 (2003) Purification and some properties of Papaya meleira virus, a novel virus infecting
2460 papayas in Brazil. *Plant Pathol* 52:389-394.

2461 2. Kitajima EW, Rodrigues CH, Silveira JS, Alves F, Ventura JA, Aragão FJL, Oliveira
2462 LHR (1993) Association of isometric viruslike particles, restricted to laticifers, with
2463 meleira (" sticky disease") of papaya (*Carica papaya*). *Fitopatol Bras* 18:118-122.

- 2464 3. Antunes TFS, Amaral RJV, Ventura JA, Godinho MT, Amaral JG, Souza FO, Zerbini
2465 PA, Zerbini FM, Fernandes PMB (2016) The dsRNA Virus Papaya Meleira Virus and
2466 an ssRNA Virus Are Associated with Papaya Sticky Disease. *PloS One* 11:e0155240.
- 2467 4. Meissner Filho P, Lima Neto F, de Oliveira C, Santana S, Dantas J (2017) Avaliação
2468 da resistência de genótipos de mamoeiro ao vírus da meleira no Semiárido. Embrapa
2469 Mandioca e Fruticultura-Boletim de Pesquisa e Desenvolvimento (INFOTECA-E).
2470 Embrapa Mandioca e Fruticultura, Cruz das Almas, BA.
- 2471 5. Ventura JA, Costa H, Tatagiba JdS (2004) Papaya Diseases and Integrated Control.
2472 In: Naqvi SAMH (ed) *Diseases of Fruits and Vegetables: Volume II: Diagnosis and*
2473 *Management*. Springer Netherlands, Dordrecht, pp 201-268.
- 2474 6. Abreu PMV, Antunes TFS, Magaña-Álvarez A, Pérez-Brito D, Tapia-Tussell R,
2475 Ventura JA, Fernandes AAR, Fernandes PMB (2015) A current overview of the Papaya
2476 meleira virus, an unusual plant virus. *Viruses* 7:1853-1870.
- 2477 7. Rodrigues SP, Galvao OP, Andrade JS, Ventura JA, Fernandes PMB (2005)
2478 Simplified molecular method for the diagnosis of Papaya meleira virus in papaya latex
2479 and tissues. *Summa Phytopathol* 31:281-283.
- 2480 8. Araújo MMMd, Tavares ÉT, Silva FRd, Marinho VLdA, Júnior MTS (2007) Molecular
2481 detection of Papaya meleira virus in the latex of *Carica papaya* by RT-PCR. *J Virol*
2482 *Methods* 146:305-310.
- 2483 9. Abreu PMV, Piccin JG, Rodrigues SP, Buss DS, Ventura JA, Fernandes PMB (2012)
2484 Molecular diagnosis of Papaya meleira virus (PMeV) from leaf samples of *Carica*
2485 *papaya* L. using conventional and real-time RT-PCR. *J Virol Methods* 180:11-17.
- 2486 10. Elnifro EM, Ashshi AM, Cooper RJ, Klapper PE (2000) Multiplex PCR: optimization
2487 and application in diagnostic virology. *Clin Microbiol Rev* 13:559-570.
- 2488 11. Tuo D, Shen W, Yang Y, Yan P, Li X, Zhou P (2014) Development and validation
2489 of a multiplex reverse transcription PCR assay for simultaneous detection of three
2490 papaya viruses. *Viruses* 6:3893-3906.
- 2491 12. Forootan A, Sjöback R, Björkman J, Sjögren B, Linz L, Kubista M (2017) Methods
2492 to determine limit of detection and limit of quantification in quantitative real-time PCR
2493 (qPCR). *Biomol Detect Quantif* 12:1-6.
- 2494 13. Broeders S, Huber I, Grohmann L, Berben G, Taverniers I, Mazzara M, Roosens
2495 N, Morisset D (2014) Guidelines for validation of qualitative real-time PCR methods.
2496 *Trends Food Sci Tech* 37:115-126.
- 2497 14. Zhao X, Liu X, Ge B, Li M, Hong B (2015) A multiplex RT-PCR for simultaneous
2498 detection and identification of five viruses and two viroids infecting chrysanthemum.
2499 *Arch Virol* 160:1145-1152.
- 2500 15. Hyun JW, Hwang RY, Jung KE (2017) Development of multiplex PCR for
2501 simultaneous detection of citrus viruses and the incidence of citrus viral diseases in
2502 late-maturity citrus trees in Jeju Island. *Plant Pathol J* 33:307.

- 2503 16. Kwon JY, Hong JS, Kim MJ, Choi SH, Min BE, Song EG, Kim HH, Ryu KH (2014)
2504 Simultaneous multiplex PCR detection of seven cucurbit-infecting viruses. J Virol
2505 Methods 206:133-139.
- 2506 17. Tao Y, Man J, Wu Y (2012) Development of a multiplex polymerase chain reaction
2507 for simultaneous detection of wheat viruses and a phytoplasma in China. Arch Virol
2508 157:1261-1267.
- 2509 18. Deng X, Zhang J, Su J, Liu H, Cong Y, Zhang L, Zhang K, Shi N, Lu R, Yan X
2510 (2018) A multiplex PCR method for the simultaneous detection of three viruses
2511 associated with canine viral enteric infections. Arch Virol 163:2133-2138.
- 2512 19. Zhang X, Peng Y, Wang Y, Zhang Z, Li D, Yu J, Han C (2016) Simultaneous
2513 detection and differentiation of three genotypes of Brassica yellows virus by multiplex
2514 reverse transcription-polymerase chain reaction. Virology J 13:189.
- 2515 20. Syller J (2012) Facilitative and antagonistic interactions between plant viruses in
2516 mixed infections. Mol Plant Pathol 13:204-216.
- 2517 21. Mascia T, Gallitelli D (2016) Synergies and antagonisms in virus interactions. Plant
2518 Sci 252:176-192.
- 2519 22. Chávez-Calvillo G, Contreras-Paredes CA, Mora-Macias J, Noa-Carrazana JC,
2520 Serrano-Rubio AA, Dinkova TD, Carrillo-Tripp M, Silva-Rosales L (2016) Antagonism
2521 or synergism between papaya ringspot virus and papaya mosaic virus in *Carica papaya*
2522 is determined by their order of infection. Virology 489:179-191.
- 2523 23. Madronero J, Rodrigues SP, Antunes TFS, Abreu PMV, Ventura JA, Fernandes
2524 AAR, Fernandes PMB (2018) Transcriptome analysis provides insights into the
2525 delayed sticky disease symptoms in *Carica papaya*. Plant Cell Rep 37:967-980.
- 2526 24. Anitha S, Monyo E, Okori P (2014) Simultaneous detection of groundnut rosette
2527 assistor virus (GRAV), groundnut rosette virus (GRV) and satellite RNA (satRNA) in
2528 groundnuts using multiplex RT-PCR. Arch Virol 159:3059-30
- 2529

2530 TABLES

2531 **Table 1.** Results of uniplex and multiplex PCR survey testing 42 plants
 2532 from greenhouse and papaya orchards in Espírito Santo, Brazil

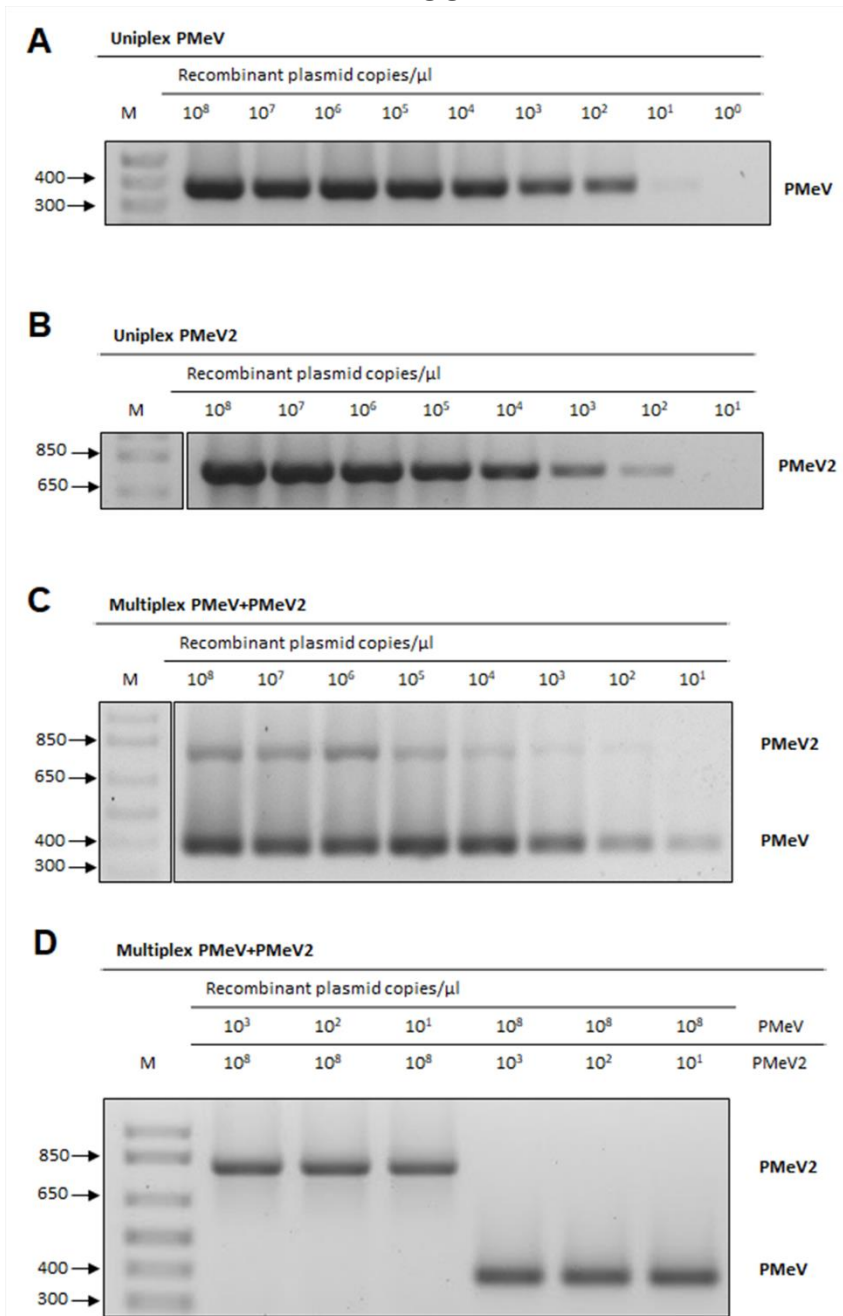
Development stage	Uniplex*		Multiplex*	
	PMeV	PMeV2	PMeV	PMeV2
Seedlings	10/10	10/0	10/10	10/0
Adult Pre-flowering	10/10	10/10	10/10	10/10
Post-flowering asymptomatic	16/16	16/12	16/12	16/12
Post-flowering symptomatic	6/6	6/6	6/4	6/6

2533 * No. of total plants/No. positives

2534

2535

SUPPLEMENTARY MATERIAL



2536

2537

2538 **MANUSCRIPT #5. EFFORTS TO UNDERSTAND TRANSMISSION OF THE**
2539 **PAPAYA MELEIRA VIRUS COMPLEX BY INSECTS**

2540

2541

2542 Manuscript in preparation for *Annals of Applied Biology* (ISSN 0003-4746; IF 2.75,
2543 2020; Qualis Biotecnologia B1)

2544

2545

2546 **Efforts to understand transmission of the papaya meleira virus complex by**
2547 **insects**

2548

2549

2550 **Marlonni Maurastoni**^a, Tathiana F. Sá-Antunes^a, José A. Ventura^{a,b}, Anna E.
2551 Whitfield^{c*} and Patricia M. B. Fernandes^{a*}

2552

2553

2554 ^aNúcleo de Biotecnologia, Universidade Federal do Espírito Santo, Vitória, Espírito
2555 Santo, Brazil

2556 ^bInstituto Capixaba de Pesquisa, Assistência Técnica e Extensão Rural, Vitória, Espírito
2557 Santo, Brazil

2558 ^cDepartment of Entomology and Plant Pathology, North Carolina State University,
2559 Raleigh, North Carolina, USA

2560 *Corresponding authors: awhitfi@ncsu.edu; patricia.fernandes@ufes.br

2561

ABSTRACT

2562

2563

2564

2565 Papaya sticky disease (PSD) is an emerging disease causing significant crop losses
2566 in some of the major papaya-growing regions of the world. The vectors of the PSD-
2567 associated viruses in Brazil are still unknown. Publications on transmission and
2568 epidemiology of PSD have increased recently with the spread of the disease to
2569 additional papaya-growing countries. In this review, we present an overview of the
2570 vector biology studies of PSD transmission. Epidemiological analyses attributed fruit
2571 thinning as a mechanism spreading the disease, but an aerial vector was not ruled out.
2572 Hemipteran insects have been implicated as vectors but a definitive conclusion on the
2573 biologically relevant vector has not been reached. Leafhoppers have a population peak
2574 a month before the PSD incidence peak in the field and their ability to vector the PMeV
2575 Mexican isolate has been demonstrated. Whiteflies (*Bemisia tabaci* Middle East-Asia
2576 Minor 1) have been reported to occur in plants close to papaya trees in Brazil and to
2577 transmit an Ecuadorian virus similar to PMeV2. In Brazil, *Trialeurodes variabilis* which
2578 colonizes papaya trees, can acquire but not transmit the PMeV complex. The
2579 conflicting reports of insect vectors for PSD and related viruses highlights the need for
2580 additional research on this important pathosystem. Elucidation of the PMeV complex
2581 vector would contribute to the efficient management of papaya sticky disease and
2582 increase understanding of the transmission mechanisms of plant-infecting toti-like
2583 viruses.

2584

2585 Keywords: sticky disease, vector, Leafhoppers, *Trialeurodes*, transmission.

2586

2587

INTRODUCTION TO PAPAYA STICKY DISEASE

2588

2589

2590

2591 Papaya sticky disease (PSD) is one of the major diseases affecting papaya orchards
2592 in Brazil (RODRIGUES *et al.*, 1989), Mexico (PEREZ-BRITO *et al.*, 2012), and
2593 Australia (PATHANIA *et al.*, 2019), and capable of causing complete crop loss. The
2594 distribution of PSD under field conditions points to possible mechanical transmission
2595 and an aerial vector but the PSD insect vector is still unknown in Brazil (ABREU, *et al.*,
2596 2015; ANTUNES *et al.*, 2020) even though, several transmission assays and
2597 epidemiology analyses have been done in the last 30 years. In Mexico, the dispersion
2598 occurs by the leafhopper *Empoasca papayae* Oman (Hemiptera: Cicadellidae)
2599 (GARCÍA-CÁMARA *et al.*, 2019), and also through the infected seeds (TAPIA-
2600 TUSSELL *et al.*, 2015). The presence of a vector in Australian orchards has not yet
2601 been confirmed, but seeds play an important role in the spread of the disease
2602 (CAMPBELL, 2019a; b).

2603 The presence of a biotic agent responsible for PSD is dated in a 1989 publication
2604 showing that inoculation of infected latex leads to symptom development in healthy
2605 plants (RODRIGUES *et al.*, 1989). The disease's etiology was initially confirmed in
2606 2003 as being caused by a virus (MACIEL-ZAMBOLIM *et al.*, 2003) and only in 2016
2607 a second virus was identified associated with diseased plants (ANTUNES *et al.*, 2016).

2608 Since the confirmation of its etiology, Brazilian researchers have tried to identify the
2609 insect vector. Initially, experiments have shown that healthy plants can develop
2610 symptoms when inoculated with macerated whiteflies (*Bemisia tabaci* Middle East-Asia
2611 Minor 1) collected near diseased papaya plants (HABIBE *et al.*, 2001). Although *B.*
2612 *tabaci* MEAM1 did not colonize papaya trees, this result paved the way to investigate
2613 the correlation of another species of whitefly associated with papaya: *Tiraleurodes*
2614 *variabilis*. From 2002 to 2003 Brazilian papaya orchards were intensively analyzed in
2615 search of a positive correlation between a population of an insect species and plants
2616 with PSD symptoms. *Tiraleurodes variabilis* does not show this correlation in the field
2617 and experiments conducted in the greenhouse have shown that despite acquiring the
2618 infectious agent, this species is not able to transmit it (ANDRADE *et al.*, 2003; LIMA *et*
2619 *al.*, 2003; RODRIGUES, S. *et al.*, 2009). Surprisingly, field analysis showed a positive

2620 correlation with leafhoppers (*Solanasca bordia*) which was confirmed in a second
2621 analysis conducted from 2017 to 2018.

2622 During these last 30 years, publications on transmission and epidemiology, written only
2623 in Portuguese, have been presented and discussed at Brazilian meetings and are
2624 available across different libraries and journals (Table 1). Recently, the number of
2625 publications and experiments carried out to identify PSD vectors has intensified since
2626 the disease has reached other countries. Thus, in this review, we have compiled these
2627 works and discussed their main findings given the molecular diagnostic techniques
2628 developed over the years and the new proposed etiology. We open an important
2629 discussion for directing new research to understand the vectors of this virus complex
2630 and the use of new management practices in papaya orchards.

2631

2632

2633

2634 COULD PMeV COMPLEX BE TRANSMITTED BY FUNGI?

2635

2636

2637 Spontaneous latex exudation from green fruits and necrosis in the edge of young
2638 leaves are the main PSD symptoms (VENTURA *et al.*, 2004) which are associated with
2639 infection by an unclassified viral complex (papaya meleira virus - PMeV and papaya
2640 meleira virus 2 - PMeV2, PMeV complex) (Figure 1) (ANTUNES *et al.*, 2016).

2641 The viral structural proteins protect the viral genome and play a role in several
2642 biological processes such as virus movement within the host, replication, translation,
2643 and specificity of transmission by a vector (BOL, 2008). In mixed infections, capsid
2644 proteins (CPs) produced by PMeV are used for the package of PMeV2 (trans-
2645 encapsidation) resulting in virions with the same morphology but containing different
2646 RNAs (ANTUNES *et al.*, 2016) which supports the idea that PMeV and PMeV2 could
2647 be transmitted by the same vectors. The trans-encapsidation phenomenon is also
2648 found between members of the *Umbravirus* genus and poleroviruses or enamoviruses
2649 (family *Solemoviridae*). Umbraviruses lack the CP gene and, as a result, do not form
2650 conventional virus particles, even though they can systematically infect a plant when
2651 mechanically inoculated (TALIANSKY; ROBINSON, 2003). Umbraviruses
2652 transmission between plants with the aid of insect vectors is only possible when the
2653 umbraviral genome is packaged by the luteovirids capsid protein, which results in the
2654 same host range (TALIANSKY *et al.*, 2000). In members of the *Totiviridae* family, the
2655 CP is typically encoded by the 5' ORF (ORF1) which generally have sizes between
2656 70–100 kDa (DE LIMA *et al.*, 2019) and are predominantly α -helical (LUQUE *et al.*,
2657 2018). Members of the *Totiviridae* family generally associated with fungi, yeast, and
2658 parasitic protozoa, have been also found infecting mollusks, arthropods, including
2659 mosquitos, ants, shrimps, and planthoppers, and plants (DE LIMA *et al.*, 2019).
2660 Besides PMeV, maize-associated totivirus (MATV), panax notoginseng virus A (PnVA)
2661 and tea-oil camellia-associated totivirus 1 (TOCaTV1) are unclassified viruses that also

2662 infect plants (AKINYEMI *et al.*, 2018; GUO *et al.*, 2016; ZHANG *et al.*, 2021). Although
2663 there are no reports of a CP coded by these viruses (except for PMeV), the PnVA,
2664 MATV and TOCaTV1 ORF1 have a conserved region which includes the LA virus coat
2665 domain (pfam09220), present in all CPs of totiviruses infecting fungi (AKINYEMI *et al.*,
2666 2018). The fact that the CP of these plant viruses is more similar to totiviruses that
2667 infect fungi than totiviruses that infect insects supports the idea that fungi may act as
2668 vectors of the PMeV complex. Given the opportunities for transfer during fungal
2669 colonization, it is possible that PMeV, MATV, PnVA and TOCaTV1 can be transmitted
2670 to plants via a fungal host species (ANDIKA *et al.*, 2017; ROOSSINCK, 2019). Under
2671 controlled conditions, *Rizoctania solani* can acquire and transmit a plant virus,
2672 cucumber mosaic virus (CMV), during plant infection (ANDIKA *et al.*, 2017). Several
2673 fungi are found infecting papaya leaves and they are included in the genus
2674 *Asperisporium*, *Stagonosporopsis* (Syn.: *Phoma*), *Colletotrichum*, and *Corynespora*,
2675 and recently an (+) ssRNA virus was found in *Phoma matteuccicola*, the causal agent
2676 of leaf blight disease in *Curcuma wenyujin* (ZHOU *et al.*, 2020). If fungi also play a role
2677 in PMeV complex transmission, important uncharacterized structural domains may be
2678 present in PMeV capsid.

2679
2680
2681

2682 **HOW DOES AN INSECT ACQUIRE PME V COMPLEX VIRIONS FROM A** 2683 **DISEASED PLANT?**

2684
2685

2686 A longstanding question in virus acquisition by an insect vector is how can they acquire
2687 PMeV virions from papaya laticifers, the only documented site of virus particle
2688 accumulation in papaya plants (KITAJIMA *et al.*, 1993). PMeV virions were visualized,
2689 using transmission electron microscopy (TEM), in laticifers cells, a structure well known
2690 for its defense role against pathogens. In *C. papaya*, laticifers are articulated,
2691 anastomosed (HAGEL *et al.*, 2008), and found in all papaya organs (FISHER, 1980;
2692 RAO *et al.*, 2013). Mature papaya laticifers are living cells that store, under high
2693 pressure, vesicles containing, carbohydrates, lipid salts, and proteins, mainly cysteine

2694 proteases (EL MOUSSAOUI *et al.*, 2001). Upon tissue wounding, latex starts to
2695 exudate and cysteine proteases are activated resulting in the clotting of the wound
2696 (SILVA *et al.*, 1997). Whereas several studies report the different strategies adopted
2697 by mandibulate herbivores, little information is available on how sap-sucking insects
2698 can feed on latex-bearing plants. Any damage to laticifers could cause an overflow of
2699 harmful compounds (e.g proteolytic enzymes such as cysteine and serine proteases,
2700 organic acids, alkaloids, and terpenes) leading to the clogging or destruction of the
2701 insect's mouthparts. However, it has been shown that when feeding in two different
2702 latex-bearing plants, *Aphis nerii* can use its stylet to reach phloem cells avoiding the
2703 laticifers or completely circumscribing them during the probing (BOTHA *et al.*, 1975a;
2704 b). It is not yet clear how the PMeV viral particles are acquired by an insect. It is
2705 possible that insects can acquire viral particles present in other cells, which due to not
2706 accumulate are not observed by TEM but could be detected with immunocytochemical
2707 techniques, hitherto unavailable. In another scenario, the physiological and
2708 biochemical changes present in laticifers of PSD plants could help viral particles to be
2709 acquired by an insect. Laticifers of PSD plants present a reduction of protease levels
2710 and activity, and an increase in its fluidity (RODRIGUES, *et al.*, 2009) which could
2711 minimize the damage and the clogging to an insect mouthpart when probing a laticifer.

2712

2713

2714

2715 **STUDIES OF PSD TRANSMISSION BY VECTORS**

2716

2717

2718 Insects are the most common vectors of plant viruses and are associated with more
2719 than 61% of virus species, and approximately 83% of insect-borne viruses are
2720 transmitted by hemipterans, e.g. aphids, whiteflies, leafhoppers, and planthoppers
2721 (reviewed in (COSTA, 2005) and (HOGENHOUT *et al.*, 2008)). Because the natural
2722 spread of viruses often depends on vectors, knowledge of the interrelationship
2723 between the virus and the vector is essential for establishing control strategies and
2724 mitigating the damage that the disease causes in plants.

2725 The possible involvement of insects as sticky disease vectors has been suggested
2726 based upon early studies on the field spread pattern of this disease, especially with
2727 evidence of the existence of an aerial vector associated with the disease (MAFFIA *et*
2728 *al.*, 1993; RODRIGUES *et al.*, 1989). Although epidemiological studies of PSD
2729 implicate the involvement of vectors in the transmission of PMeV and PMeV2 viruses,
2730 the identity of the vector has not been determined in Brazil and in the other regions
2731 where the disease is present. Insects of the order Hemiptera, suborder Homoptera,
2732 have a large number of species that are reported as vectors of approximately 90% of
2733 the viruses transmitted by insects (COSTA, 2005). In addition to aphids (Family:
2734 *Aphididae*) reported as vectors of *Papaya ringspot virus* (PRSV-P), other homopterans,
2735 such as leafhoppers (Family: *Cicadellidae*) and whiteflies (Family: *Aleyrodidae*), are
2736 also reported as vectors of other diseases in papaya (LIMA *et al.*, 2003).

2737 It is important to clarify that until 2007 most studies on PSD were based on virus
2738 detection through the visualization of the viral PMeV dsRNA. However, this technique
2739 requires that samples display a large amount of both viruses. The sequencing of both
2740 PMeV and PMeV2 (ABREU *et al.*, 2015; ANTUNES *et al.*, 2016; ARAÚJO *et al.*, 2007)
2741 allowed the development of more sensitive techniques such as RT-PCR (ABREU *et*
2742 *al.*, 2012; ANTUNES *et al.*, 2016; MAURASTONI *et al.*, 2020) and qRT-PCR (ABREU
2743 *et al.*, 2012) which have been applied to understand critical aspects of the PSD
2744 epidemiology. Through RT-PCR it was able to show that papaya plants infected by
2745 PMeV can remain asymptomatic in the field acting as a viral source for uninfected
2746 plants (ANTUNES *et al.*, 2016).

2747

2748

2749

2750 **DO LEAFHOPPERS TRANSMIT PSD-ASSOCIATED VIRUSES?**

2751

2752

2753 Leafhoppers (Hemiptera: *Cicadellidae*) are threatening papaya pests because they
2754 cause significant damage and are potential vectors of viruses, phytoplasmas, and
2755 rickettsia. Leafhoppers emerged as potential vectors of the PMeV complex since their

2756 distribution in the field is related to the spread of the PSD (LIMA *et al.*, 2003; VENTURA
2757 *et al.*, 2003). Surveys of leafhopper populations in papaya orchards in Brazil were
2758 conducted using sticky traps and circular sweep nets. During the one-year sampling
2759 period, most leafhoppers collected were identified as *Solanasca bordia* (Hemiptera:
2760 Cicadellidae: Typhlocybinae), accounting for 80% of the total, followed by species of
2761 the genus *Empoasca*, accounting for 5% of the total (GOUVEA *et al.*, 2018). Studies
2762 on the involvement of leafhoppers, especially those of the genus *Solanasca*, as vectors
2763 of PMeV have shown a high correlation between the insect population and the
2764 incidence of diseased plants (Figure 2). The population peak of leafhoppers precedes
2765 the highest peak of PSD incidence, which occurs about one month later (GOUVEA *et*
2766 *al.*, 2018). A delay of 45 days for symptom onset was also shown when papaya plants
2767 are mechanically inoculated with disease latex (VENTURA *et al.*, 2001). These results
2768 indicate that leafhoppers can be potential vectors of the PSD in Brazil and must be
2769 considered in further transmission assays (GOUVEA *et al.*, 2018; LIMA *et al.*, 2003;
2770 VENTURA *et al.*, 2003).

2771 The population fluctuation of leafhoppers is compatible with the analysis of temporal
2772 evolution of papaya sticky disease and provides subsidies to verify the dispersion and
2773 generate information about the influence of biological and environmental factors on the
2774 population dynamics of the pathogen/disease. The most favorable period of the year
2775 for the disease development were colder and dry months, while the warmest and
2776 wettest months favored the mitigation of symptoms, and the model that best fitted the
2777 disease epidemics is the Gompertz (COSMI *et al.*, 2017).

2778 In Mexico, the ability of the leafhopper *E. papayae* adults, but not nymphs, to transmit
2779 PMeV-Mx to *C. papaya* 'Maradol' has been proven. PMeV-Mx is an umbravirus-like
2780 associated RNA (ulaRNA) found infecting papaya plants in Mexico. It is 71% and 79%
2781 identical at nucleotide level to PMeV2 and the Ecuadorian virus, papaya virus Q
2782 (PpVQ) respectively. Under controlled conditions, *E. papayae* can acquire PMeV-Mx
2783 six hours after exposure to infected plants, and viral titer increases if the exposure time
2784 is longer up to 5 days (Figure 3). Little is known about the biology of *E. papayae*, and
2785 research is now focused on understanding the behavior of this insect in the field
2786 (GARCÍA-CÁMARA *et al.*, 2019). Despite the lower abundance among the collected

2787 species, insects from the family *Cicadelidae* (*Agallia constricta*, *Agalliopsis novella*, *E.*
2788 *papayae*, *Draeculacephala soluta*, *Hortensia* sp., and *Xyphon* sp.) and *Aphididae*
2789 (*Aphis* sp. and *Uroleucon taraxaci*) were also identified containing the PMeV-Mx but
2790 their potential as vectors has yet to be studied.

2791 Research teams in Brazil are currently conducting experiments to identify the virus
2792 vector and elucidate the transmission mechanism. Under field conditions, research on
2793 the papaya-producing region of the north of Espírito Santo state found the most
2794 frequent leafhoppers in papaya plants belonging to *Cercopyidae*, *Cicadellidae*,
2795 *Membracidae*, and *Delphacidae* families (VENTURA, J.A.; unpublished data).

2796

2797

2798

2799 **DO WHITEFLIES TRANSMIT PSD-ASSOCIATED VIRUSES?**

2800

2801

2802 Whiteflies are considered secondary pests of papayas worldwide because they do not
2803 cause important damage to plants or fruits in field orchards. Among the whitefly species
2804 reported worldwide two species, *Bemisia tabaci* MEAM1 and *Trialeurodes variabilis*,
2805 have been reported occurring in different areas of Brazilian papaya orchards
2806 (MARTINS *et al.*, 2016) (Figure 4), and its ability to transmit the infectious agent of
2807 PSD in Brazil, was evaluated in three different works through the visualization of PMeV
2808 dsRNA (HABIBE *et al.*, 2001; RODRIGUES. *et al.*, 2009; VIDAL *et al.*, 2003).

2809 *B. tabaci* MEAM1, despite being reported to cause damage to papaya in other
2810 biogeographic regions of the world, so far it has limited occurrence to protected
2811 cultivation environments and is not considered a papaya pest in Brazil under field
2812 conditions (VENTURA *et al.*, 2004). As a polyphagous insect, the whitefly colonizes
2813 and multiplies on numerous cultivated, wild, and invasive plants. The ability of *B. tabaci*
2814 MEAM1 to acquire and transmit the PSD infectious agent was assessed by two
2815 different experiments. Habibe *et al.*, (2001) inoculated macerated bodies of whiteflies
2816 collected from areas with PSD into healthy papaya plants. Ninety days after inoculation,
2817 healthy plants presented viral dsRNA of similar size to that detected in PSD plants,

2818 which suggested that *B. tabaci* MEAM1 is capable of acquiring the infectious form of
2819 the PMeV complex (HABIBE *et al.*, 2001). In another experiment, the ability of *B. tabaci*
2820 MEAM1 to transmit the PSD infectious agent was determined when the dsRNA of
2821 PMeV was detected in asymptomatic plants exposed for 24-72h to whiteflies that have
2822 previously been forced feeding for 48h and 30min on diseased papaya plants (Figure
2823 5.A) (VIDAL *et al.*, 2003). In this experiment, the authors do not mention any diagnostic
2824 test in asymptomatic plants. After the development of sensitive techniques for PSD-
2825 associated virus diagnosis (e.g RT-PCR), it is not uncommon to detect viral RNA in
2826 asymptomatic plants (ANTUNES *et al.*, 2016). This supports the idea that
2827 asymptomatic but infected plants were used for the experiment, instead of virus-free
2828 plants. Moreover, the fact that few plants were exposed to the whiteflies raises the
2829 necessity to include a higher number of plants in this experiment. This group also
2830 tested the virus transmission by aphid species, *Toxoptera citricidus*, and *Myzus*
2831 *persicae*, but they were unable to transmit the PMeV dsRNA to healthy plants. Under
2832 field conditions, Martins *et al.* (2016) when studying aphid population species and their
2833 host plants in commercial papaya orchards, found no evidence that these insects were
2834 involved in the transmission of PSD.

2835 *T. variabilis* initially infest papaya leaves on the top of the canopies and then move to
2836 newly developed leaves. Eggs and nymphs are found in all parts of the canopy, but
2837 insects preferentially feed and lay their eggs on new leaves. Also, it is common to see
2838 oviposition concentrated in the basal region, and nymphs more frequently in the central
2839 part of older leaves (MARTINS *et al.*, 2016). The ability of *T. variabilis* to transmit the
2840 PMeV dsRNA was assessed under greenhouse conditions (Figure 5.B). Twenty-four
2841 plants were inoculated with papaya diseased-latex, and one month later, they were
2842 infested with a population of *T. variabilis* collected from fields with asymptomatic
2843 papaya plants. One month later, three healthy papaya plants of different cultivars each
2844 (cvs. Taiwan, Golden, and Sunrise Solo) were added inside the greenhouse to be
2845 infested by the whiteflies. Twenty days later, dsRNA was detected in plants used as
2846 initial inoculum, and in adults and nymphs exposed to latex-inoculated plants but not
2847 in healthy plants that were exposed to "viruliferous" whiteflies. The authors suggested
2848 that *T. variabilis* can acquire the virus from infected plants and it is not able to transmit
2849 it to healthy plants under controlled conditions (RODRIGUES *et al.*, 2009). The amount

2850 of virus inoculated through latex injection is higher than through vector transmission.
2851 This difference could result in a lower virus load in plants that were exposed to
2852 "viruliferous" whiteflies, undetectable for dsRNA visualization.

2853 Epidemiological analysis revealed that PSD spread does not follow the same pattern
2854 as the fluctuation of the whitefly population (ANDRADE *et al.*, 2003; LIMA *et al.*, 2003).
2855 PSD occurs initially scattered and randomly in the orchard, later evolving to
2856 aggregation. Clouds of whiteflies are regularly observed in papaya crops during peak
2857 periods of the insect population and low incidence of plants with PSD, which suggests
2858 that whiteflies could not be the major insect involved in PSD spreading (MARTINS, D.
2859 *et al.*, 2016) (Figure 6). Whiteflies have a preference for certain hosts and even though
2860 they acquire viruses they only transmit a few, for example, viruses belonging to the
2861 genera *Begomovirus*, *Carlavirus*, *Crinivirus* and *Polerovirus* (GHOSH *et al.*, 2019).

2862 In Ecuador, the latest transmission tests pointed to whiteflies (*B. tabaci*) as vectors of
2863 the ulRNA PpVQ. Epidemiology data suggests an aerial vector for PpVQ which
2864 commonly occurs associated with *Papaya ringspot virus* (PRSV). However, efforts to
2865 transmit the virus from plants using aphids were only successful for PRSV but not for
2866 PpVQ (QUITO-AVILA *et al.*, 2015). To understand the vector of PpVQ in Ecuador, a
2867 field survey identified whiteflies, red mites, and mealybugs as the main arthropods
2868 present in papaya-infected plants and detected PpVQ in all three groups. These
2869 arthropods were collected and transferred to PpVQ virus-free papaya plants where
2870 they fed for 7 days. Ninety days after exposure to whiteflies, the virus was detected in
2871 three out of ten plants which whiteflies had fed, but not in field-collected whiteflies 7
2872 days after feeding in PpVQ virus-free plants. None of the plants exposed to field-
2873 collected red mites and mealybugs tested positive for PpVQ (CORNEJO-FRANCO *et*
2874 *al.*, 2018).

2875 Overall, the role of whiteflies as vectors of PSD needs to be carefully assessed since
2876 the experiments and analyzes carried out so far reach different conclusions. *T.*
2877 *variabilis* does not have a field distribution correlated with the incidence of diseased
2878 plants and is not able to transmit the infectious form of the viral complex to healthy
2879 plants. *B. tabaci* MEAM1 is not found colonizing papaya plants in the field which does

2880 not support its role as a vector even though, they can acquire the PMeV dsRNA from
2881 papaya plants under greenhouse conditions.

2882

2883

2884

2885 **CONCLUSIONS**

2886

2887

2888 For the past 30 years, research groups studying PSD have made efforts to understand
2889 the vector of PSD causative agents in the main papaya producers in the world. It is still
2890 challenging to assign a specific vector but epidemiological analysis shows insects as
2891 potential spreaders, among them leafhoppers and whiteflies. In Mexico and Ecuador,
2892 the question: "who are the vectors of the causal agents of the PSD?" is partially
2893 answered. Although leafhoppers and whiteflies were not found during survey analyzes
2894 conducted in Ecuador and Mexico, respectively, the sequence and genome
2895 organization similarity of PpVQ and PMeV-Mx supports the idea that both can be
2896 transmitted by the two insects. In Brazil, the results of the experiments conducted with
2897 whiteflies so far are contradictory but we cannot rule out that these insects may play a
2898 role in the dispersion of viruses in the field, among invasive plants as sources of
2899 inoculum. Leafhoppers need to be studied as potential vectors of the PMeV complex
2900 in Brazil, since these insects already play a role in the disease spread in Mexico and
2901 that their population fluctuation is related to the PSD occurrence in Brazil. Importantly,
2902 previous experiments need to be repeated and analyzed now that more sensitive
2903 molecular diagnostic techniques are available and with considerations of how the virus
2904 complex of a toti-like virus (PMeV) and the ulaRNA (PMeV2) may impact disease
2905 physiology and vector transmission. Knowledge about the diversity of viruses
2906 tentatively classified in the family *Totiviridae* infecting plants is very limited, as well as
2907 their modes of transmission. Therefore, studies that elucidate the PMeV complex
2908 vector and its transmission mechanisms could reveal uncharacterized relationships
2909 between viral structural proteins and insect vectors.

2910

2911 REFERENCES

2912

2913

2914 ABREU, E. F. M.; DALTRO, C. B.; NOGUEIRA, E. O.; ANDRADE, E. C.; ARAGÃO, F.
2915 J. Sequence and genome organization of papaya meleira virus infecting papaya in
2916 Brazil. **Archives of virology**, 160, n. 12, p. 3143-3147, 2015.

2917 ABREU, P. M. V.; ANTUNES, T. F. S.; MAGAÑA-ÁLVAREZ, A.; PÉREZ-BRITO, D.;
2918 TAPIA-TUSSELL, R.; VENTURA, J. A.; FERNANDES, A. A. R.; FERNANDES, P. M.
2919 B. A current overview of the Papaya meleira virus, an unusual plant virus. **Viruses**, 7,
2920 n. 4, p. 1853-1870, 2015.

2921 ABREU, P. M. V.; PICCIN, J. G.; RODRIGUES, S. P.; BUSS, D. S.; VENTURA, J. A.;
2922 FERNANDES, P. M. B. Molecular diagnosis of Papaya meleira virus (PMeV) from leaf
2923 samples of *Carica papaya* L. using conventional and real-time RT-PCR. **Journal of**
2924 **Virological Methods**, 180, n. 1, p. 11-17, 2012/03/01/ 2012.

2925 AKINYEMI, I. A.; WANG, F.; CHANG, Z.-X.; WU, Q. Genome characterization of the
2926 newly identified maize-associated totivirus Anhui. **Archives of Virology**, 163, n. 10, p.
2927 2929-2931, 2018/10/01 2018.

2928 ANDIKA, I. B.; WEI, S.; CAO, C.; SALAIPETH, L.; KONDO, H.; SUN, L.
2929 Phytopathogenic fungus hosts a plant virus: A naturally occurring cross-kingdom viral
2930 infection. **Proceedings of the National Academy of Sciences**, 114, n. 46, p. 12267-
2931 12272, 2017.

2932 ANDRADE, J. D. S.; VENTURA, J. A.; RODRIGUES, S. P.; COUTO, A. D. O. F.; LIMA,
2933 R. D. C. A.; TATAGIBA, J. D. S.; FERNANDES, P. M. B.; MARTINS, D. D. S. Evidência
2934 da não transmissão do vírus da meleira por mosca-branca *Trialeurodes variabilis*
2935 (Quaintance, 1900). *In*: Papaya Brasil: qualidade do mamão para o mercado interno,
2936 2003, Vitória-ES, Brazil. p. 605-608.

2937 ANTUNES, T. F. S.; AMARAL, R. J. V.; VENTURA, J. A.; GODINHO, M. T.; AMARAL,
2938 J. G.; SOUZA, F. O.; ZERBINI, P. A.; ZERBINI, F. M.; FERNANDES, P. M. B. The
2939 dsRNA Virus Papaya Meleira Virus and an ssRNA Virus are Associated with Papaya
2940 Sticky Disease. **PloS One**, 11, p. e0155240, 2016.

2941 ANTUNES, T. F. S.; MAURASTONI, M.; MADROÑERO, L. J.; FUENTES, G.;
2942 SANTAMARÍA, J. M.; VENTURA, J. A.; ABREU, E. F.; FERNANDES, A. A. R.;
2943 FERNANDES, P. M. B. Battle of Three: The Curious Case of Papaya Sticky Disease.
2944 **Plant Disease**, 104, n. 11, p. 2754-2763, 2020.

2945 ARAÚJO, M. M. M. D.; TAVARES, É. T.; SILVA, F. R. D.; MARINHO, V. L. D. A.;
2946 JÚNIOR, M. T. S. Molecular detection of Papaya meleira virus in the latex of *Carica*
2947 *papaya* by RT-PCR. **Journal of Virological Methods**, 146, n. 1, p. 305-310,
2948 2007/12/01/ 2007.

- 2949 BOL, J. F. Role of Capsid Proteins. *In*: FOSTER, G. D.; JOHANSEN, I. E., *et al* (Ed.).
 2950 **Plant Virology Protocols: From Viral Sequence to Protein Function**. Totowa, NJ:
 2951 Humana Press, 2008. p. 21-31.
- 2952 BOTHA, C. E. J.; EVERT, R. F.; WALMSLEY, R. D. Observations of the penetration of
 2953 the phloem in leaves of *Nerium oleander* (Linn.) by stylets of the aphid, *Aphis nerii* (B.
 2954 de F.). **Protoplasma**, 86, n. 4, p. 309-319, 1975/12/01 1975a.
- 2955 BOTHA, C. E. J.; EVERT, R. F.; WALMSLEY, R. D. Studies on *Gomphocarpus*
 2956 *physocarpus*: Further evidence of preferential feeding by the aphid, *Aphis nerii* on the
 2957 internal phloem. **Protoplasma**, 84, n. 3, p. 345-356, 1975/09/01 1975b.
- 2958 CAMPBELL, P. Papaya Press. Papaya Clean Seed Program Underway. KATH, G.
 2959 Australia: 1 p. 2019a.
- 2960 CAMPBELL, P. Papaya Press. Papaya clean seed update KATH, G. Australia: 1 p.
 2961 2019b.
- 2962 CORNEJO-FRANCO, J. F.; ALVAREZ-QUINTO, R. A.; QUITO-AVILA, D. F.
 2963 Transmission of the umbra-like Papaya virus Q in Ecuador and its association with
 2964 meleira-related viruses from Brazil. **Crop Protection**, 110, p. 99-102, 2018/08/01/
 2965 2018.
- 2966 COSMI, F. C.; ALVES, K. D. S.; MORAES, W. B.; VENTURA, J. A.; MORAES, S. D.
 2967 P. C. B.; MORAES, W. B.; JESUS JÚNIOR, W. C. D. Análise epidemiológica da
 2968 evolução temporal da meleira do mamoeiro. **Summa Phytopathologica**, 43, p. 303-
 2969 309, 2017.
- 2970 COSTA, C. L. As inter-relações vírus-afídeos vetores e o controle da mancha anelar
 2971 do mamoeiro causada pelo Papaya ringspot virus-P. *In*: Papaya Brasil: mercado e
 2972 inovações tecnológicas para o mamão, 2005, Vitória-ES, Brazil. p. 183-191.
- 2973 DE LIMA, J. G. S.; TEIXEIRA, D. G.; FREITAS, T. T.; LIMA, J. P. M. S.; LANZA, D. C.
 2974 F. Evolutionary origin of 2A-like sequences in *Totiviridae* genomes. **Virus Research**,
 2975 259, p. 1-9, 2019/01/02/ 2019.
- 2976 EL MOUSSAOUI, A.; NIJS, M.; PAUL, C.; WINTJENS, R.; VINCENTELLI, J.;
 2977 AZARKAN, M.; LOOZE, Y. Revisiting the enzymes stored in the laticifers of *Carica*
 2978 *papaya* in the context of their possible participation in the plant defence mechanism.
 2979 **Cellular and Molecular Life Sciences**, 58, p. 556-570, 2001.
- 2980 FISHER, J. B. The vegetative and reproductive structure of papaya (*Carica papaya*).
 2981 **Lyonia**, 1, n. 4, p. 191-208, 1980.
- 2982 GARCÍA-CÁMARA, I.; TAPIA-TUSSELL, R.; MAGAÑA-ÁLVAREZ, A.; CORTÉS
 2983 VELÁZQUEZ, A.; MARTÍN-MEX, R.; MORENO-VALENZUELA, O.; PÉREZ-BRITO, D.
 2984 *Empoasca papayae* (Hemiptera: *Cicadellidae*)-mediated transmission of papaya
 2985 meleira virus-mexican variant in Mexico. **Plant Disease**, 103, n. 8, p. 2015-2023, 2019.

- 2986 GHOSH, S.; KANAKALA, S.; LEBEDEV, G.; KONTSEDALOV, S.; SILVERMAN, D.;
2987 ALON, T.; MOR, N.; SELA, N.; LURIA, N.; DOMBROVSKY, A.; MAWASSI, M.; HAVIV,
2988 S.; CZOSNEK, H.; GHANIM, M. Transmission of a new polerovirus infecting pepper by
2989 the whitefly *Bemisia tabaci*. **Journal of Virology**, 93, n. 15, p. e00488-00419, 2019.
- 2990 GOUVEA, R.; DA VITÓRIA, R.; ROSA, R.; ALVES, W. D. S.; GIURIATTO, N.;
2991 CALATRONI, D.; FANTON, C.; MARTINS, D. D. S.; QUEIROZ, R. Flutuação
2992 populacional de cigarrinhas (Hemiptera: *Cicadellidae*) e ocorrência do vírus da meleira
2993 do mamoeiro. *In*: VII Simpósio do Papaya Brasileiro. Produção e Sustentabilidade,
2994 2018, Vitória-Espírito Santo, Brazil. 22-25 August.
- 2995 GUO, L.; YANG, X.; WU, W.; TAN, G.; FANG, S.; ZHANG, S.; LI, F. Identification and
2996 molecular characterization of Panax notoginseng virus A, which may represent an
2997 undescribed novel species of the genus Totivirus, family *Totiviridae*. **Archives of**
2998 **Virology**, 161, n. 3, p. 731-734, 2016/03/01 2016.
- 2999 HABIBE, T. C.; VIDAL, C. A.; NASCIMENTO, A. S. Transmissão da meleira para
3000 mamoeiros inoculados com macerados de moscas-brancas *Bemisia tabaci* Genn.
3001 biótipo B. **Fitopatologia Brasileira**, 26 (supl.), p. 526-526, 2001.
- 3002 HAGEL, J. M.; YEUNG, E. C.; FACCHINI, P. J. Got milk? The secret life of laticifers.
3003 **Trends in Plant Science**, 13, n. 12, p. 631-639, 2008.
- 3004 HOGENHOUT, S. A.; AMMAR, E.-D.; WHITFIELD, A. E.; REDINBAUGH, M. G. Insect
3005 Vector Interactions with Persistently Transmitted Viruses. **Annual Review of**
3006 **Phytopathology**, 46, n. 1, p. 327-359, 2008.
- 3007 KITAJIMA, E. W.; RODRIGUES, C. H.; SILVEIRA, J. S.; ALVES, F.; VENTURA, J.
3008 A.; ARAGÃO, F. J. L.; OLIVEIRA, L. H. R. Association of isometric viruslike particles,
3009 restricted to laticifers, with "meleira" (sticky disease) of papaya (*Carica papaya*).
3010 **Fitopatologia Brasileira**, 18, p. 118, 1993.
- 3011 LIMA, R. C. A.; COUTO, A. O. F.; ANDRADE, J. S.; MARTINS, D. D. S.; VENTURA,
3012 J.; TATAGIBA, J.; COSTA, H. Flutuação populacional de insetos vetores de doenças
3013 do mamoeiro e sua relação com a ocorrência de doenças viróticas. *In*: Papaya Brasil:
3014 qualidade do mamão para o mercado interno, 2003, Vitória-ES, Brazil. p. 539-541.
- 3015 LUQUE, D.; MATA, C. P.; SUZUKI, N.; GHABRIAL, S. A.; CASTÓN, J. R. Capsid
3016 structure of dsRNA fungal viruses. **Viruses**, 10, n. 9, p. 481, 2018.
- 3017 MACIEL-ZAMBOLIM, E.; KUNIEDA-ALONSO, S.; MATSUOKA, K.; DE CARVALHO,
3018 M. G. *et al.* Purification and some properties of Papaya meleira virus, a novel virus
3019 infecting papayas in Brazil. **Plant Pathology**, 52, n. 3, p. 389-394, 2003.
- 3020 MAFFIA, L. A.; RODRIGUES, C. H.; VENTURA, J. A. Significância epidemiológica do
3021 conhecimento do arranjo espacial de plantas doentes em campo. I - Meleira do
3022 mamoeiro. **Fitopatologia Brasileira**, 18 (Supl.), p. 315, 1993.
- 3023 MARTINS, D. D. S.; LIMA, A. F.; FORNAZIER, M. J.; BARCELLOS, B. D.; QUEIROZ,
3024 R. B.; FANTON, C. J.; JUNIOR, J. S. Z.; FORNAZIER, D. L. Whiteflies (Hemiptera:

- 3025 *Aleyrodidae*) associated with papaya (*Carica papaya* L.). **Revista Científica Intelletto**,
3026 2, n. 1, p. 78-86, 2016.
- 3027 MARTINS, D. D. S.; VENTURA, J. A.; PAULA, R. D. C. A. L.; FORNAZIER, M. J.;
3028 REZENDE, J. A. M.; CULIK, M. P.; FERREIRA, P. S. F.; PERONTI, A. L. B. G.; ZONTA
3029 DE CARVALHO, R. C.; SOUSA-SILVA, C. R. Aphid vectors of Papaya ringspot virus
3030 and their weed hosts in orchards in the major papaya producing and exporting region
3031 of Brazil. **Crop Protection**, 90, p. 191-196, 2016/12/01/ 2016.
- 3032 MARTINS, D.; FORNAZIER, M.; FANTON, C.; QUEIROZ, R.; ZANUNCIO JUNIOR, J.
3033 Pragas do mamoeiro (Pests of Papaya). **Informe Agropecuário**, 37, p. 30-43, 01/01
3034 2016.
- 3035 MAURASTONI, M.; ANTUNES, T. F. S.; OLIVEIRA, S. A.; SANTOS, A. M. C.;
3036 VENTURA, J. A.; FERNANDES, P. M. B. A multiplex RT-PCR method to detect papaya
3037 meleira virus complex in adult pre-flowering plants. **Archives of Virology**, 165, n. 5,
3038 p. 1211-1214, 2020/05/01 2020.
- 3039 PATHANIA, N.; VALERIANA JUSTO; PABLITO MAGDALITA; FE DE LA CUEVA *et al.*
3040 Integrated disease management strategies for the productive, profitable and
3041 sustainable production of high quality papaya fruit in the southern Philippines and
3042 Australia (FR2019-89). ACIAR. Australia: Australian Centre for International
3043 Agricultural Research (ACIAR) 2019: 64 p. 2019.
- 3044 PEREZ-BRITO, D.; TAPIA-TUSSELL, R.; CORTES-VELAZQUEZ, A.; QUIJANO-
3045 RAMAYO, A.; NEXTICAPAN-GARCEZ, A.; MARTÍN-MEX, R. First report of papaya
3046 meleira virus (PMeV) in Mexico. **African Journal of Biotechnology**, 11, p. 13564-
3047 13570, 2012.
- 3048 QUITO-AVILA, D. F.; ALVAREZ, R. A.; IBARRA, M. A.; MARTIN, R. R. Detection and
3049 partial genome sequence of a new umbra-like virus of papaya discovered in Ecuador.
3050 **European Journal of Plant Pathology**, 143, n. 1, p. 199-204, 2015/09/01 2015.
- 3051 RAO, K. S.; RAJPUT, K. S.; KIM, Y. S. Secondary growth and occurrence of laticifers
3052 in the root of papaya (*Carica papaya* L.). **Acta Botanica Gallica**, 160, n. 3-4, p. 255-
3053 260, 2013/12/01 2013.
- 3054 RODRIGUES, C.; VENTURA, J.; MAFFIA, L. Distribuição e transmissão da meleira
3055 em pomares de mamão no Espírito Santo. **Fitopatologia Brasileira**, 14, p. 118, 1989.
- 3056 RODRIGUES, S. P.; DA CUNHA, M.; VENTURA, J. A.; FERNANDES, P. M. B. Effects
3057 of the Papaya meleira virus on papaya latex structure and composition. **Plant Cell**
3058 **Reports**, 28, p. 861-871, 2009.
- 3059 RODRIGUES, S.; ANDRADE, J.; VENTURA, J.; LINDSEY, G.; FERNANDES, P.
3060 Papaya meleira virus is neither transmitted by infection at wound sites nor by the
3061 whitefly *Trialeurodes variabilis*. **Journal of Plant Pathology**, 91, n. 1, p. 87-91, 2009.
- 3062 ROOSSINCK, M. J. Evolutionary and ecological links between plant and fungal
3063 viruses. **New Phytologist**, 221, n. 1, p. 86-92, 2019.

- 3064 SILVA, L.; GARCIA, O.; LOPES, M.; SALAS, C. Changes in protein profile during
3065 coagulation of latex from *Carica papaya*. **Brazilian Journal of Medical and Biological**
3066 **Research**, 30, n. 5, p. 615-616, 1997.
- 3067 TALIAISKY, M. E.; ROBINSON, D. J. Molecular biology of umbraviruses: phantom
3068 warriors. **Journal of General Virology**, 84, n. 8, p. 1951-1960, 2003.
- 3069 TALIAISKY, M. E.; ROBINSON, D.; MURANT, A. Groundnut rosette disease virus
3070 complex: biology and molecular biology. **Advances in virus research**, 55, p. 357-
3071 408, 2000.
- 3072 TAPIA-TUSSELL, R.; MAGAÑA-ALVAREZ, A.; CORTES-VELAZQUEZ, A.; ITZA-
3073 KUK, G. *et al.* Seed transmission of Papaya meleira virus in papaya (*Carica papaya*)
3074 cv. Maradol. **Plant Pathology**, 64, n. 2, p. 272-275, 2015.
- 3075 VENTURA, J. A.; COSTA, H.; TATAGIBA, J. D. S. Papaya Diseases and Integrated
3076 Control. *In*: NAQVI, S. A. M. H. (Ed.). **Diseases of Fruits and Vegetables: Volume**
3077 **II: Diagnosis and Management**. Dordrecht: Springer Netherlands, 2004. p. 201-268.
- 3078 VENTURA, J. A.; COSTA, H.; TATAGIBA, J. D. S.; ANDRADE, J. D. S. Meleira do
3079 mamoeiro: Etiologia, sintomas e epidemiologia. *In*: Papaya Brasil: Qualidade do
3080 mamão para o mercado interno, 2003, Vitória-Espírito Santo, Brazil. p. 267-276.
- 3081 VENTURA, J.; COSTA, H.; TATAGIBA, J. D. S. Sintomatologia da meleira do
3082 mamoeiro e sua importância para o "roguing". **Fitopatologia Brasileira**, 26, n. 1, 2001.
- 3083 VIDAL, C.; NASCIMENTO, A.; HABIBE, T. Transmissão do vírus da meleira do
3084 mamoeiro por insetos. *In*: Papaya Brasil: Qualidade do Mamão Para o Mercado
3085 Interno, 2003, Vitória, Espírito Santo, Brazil. p. 612-615.
- 3086 ZHANG, Z. Y.; HUANG, H.; HAN, X. X.; LI, R.; WU, L. P.; WU, L. Identification and
3087 molecular characterization of tea-oil camellia-associated totivirus 1. **Archives of**
3088 **Virology**, 2021/04/17 2021.
- 3089 ZHOU, J.; WANG, Y.; LIANG, X.; XIE, C.; LIU, W.; MIAO, W.; KANG, Z.; ZHENG, L.
3090 Molecular Characterization of a Novel Ourmia-Like Virus Infecting *Phoma*
3091 *matteucciicola*. **Viruses**, 12, n. 2, p. 231, 2020.

3092 TABLES

3093

3094

3095 Table 1. Summary of transmission assays conducted to date

Experiment details						
Country	Virus	Virus detection method	Vector implicated	Transmission assay	Main Conclusion	Citation
Brazil	PMeV-ES	Visualization of viral dsRNA	<i>Bemisia tabaci</i> MEAM1*	A macerated of insects collected from diseased plants was inoculated in healthy plants which developed symptoms later	<i>B. tabaci</i> MEAM1 is capable of acquiring the infectious form of the PMeV complex	Habibe, 2001
Brazil	PMeV-ES	Visualization of symptoms	<i>Bemisia tabaci</i> MEAM1; <i>Toxoptera citricidus</i> ; <i>Myzus persicae</i>	Asymptomatic plants were exposed to whiteflies and aphids that were forced to feed on diseased papaya plants	<i>B. tabaci</i> MEAM1 but not <i>Toxoptera citricidus</i> and <i>Myzus persicae</i> are capable to transmit the infectious form of the PMeV complex.	Vidal, 2003

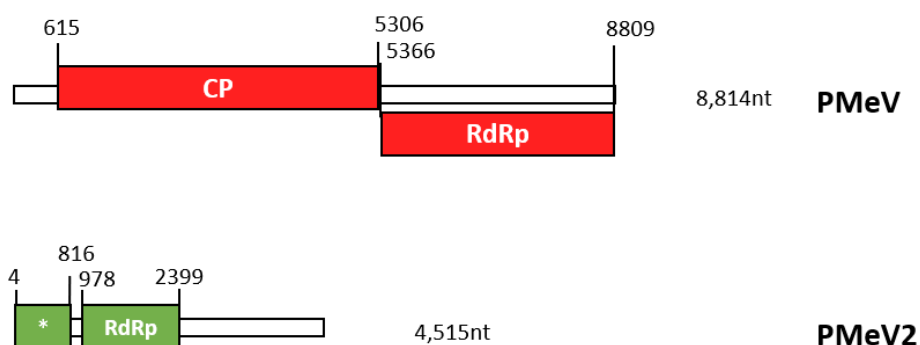
Brazil	PMeV-ES	Visualization of viral dsRNA	<i>Trialeurodes variabilis</i>	Plants inoculated with papaya diseased-latex were infested with <i>T. variabilis</i> collected from fields with non-symptomatic papaya plants. Three healthy papaya plants of different cultivars were added into the greenhouse to be infested by the whiteflies.	<i>T. variabilis</i> can acquire the virus from infected plants and it is not able to transmit it to healthy plants under controlled conditions	Rodrigues et al., 2009
Ecuador	PpVQ	RT-PCR	<i>Bemisia tabaci</i>	Whiteflies, red mites, and mealybugs collected from infected plants were transferred to virus-free plants to feed for 7 days.	Papaya virus Q (PpVQ) is transmitted by the whitefly <i>Bemisia tabaci</i> .	Cornejo-Franco et al., 2018
Mexico	PMeV-Mx	qRT-PCR and visualization of symptoms	<i>Empoasca papayae</i>	After determination of optimal acquisition access period, "viruliferous" insects were allowed to fly from cages containing infected plants to healthy plants. Exposed	<i>E. papayae</i> can acquire the virus six hours after exposure to infected plants and transmit it to <i>C. papaya</i> 'Maradol'.	Garcia-camara et al., 2019

plants were transferred to green-house.

3096

1* *Bemisia tabaci* is not considered a papaya pest in Brazil, but have been reported to occur in plants near papaya trees

3098 FIGURES



3099

3100

3101

3102

3103

3104

3105

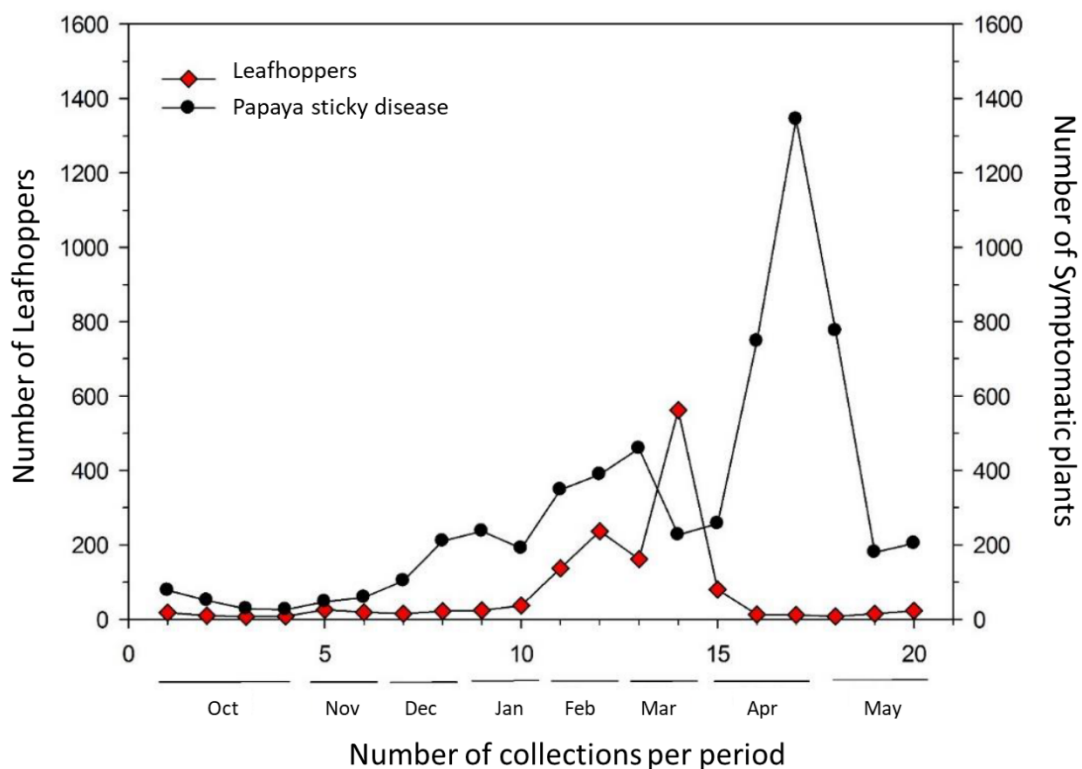
3106

3107

3108

3109

Figure 1. Genomic organization of PMeV-ES (red) and PMeV2 (green) isolates showing their open reading frames and their putative encoded proteins. PMeV is a double-stranded RNA (dsRNA) virus enclosed in a 42-nm-diameter icosahedral particle with its genome organized in two ORFs in different reading frames. ORF1 encodes a polypeptide predicted to be 1,563 amino acids long (177.6 kDa) in which a segment of the capsid from aa 356 to 785 was proved to be part of the virion. It is 75% identical to another Brazilian isolate of PMeV (PMeV-RN) and 20-26% identical to viruses infecting plant pathogenic fungi. Both PMeV-ES and PMeV-RN isolates are tentatively classified in the family *Totiviridae* (ANTUNES *et al.*, 2016; ANTUNES *et al.*, 2020; ABREU *et al.*, 2015).

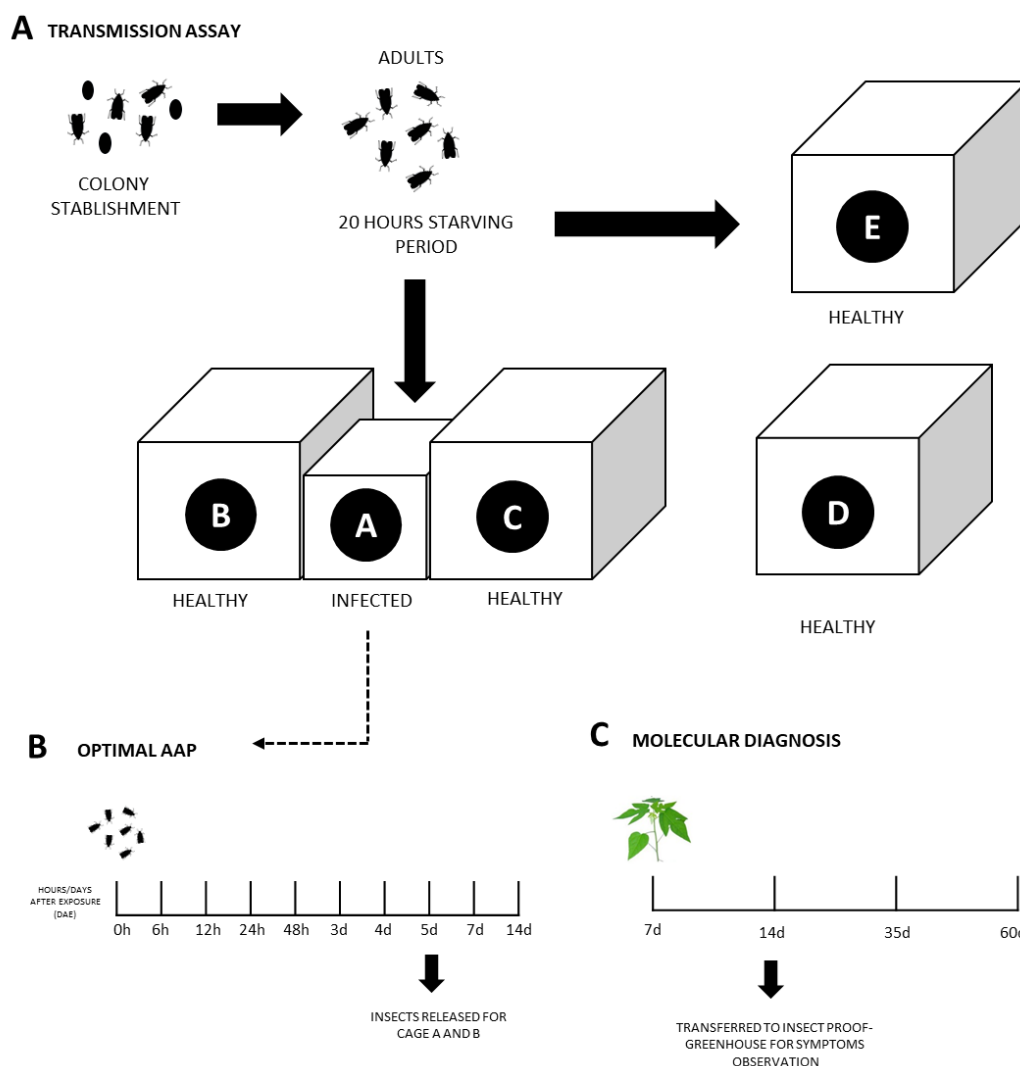


3110

3111

3112 Figure 2. Population fluctuation of leafhoppers and incidence of plants with symptoms of
 3113 papaya sticky disease in Northern Espírito Santo state, Brazil, with roguing management
 3114 applied to control the PSD. Source: (GOUVEA et al., 2018).

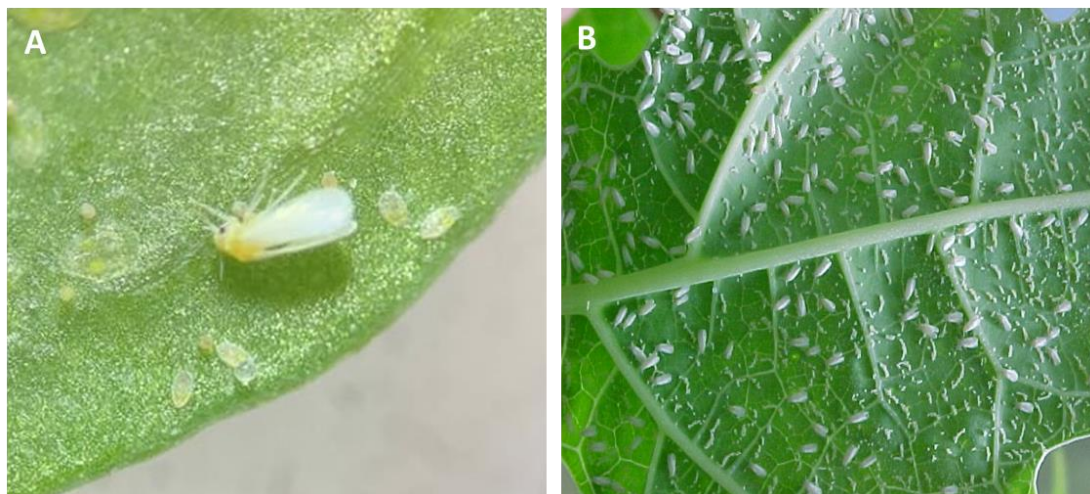
3114



3115

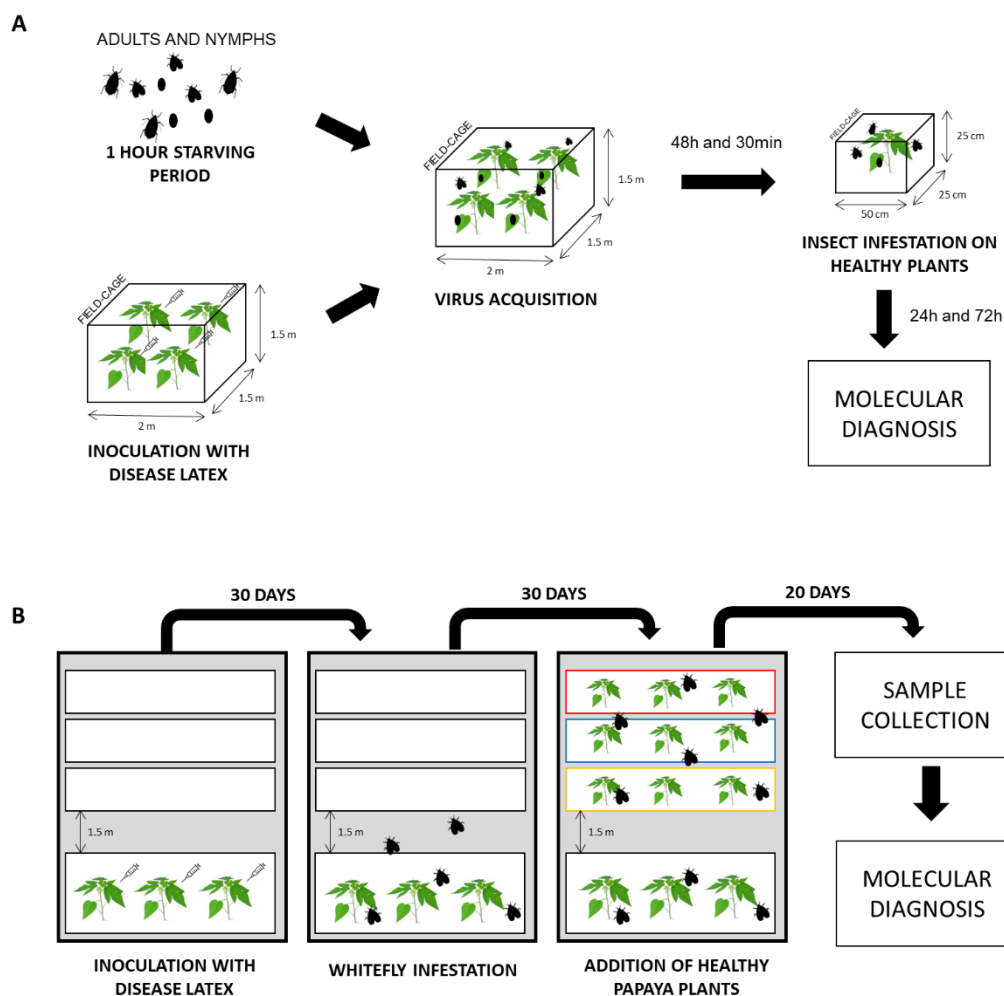
3116 Figure 3. Schematic representation of the transmission assay of papaya meleira virus Mexican
 3117 variant (PMeV-Mx) by *Empoasca papayae*. **a** A colony of *E. papayae* was established in the
 3118 laboratory and periodically diagnosed for PMeV-Mx or phytoplasma infection. Two hundred
 3119 adult insects were transferred to a cage containing PMeV-Mx infected plants after a 20-hour
 3120 starvation period. **b** The optimal acquisition access period was determined by qRT-PCR at
 3121 different time points after exposure to infected plants. Five days after exposure (optimal AAP)
 3122 insect-proof meshes that separate cage A from two other cages, named B and C, were
 3123 removed allowing insects to fly from infected plants to healthy plants. **c** The plants in cages B
 3124 and C were diagnosed at 7, 14, 35, and 60 days after exposure to insects that had fed on
 3125 infected plants. After 14 days the plants were transferred to a greenhouse. Symptoms were
 3126 observed within 3 to 4 months after insect exposure. Two controls were included in this
 3127 experiment represented on cages D and E (a). In cage D six plants were exposed to 100 adult
 3128 insects that had not fed on infected plants. In cage E, six plants were not exposed to insects.
 3129 Plants in both cages remained healthy throughout the experiment.

3130



3131

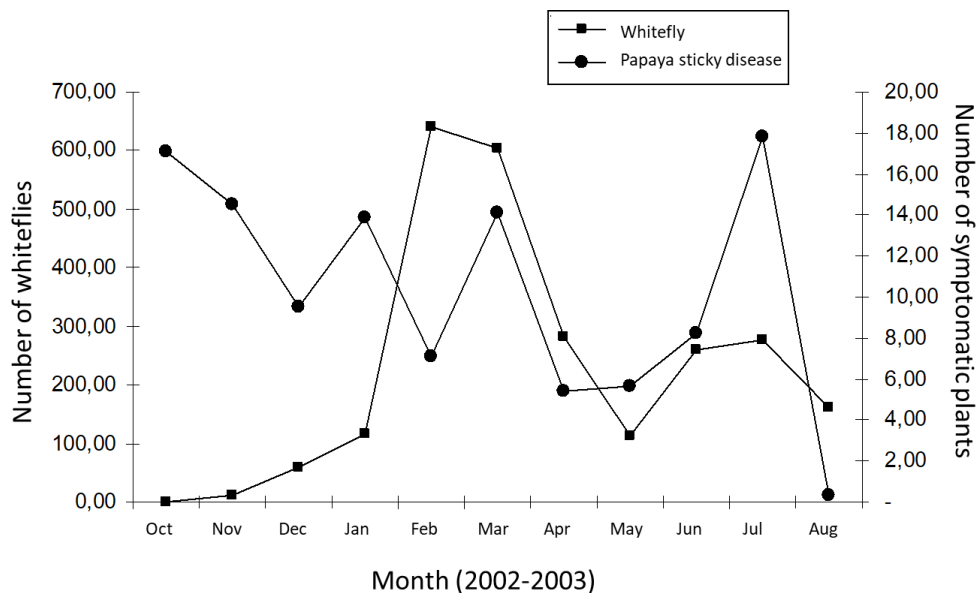
3132 Figure 4. Whitefly species reported occurring in different areas of Brazilian papaya orchards. **a**
3133 *Bemisia tabaci* MEAM1 in a tomato leaf. The species is reported to occur in plants close to
3134 papaya trees Source: A. Nogueira-UFV. **b** High incidence of *Trialeurodes variabilis* population
3135 in the papaya leaf cv. Golden. Source: JA Ventura-Incaper
3136



3137

3138 Figure 5. Transmission assays conducted to test the ability of whiteflies (A and B) to transmit
 3139 the PMeV dsRNA. **a** Plants inoculated with latex collected from disease fruits were kept under
 3140 cages until the experimental assay. Aphids (*Toxoptera citricidus* and *Myzus persicae*) and
 3141 whiteflies (*Bemisia tabaci* MEAM1) were kept in separate cages containing asymptomatic
 3142 papaya plants. 10-20 nymphs and adults were kept in a starving period of 1 hour. Then, insects
 3143 were transferred to a diseased plant for 48h and 30min (virus acquisition). Then 10-20 insects
 3144 of each species were transferred to a cage containing a 3 month-old asymptomatic papaya
 3145 plant where they fed for 24-72h. Insects obtained from the same colonies but submitted to
 3146 feeding in healthy plants were used as negative controls. Infested plants were kept in a
 3147 greenhouse for 30 days and subsequently transferred to field cages (two plants per cage) for
 3148 9 months or until fructification. Three and eight months after the virus acquisition, new
 3149 emerging leaves of all plants were collected and submitted for diagnosis by detection of the
 3150 viral dsRNA. Plants were monitored monthly until the visualization of symptoms. **b** This
 3151 experiment was conducted in greenhouse conditions. A total of 32 plants were analyzed: 24
 3152 were inoculated with diseased latex and 8 were kept non-inoculated. One month after latex
 3153 inoculation, plants were infested with a population of *T. variabilis* collected from fields with
 3154 asymptomatic papaya plants. 30 days after the infestation, three healthy plants of different
 3155 cultivar each (cv. Taiwan, cv. Golden and cv. Sunrise – outlined red, blue, and yellow rectangle,
 3156 respectively) were added inside the greenhouse. 20 days after the exposition, latex from all

3157 plants was collected for detection of the viral dsRNA. Adults and nymphs exposed to healthy
 3158 plants and inoculated plants were collected and submitted to molecular diagnosis by detection
 3159 of the viral dsRNA.
 3160



3161
 3162 Figure 6. Population of whitefly (*Trialeurodes variabilis*) and incidence of plants with
 3163 symptoms of PSD in Northern Espírito Santo, Brazil. Source: (Andrade et al., 2003).
 3164

3165 **THESIS CONCLUSIONS AND FUTURE PERSPECTIVES**

3166

3167

3168 Since the identification of a virus as an etiological agent, researchers have had to try
3169 to understand papaya sticky disease in three major spheres: the biology of the etiologic
3170 agent and its host, the spread of the disease in the field, and the development of
3171 technologies for its management. Here, we compiled and analyzed critically the latest
3172 publications on the disease. Through the first manuscript, we highlighted the points of
3173 the greatest progress in the last 30 years and those that still need further investigation.
3174 Among them, “what is the tolerance mechanism that plants present at the pre-flowering
3175 stage?”, “how is the virus able to infect laticifers?”, “who is the vector?”, “is the virus
3176 transmitted through the seed?”, “How can we diagnose the disease early?”.

3177 In the sphere of virus-host interaction, we show that the PMeV complex accumulates
3178 preferentially in the laticifers of the main vein and that PMeV2 can infect alone laticifers
3179 in the mesophyll. Here, we proposed that the PMeV complex reaches mature laticifers
3180 early in its differentiation. Two pieces of evidence were presented here supporting this
3181 idea: the absence of plasmodesmata in mature laticifer cells and the detection of PMeV
3182 in non-laticifer tissue systems.

3183 The virus-host interaction was also explored in the fourth manuscript, where we show
3184 that the PMeV capsid protein is mainly composed of two major polypeptides with
3185 overlapping sequences. We also show that the central fragment of these polypeptides
3186 can interact with an *Arabidopsis* ribosomal protein, RPL17, potentially modulating an
3187 important pathway for virus infection. This pathway is mainly composed of translation-
3188 associated proteins which are mostly down-regulated at pre-flowering. The meaning of
3189 this interaction is still unknown, but we can speculate that reducing the levels of these
3190 proteins could be important to avoid virus accumulation. This could be an important
3191 strategy presented by pre-flowering plants to tolerate virus effects. The effect of
3192 silencing or overexpression of RPL17 in virus replication could give additional thoughts
3193 in the RPL17 or another capsid protein-interacting proteins in the virus life cycle.

3194

3195

3196 To contribute to disease management, a new diagnostic method is proposed in this
3197 thesis for the detection of the viral complex in adult-pre-flowering asymptomatic plants.
3198 This method takes into account the new proposed etiology and will contribute to a
3199 better understanding of PSD epidemiology. Several new diagnostic procedures are
3200 available across the literature and have been used in the diagnosis of plant viruses.
3201 With some adaptations, methods like loop-mediated isothermal amplification (LAMP)
3202 could be an alternative diagnosis of PMeV complex virus. Other approaches could also
3203 be explored for diagnosis focusing on the changes of metabolite composition of
3204 infected and healthy plants, including paper chromatography or detection of volatile
3205 organic compounds (VOCs). Quantitative Elisa and lateral flow tests targeting viral
3206 proteins could also be explored once established a threshold of protein accumulation
3207 when comparing infected and healthy plants.

3208 The last manuscript focused on a major unresolved problem in Brazil, the vector of the
3209 PMeV complex. We can conclude that the role of whiteflies and leafhoppers as vectors
3210 needs to be addressed. Previous experiments need to be repeated using new more
3211 sensitive diagnostic methodologies, which were developed due to advances in the
3212 understanding of etiology. Also, the possibility of fungi as vectors of PMeV complex
3213 also needs to be assessed due to the similarities of PMeV capsid protein, a plant virus,
3214 with other viruses infecting fungi.

3215 The PSD pathosystem does not follow several common topics in plant virology, starting
3216 with the cells PMeV complex are capable to infect. Besides the questions presented
3217 above, which are still open, the results in this thesis pave the way for new research to
3218 understand the papaya sticky disease pathosystem.

3219

3220

3221 ANNEX

3222

ANNEX #1

3223

**PERMISSION TO REUSE A MATERIAL PUBLISHED IN PAPAYA BRAZIL**

The Editor of Papaya Brazil agrees that you use in Archives of Virology, the Figure 1 of the article: Evidência da não transmissão do vírus da meleira por mosca-branca *Trialeurodes variabilis* (Quaintance, 1900), in Papaya Brasil: qualidade do mamão para o mercado interno, D.d.S. MARTINS, Editor. 2003: Vitória-ES, Brazil. p.605-608, and Figure 1 of the article: Flutuação populacional de cigarrinhas (Hemiptera: cicadellidae) e ocorrência do vírus da meleira do mamoeiro, in VII Simpósio do Papaya Brasileiro. Produção e Sustentabilidade. 2018: Vitória-Espírito Santo, Brazil. Proper credits to the authors and journal/publication should be provided.


David dos Santos Martins

Editor Papaya Brazil
Instituto Capixaba de Pesquisa, Assistência Técnica e Extensão Rural-Incaper
Rua Afonso Sarlo 160, (Bento Ferreira)
29052-010, Vitória-ES, Brasil.

3224

3225

3226

ANNEX #2

3227

3228

3229

3230

PROTOCOLS

3231

3232

3233

Preparation of competent yeast cells for co-transformation

3234

Clontech Matchmaker Gold Yeast Two-Hybrid System [Cat#630489]

3235

Yeast strains included in the kit: Y187 and 2YHGold

3236

3237

3238

3239

For co-transformation use 2YHGold. If single plasmids need to be transformed into yeast do as follows: pGADT7 in 2YHGold (resuspending the cells in -Leu plates at the last step) and pGBKT in Y187 (-Trp plates). This protocol is different from “Yeastmaker Yeast transformation system 2 User Manual” but solutions and media preparation are the same.

3240

This procedure can make 12 transformation reactions and the whole protocol

3241

takes 2 days

1.1X TE/LiAc	10mL	PEG/LiAc	10ml
10X TE	1.1 mL	50 % PEG 4000 or 3350	8 mL
10X LiAc	1.1 mL	10X TE	1 mL
ddH ₂ O (sterilized)	7.8 mL	10X LiAc	1 mL

These two solutions need to be prepared freshly before transformation and pH of all DROPOUT media should be adjusted to 5.8.

3242

3243 YPDA = YPD + Adenine hemisulfate (15 mL 0.2 % for 1 L), no need to adjust the pH
3244 (autoclavable), but it is added to the media before pouring. The adenine hemisulfate is filter
3245 sterilized.

3246

3247 **Methods:**

3248 1. From glycerol stock: streak a **YPDA** agar plate with Y2HGold and incubate at 30 °C
3249 for ~2days. If it is from a streaked plate, just take one colony and streak it again (no
3250 more than 3 times).

3251 **NOTE: Use filter tips for all steps that need to pipette.**

3252 **1st Day**

3253 2. Inoculate a 2-3mm colony into 5 mL YPDA in a falcon tube (it is better to use yeasts
3254 that were in the plate no more than 2 weeks, otherwise, it will take a longer time to
3255 reach the desired OD600). Incubate on a shaker at 250 rpm at 30 °C for 8 h (start
3256 from 8 am to 4 pm)

3257 3. Inoculate 5 µL to 50 mL YPDA in a 250 mL erlenmeyer flask. Incubate in a shaker at
3258 250 rpm overnight (16-20 h) until the OD600 reaches 0.15-0.3 (check in the next
3259 morning).

3260 **2nd Day**

3261 4. Check at 8 am the OD600 from overnight culture from step 3.

3262 5. Spin down cells at 700-1000 g for 7 min at RT. Discard the supernatant and gently
3263 resuspend the pellet in 100 mL of fresh YPDA in a 500 mL Erlenmeyer flask.

3264 6. Incubate in a shaker at 250 rpm at 30 °C for another 3-5 h until the OD600 reaches
3265 0.4-0.6.

3266 7. Spin down cells using 2x 50 mL falcon tubes at 700 g for 7 min at RT.

3267 8. Discard the supernatant and resuspend each pellet using 30 mL of sterile ddH₂O.
3268 Spin down at 700 g for 7 min at RT. Total of 60 mL of ddH₂O. As soon as you add the
3269 water, pellets will resuspend.

- 3270 9. Discard the supernatant and resuspend each pellet using 1.5 mL 1.1X TE/LiAc (total
3271 3 mL 1.1X TE/LiAc solution). **Do not pour!** Use a serological pipette. Yeast pellets do
3272 not attach very well. Otherwise, you will lose some pellets.
- 3273 10. Transfer cell suspension to 1.5 mL microtube (2 tubes).
- 3274 11. Spin down 14 000 rpm 30 s RT in a centrifuge bench
- 3275 12. Remove supernatant. **Do not pour!** Use a micropipette. Yeast pellets do not attach
3276 very well. Otherwise, you will lose some pellets.
- 3277 13. Use a total of 1.2 mL of 1.1X TE/LiAc to resuspend all pellets (for example step 9 I
3278 used 2 tubes, so 600 μ L of 1.1X TE/LiAc will be added into each tube. Given that
3279 every 100 μ L competent cell will be used for one co-transformation reaction, this
3280 procedure can make 12 transformation reactions, if more reactions are needed, scale-
3281 up. **These competent cells cannot be frozen! They stay competent for several**
3282 **hours at room temperature.**
- 3283
- 3284

3285 Yeast co-transformation protocol

3286 Prepare all combinations of prey+bait+carrier DNA during step 6 of the previous
3287 protocol.

3288

3289 1. Perform in a hood: In each 1.5 mL sterile microtube add sequentially: 1500 ng prey
3290 plasmid (pGADT7) + 1500 ng of bait plasmid (pGBKT7) + 5 μ L denatured carrier DNA
3291 [Cat#630440]. Close the tubes, vortex to mix, and do a short spin. Spray 70% ethanol
3292 on tubes before bringing to hood.

3293 2. Add 100 μ L of freshly made competent cells (Y2HGold) in each tube, mix by pipetting
3294 2-3 times.

3295 3. Add 500 μ L PEG/LiAc to each tube, mix by inverting tubes or short vortex. The
3296 PEG/LiAc solution is viscous, after adding them to cells+DNA make sure that they are
3297 well mixed.

3298 4. Incubate at 30 °C in a water bath for 30 min (mix by inverting tubes every 15 min).

3299 5. Spray 70% ethanol before returning the tubes to the hood. Add 20 μ L of DMSO to
3300 each tube and mix by inverting tubes.

3301 6. Incubate at 42 °C for 20 min, mix every 5 min. **Do not shake! just mix gently.**

3302 7. Spin down cells at 14 000 rpm (bench centrifuge) for 30 s.

3303 8. Perform in a hood: Remove supernatant and resuspend cells using 800 μ L - 1mL of
3304 YPDA. Because PEG was added, cells are very sticky, so pipette carefully.

3305 9. Incubate at 30 °C for 90 min in a shaker at 225 rpm.

3306 10. Spin down cells at 14 000 rpm (bench centrifuge) for 30 s.

3307 11. Perform in a hood: Remove YPDA and resuspend in 150 μ L 0.9 % NaCl (sterile). This
3308 volume is recommended for 1 plate. Spread on DDO (SD/-Leu/-Trp) and QDO media
3309 (SD/-Ade/-Leu/-Trp/-His)

3310 Positive control: pGADT7-T + pGBKT7-53 show colonies on both DDO + QDO plates

3311 Negative control: pGADT7-T + pGBKT7-Lam show colonies only on DDO media

3312 If show colonies in DDO = cotransformation work

3313 If show colonies in QDO = interaction occur.

3314

3315

3316 **Protocol for protein-protein interaction map building on String using**
3317 **Arabidopsis orthologs.**

3318

3319 **Obtaining the orthologs**

- 3320 1. Open the Phytozome website, select “Tools” and then “Biomart”
- 3321 2. In the Biomart software go to the dropdown menu “Choose database” and select “ V13
3322 Genomes and Families”. Then in the dropdown menu “Choose dataset” select
3323 “Phytozome V13 Genomes”.
- 3324 3. Now you’re going to add your input data, which means the list of the proteins from a
3325 certain species that you’re looking for in the orthologs in the other. In my case, I used
3326 the PAC transcript ID, which refers to the papaya transcript, available in the dataset
3327 from Soares, 2016.
- 3328 1. Go to “Filters - click to specify” on the left menu and select “Organism”
- 3329 2. Then, select on the list on your left “*Carica papaya* ASGPBv0.4:
- 3330 3. Then open the GENE tab and select “ID List Filter”
- 3331 4. In the dropdown menu “Gene name(s)”, select PAC transcript ID and add your list
3332 of ID in the box below.
- 3333 4. Now you’re going to choose the species that you want the orthologs. In my case,
3334 Arabidopsis
- 3335 a. Go in “Attributes - click to specify” on the left menu and select “Orthologs”
- 3336 b. Click on the box “Select all”
- 3337 c. Choose the species you want the orthologs, in my case “Arabidopsis TAIR 100”
- 3338 5. Click on results
- 3339 6. The results are displayed and downloadable in text format, you have to convert for a
3340 table format in excel.

3341 It is important to note that one gene can retrieve more than one ortholog and some genes
3342 do not have orthologs identified in that species. As output, you will have the gene name (ex.
3343 evm.TU.supercontig_12.98), and the TAIR code corresponded to that papaya gene in
3344 Arabidopsis. You have to organize your data in the excel table to match the gene name with
3345 your PAC transcript ID and TAIR code. Now with the TAIR codes, we can proceed to the String
3346 analysis.

3347

3348 **Creating the PPI network on String**

- 3349 1. Go to string website <https://string-db.org/>
- 3350 2. Select "Search"
- 3351 3. On the menu on your left, select "Multiple proteins"
- 3352 4. In "List of names" Add the list of proteins that you obtained from the previous analysis.
3353 In my case, I included the TAIR codes of proteins that I found interacting with the PMeV
3354 ORF1 segment used to test the interaction.
- 3355 5. Select "Organism", which in my case would be Arabidopsis, and press search
- 3356 6. A list of proteins based on the codes you provided will appear and sometimes more
3357 than one option for a protein will be present. Select the best one for your case and
3358 press "Continue"
- 3359 7. Now your map is built. In my case, I went to "Settings" and selected high confidence in
3360 the dropdown menu "minimum required interaction score".
- 3361 8. You can now export your network as JPG or for a different software, including
3362 Cytoscape.

3363

3364 **Purification of PMeV complex viral particles from papaya latex**

3365

3366 This protocol was written based on a procedure performed at CENARGEN under the
3367 guidance of Dr. Márcio Sanches, Dr. Tathiana Antunes (UFES), Dr. Murilo Zerbini (UFV) and
3368 Dr. Simone Ribeiro. Therefore, for any questions regarding the procedure, contact these
3369 experts. The protocol was based on Zambolim et al., 2003. and Lane (1992).

3370 The procedure is described for purification from the supernatant of papaya latex.
3371 However, some adaptations can be made if the procedure is performed from leaves.
3372 Considering that most particles are found in latex, the ideal is to use this plant material for the
3373 procedure.

3374

3375 **Material collection:**

3376 1. One day before collection, prepare 0.1M sodium citrate buffer pH 5.0 containing
3377 protease inhibitor E64 at a final concentration of 10 μ M. We usually prepare enough for
3378 4 falcon tubes (100ml). Distribute 25 mL of the buffer in each falcon and store in the
3379 refrigerator.

3380 2. Collect latex from the fruits of diseased plants in the buffer. Maintain the 1:1 latex: buffer
3381 volume ratio. We usually do it from a pool of plants, because that's the only way we can
3382 get enough latex volume. Once collected, the material should be stored on ice. **Must**
3383 **not freeze!!** this can denature the proteins.

3384

3385 **Separation of viral particles:**

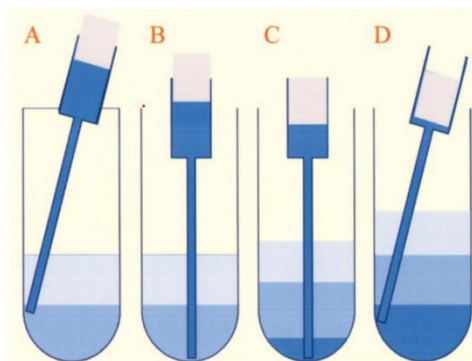
3386 **The entire procedure must be performed on ice.**

3387 3. Add 2 volumes (~20ml) of 0.1M ammonium citrate pH 6.5 containing 0.037M of
3388 iodoacetamide, 0.15M of NaDIECA and 100 μ g/ml of PMSF (iodoacetamide, NaDIECA
3389 and PMSF have to be add freshly) to 10ml of the latex:sodium citrate solution. Vortex
3390 the solution to mix. If there are problems with the solubility of NaDIECA, omit it from the
3391 preparation. It is ideal to use a PMSF that sells already solubilized.

- 3392 4. Centrifuge the mixture at 3800g for 10min at 4°C (Falcon Centrifuge 5804R-Eppendorf).
3393 Collect supernatant (~30mL).
- 3394 5. Transfer supernatant to a beaker on ice. Add Triton X-100 3% (v/v) dropwise to the
3395 supernatant (this step should be done in the hood). After the addition of the triton, clear
3396 clumps will form. Stir in a cold chamber for 3 h with the aid of a magnetic stirrer. Stirring
3397 should not be too fast or too slow, but gently. After 3h the solution turns slightly yellow
3398 and the clumps disappear.
- 3399 6. Ultracentrifuge at 100,000 g for 90 min (add 10min to centrifuge reach the speed) at
3400 4°C, in fixed angle rotor through a 20% (w/v) sucrose cushion. Use a proportion of 4 of
3401 viral preparation and 1 of 20% (w/v) sucrose.
- 3402 a. Prepare the 20% (w/v) sucrose solution with the buffer used in step 3;
- 3403 b. Transfer the viral preparation to the tubes of the fixed angle rotor. These tubes have
3404 a capacity of 30ml. So, I transferred 15ml of viral preparation into 2 different tubes.
3405 Add 3.75 ml of sucrose solution by placing the pipette at the bottom of the tube and
3406 gently releasing it.
- 3407 c. Weigh tubes and balance in pairs adding more buffer from step 3 if necessary. Place
3408 a beaker on the scale (previously tared) to keep the tube upright. As the process is
3409 carried out on the ice, it is necessary to dry the tubes well with paper before
3410 weighing them so that water does not interfere with the weight. Be careful when
3411 handling the tubes to not disturb the sucrose cushion.
- 3412 7. Remove supernatant and refrigerate, in case something goes wrong you still have the
3413 supernatant stored.
- 3414 8. Add 500µL of ice-cold 0.01M borate buffer pH 9.0 to each pellet. Keep the tubes slanted
3415 in the refrigerator (so that the solution completely covers the pellet) overnight.
- 3416 9. Prepare different 10, 20, 30 and 40% (w/v) sucrose solutions in 0.01M borate buffer pH
3417 9.0.
- 3418 a. Mount the gradient in polycarbonate tubes for ultracentrifugation in a Swing Bucket
3419 rotor. **TUBES MUST BE POLYCARBONATE OR ANY VERY TRANSPARENT**
3420 **MATERIAL. OTHERWISE, IT WILL NOT BE POSSIBLE TO SEE THE BANDS**
3421 **BY REFRACTION OF THE LIGHT.** The tube has a capacity of 8ml. Therefore, it

3422 fitted approximately 1.4ml of each sucrose fraction and 1-2ml of the viral
3423 preparation.

3424 b. This process requires a lot of patience, so be calm and relaxed. Add 10% solution
3425 to each tube. With the aid of a Pasteur pipette (glass) coupled to an automatic
3426 pipettor (these instruments are important as the procedure requires great care and
3427 precision) add the 20% solution by touching the pipette to the bottom of the tube
3428 and gently releasing (always pipette 0.5 mL more volume than you want to pipette
3429 as part of the solution does not come out of the pipette. There must be no bubbles,
3430 this will disturb your gradient!! Always dry the Pasteur pipette before placing it in
3431 your gradient tube. When you remove the pipette, it is normal for part of the solution
3432 to come off creating a trail along with the sucrose layers). The lighter solution (10%)
3433 will float above the 20% solution. Do the same with the next denser solutions up to
3434 40%. Avoid sudden shaking with the tubes!! this will destroy your gradient. You
3435 need to see the layers as they are added, if you don't see, something is wrong with
3436 your sucrose solution. Over time the layers become less defined, but if you pay
3437 attention it is possible to observe a subtle transparent line between each layer.
3438 Leave the tubes in the refrigerator overnight. This will cause the regions between
3439 two layers to slowly homogenize creating a continuous gradient. The figure below
3440 illustrates how to perform the gradient.



3441

3442 10. The next day, ultracentrifuge the resuspended pellets through the sucrose gradient.

3443 11. Transfer the gradient tubes to the rotor adapters supported on a hack to avoid sudden
3444 movement and gradient dispersion.

3445 a. Resuspend the pellets that stayed overnight in the refrigerator (ideally, the solution
3446 is very homogeneous, despite having some small clumps). Mix the resuspended
3447 pellet from 2 different tubes (1-2ml total, do not add more buffer!). Slowly load the

3448 resuspended solution over the sucrose solution in the gradient tube. This solution
3449 is whiter than the transparent gradient.

3450 b. Weigh tubes with their adapters by balancing in pairs. Use 0.01M borate buffer pH
3451 9.0, if necessary. Also prepare a tube to balance if necessary.

3452 c. Place the tubes in the rotor and ultracentrifuge at 114,000g for 90 min at 4°C under
3453 vacuum. (The centrifuge time is 80 min; the extra 10 min is needed to reach speed).
3454 If the centrifuge loses the vacuum, the run is lost as it slows down.

3455 12. Analyze the viral bands that scatter light. The environment must be as dark as possible
3456 (a small room with a closed door and no windows is ideal). Place a flashlight light (the
3457 light source must be powerful) under the tube. The ideal is to assemble a box in which
3458 only one hole of approx. 0.5 cm of light pass. Place the tube supported with claws or
3459 on support over this light string. Photograph and collect the bands. In the purification of
3460 latex from diseased plants usually, 3 opalescent layers appear, the heavier one being
3461 more separated from the others and tending to form a band.

3462 13. The collection of bands is performed with a 3mL syringe and a hypodermic needle. The
3463 needle must be as thin as possible. With the tube positioned over the light, collect the
3464 lighter bands (the ones on top) by slowly pulling the syringe plunger and transfer to the
3465 polycarbonate tubes (3-5mL) for ultracentrifugation, previously identified as TOP,
3466 MIDDLE, AND BOTTOM.

3467 14. Ultracentrifuge at 100,000g for 2 hours at 4 °C. After ultracentrifugation, it is possible
3468 (sometimes not) to see a transparent and gelatinous pellet at the bottom of the tube.
3469 Remove the supernatant (refrigerate if necessary) and resuspend the pellet in 100µL
3470 of 0.01M borate buffer pH 9.0. Wash and scrub with the pipette tip the tube walls well
3471 where the pellet may be.

3472 15. Quantify in nanodrop on A280 or UV.

3473 a. Commonly found values:

3474

Sample	Protein	Unit	A 260/280
T	0.496	mg/mL	1.66
M	2.283	mg/mL	1.07
B	1.427	mg/mL	1.56

3475

3476 16. The purification using Cesium chloride is done similarly to the sucrose. All the care
3477 applied for sucrose purification is also applied here.

3478 a. Load 1mL of the three collected fractions over 4mL of a 50% (w/v) CsCl solution in
3479 0.01M borate buffer pH 9.0.

3480 b. Centrifuge at 145,000 g for 18 h in the swing bucket rotor.

3481 c. Visualize and collect the opalescent bands in the same way for the sucrose solution

3482 d. Centrifuge at 35,000 g for 3.5 h to pellet the viral particles

3483 17. Resuspend the pellet in 100 μ L 0.01M borate buffer pH 9.0buffer

3484 18. Quantify in nanodrop A280 or UV

3485 a. Commonly found values:

3486

Sample	Protein	Unit	A 260/280
T	0.471	mg/mL	
M	0.994	mg/mL	
B	0.437	mg/mL	

3487

3488

3489

ANNEX #3



31/01/2018 870180008444
13:19
29409161800979443

**Pedido nacional de Invenção, Modelo de Utilidade, Certificado de
Adição de Invenção e entrada na fase nacional do PCT**

Número do Processo: BR 10 2018 002105 2

Dados do Depositante (71)

Depositante 1 de 1

Nome ou Razão Social: UNIVERSIDADE FEDERAL DO ESPÍRITO SANTO - UFES

Tipo de Pessoa: Pessoa Jurídica

CPF/CNPJ: 32479123000143

Nacionalidade: Brasileira

Qualificação Jurídica: Instituição de Ensino e Pesquisa

Endereço: RUA FERNANDO FERRARI,514

Cidade: Vitória

Estado: ES

CEP: 29075-910

País: Brasil

Telefone: 027-4009-7885

Fax:

Email: josecarlos.init@gmail.com

**PETICIONAMENTO
ELETRÔNICO**

Esta solicitação foi enviada pelo sistema Peticionamento Eletrônico em 31/01/2018 às
13:19, Petição 870180008444

Petição 870180008444, de 31/01/2018, pag. 1/21

3490

3491